Electronic Thesis and Dissertation Repository

6-16-2014 12:00 AM

Analysis of the Vascular Phenotype of the ENT1-null mouse

Keisha A. Best, *The University of Western Ontario*

Supervisor: Dr. James Hammond, *The University of Western Ontario*
A thesis submitted in partial fulfillment of the requirements for the Master of Science degree in Pharmacology and Toxicology
© Keisha A. Best 2014

Recommended Citation

Analysis of the Vascular Phenotype of the ENT1-null mouse

(Thesis Format: Monograph)

by

K. Arielle Best

Graduate Program of Pharmacology and Toxicology

A thesis submitted in partial fulfillment
of the requirements for the degree of
Master of Science

School of Graduate and Postdoctoral Studies
The University of Western Ontario
London, Ontario, Canada

© K. A. Best 2014

ABSTRACT

Adenosine is important in the regulation of vascular tone and the Equilibrative Nucleoside Transporter 1 (ENT1) is a regulator of adenosine concentrations. Thus, changes in ENT1 expression and activity may alter vascular tone regulation. We therefore examined the cardiovascular phenotype of ENT1-null (ENT1$^{-/-}$) as compared to wild type mice (ENT1$^{+/+}$). Heart rates (HRs) and blood pressures (BPs) of ENT1$^{-/-}$ and ENT1$^{+/+}$ littermate male mice were obtained while conscious and anaesthetized, and metabolic data were collected over a 24 hr period. Vascular reactivity was assessed in aortic ring segments obtained from 3 month old ENT1$^{-/-}$ and ENT1$^{+/+}$ mice during both normoxic and hypoxic conditions. Gene expression was obtained using qPCR. KCl administration mediated significantly greater constriction (~32% increase independent of tension applied or age) in ENT1$^{-/-}$ rings compared to ENT1$^{+/+}$. However, no significant differences between the two genotypes were observed for the different receptor agonists. KCl works independent of receptors and carries out direct vasoconstriction via depolarization whereas receptor agonists work indirectly through cellular signaling mechanisms. In hypoxic conditions, ENT1$^{-/-}$ mice exhibited diminished response to phenylephrine following pretreatment with increasing concentration of adenosine as well as in the presence of ENT1 inhibitor NBMPR suggesting an ENT1 independent effect of NBMPR. Length tension curves on the aortas were carried out and resulted in an increase in ENT1$^{-/-}$ curve when the same tension was applied. HR and BP analysis showed elevated blood pressure while the mice were conscious. Morphological assessment of vascularized tissues was performed using H&E and Alizarin Red Staining. Visualization of H&E stain yielded significant differences in luminal area however no significant differences were seen in arterial wall thickness between ENT1$^{+/+}$ and ENT1$^{-/-}$ mice at the age of 3 months. Alizarin Red staining yielded no evidence of calcium

deposits in the arterial walls. The enhanced effect of KCl in ENT1$^{-/-}$ aortic rings suggests a physiological difference in the regulation of the vasoconstriction response. The increased blood pressure coupled with the stiffening of the aortic wall suggests an increase on the mechanical load of the heart, possibly the early stages of hypertension. The studies suggest a vascular phenotype associated with a loss of ENT1. This model will continue to aid in unraveling the role of adenosine in vascular regulation.

ACKNOWLEDGEMENTS

TABLE OF CONTENTS

LIST OF TABLES

LIST OF FIGURES

LIST OF APPENDICES

Appendix A: Ethics Approval of the Animal Use

Appendix B: Copyright Permission for Reproduction from Journal of Nature Neuroscience

LIST OF ABBREVIATIONS

Ada   adenosine deaminase

Adk   adenosine kinase

ADP   adenosine diphosphate

AMI   acute myocardial infarction

AMP   adenosine monophosphate

ATP   adenosine triphosphate

BP   blood pressure

cAMP   cyclic adenosine monophosphate

CD39   ectonucleoside triphosphate diphosphohydrolase 1

CD73   5□-nucleotidase

CNS   central nervous system

CNT   concentrative nucleoside transporter

DAG   diacylglycerol

DISH   diffuse idiopathic skeletal hyperostosis

DMSO   dimethyl sulfoxide

DNA   deoxyribonuclei acid

EC$_{50}$	half maximal effective concentration
EDHF	endothelium-derived hyperpolarizing factor
EDRF	endothelium-derived relaxing factor
ENBT1	equilibrative nucleobase transporter 1
ENT1	equilibrative nucleoside transporter 1
ENT2	equilibrative nucleoside transporter 2
ENT3	equilibrative nucleoside transporter 3
ENT4	equilibrative nucleoside transporter 4
FP	Prostaglandin F
GPCR	G-protein coupled receptors
HR	heart rate
H&E	haematoylin and eosin
IP$_3$	inositol 1,4,5-trisphosphate
MAP	mean arterial pressure
MAP kinase	mitogen-activated protein kinase
NBMPR	nitrobenzylthioinosine, nitrobenzylmercaptopurine riboside
NOS	nitric oxide synthase

PGE$_1$	prostaglandine E$_1$
PGF2α	prostaglandin F2α
PKA	protein kinase A
PLC	phospholipase C
RNA	ribonucleic acid
ROS	reactive oxygen species
SCH58261	A$_{2A}$ selective antagonist
SNS	sympathetic nervous system
TGF	transforming growth factor
VEGF	vascular endothelial growth factor
5HT$_2$	5 hydroxytryptamine

Chapter 1:

Introduction

1.1 Adenosine and Receptor Signaling

Adenosine is a molecule that is found ubiquitously throughout the body. It functions in cellular signaling and ATP (adenosine triphosphate) formation, which contributes to energy supply within tissues [1]. Adenosine formation and catabolism take place both intra- and extra-cellularly and require either adenosine monophosphate (AMP) or *S*-adenosylhomocysteine [2].

The enzyme 5□-nucleotidase is responsible for adenosine formation from substrate AMP [3]. A distinction is made between the extracellular and intracellular formation of adenosine by way of renaming the enzyme *ecto*-5□-nucleotidase (CD73) when dealing extracellularly, and this is done because this particular enzyme does not participate in the formation of intracellular adenosine. Similar to CD73, the intracellular 5□-nucleotidase has the ability to hydrolyze multiple 5□-monophosphates but its affinity for AMP is much greater. AMP is derived from ADP (adenosine diphosphate) and ATP, and within the cytosol, a decrease in the need for energy and therefore decrease in ATP generation results in more adenosine production.

The breakdown of nucleotides is performed by a cascade effect in which using the example of ATP or ADP, the ecto-apyrase CD39 converts to AMP, and CD73 further converts AMP to adenosine [4]. Extracellular purinergic modulation is achieved by CD39, functioning as a family of nucleotidases that hydrolyze the di- and triphosphate nucleotides, whereas the glycosyl phosphatidylinositol linked membrane bound glycoprotein CD73, functions to hydrolyze extracellular nucleoside monophosphates [5,3] (Figure 1.1).
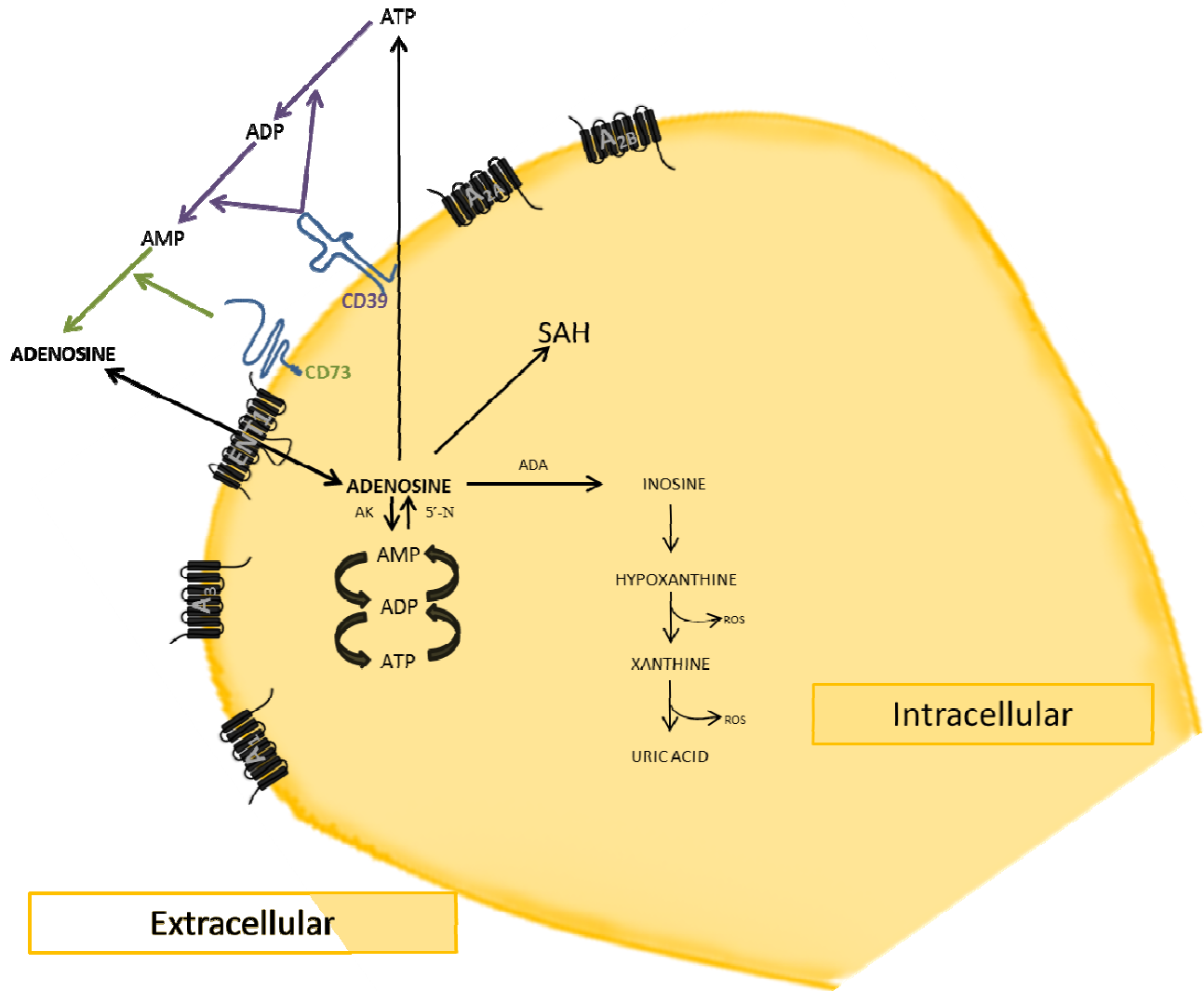
Figure 1.1: Intracellular and extracellular adenosine formation pathways. Adenosine formation and catabolism takes place both intra- and extra-cellularly and requires either adenosine monophosphate (AMP) or *S*-adenosylhomocysteine. The enzyme 5□-nucleotidase is responsible for adenosine formation from substrate AMP intracellularly. CD39 converts ATP and ADP to AMP, and CD73 further converts AMP to adenosine extracellularly.

Hydrolysis occurs in the *S*-adenosylhomocysteine pathway by way of *S*-adenosylhomocysteine hydrolase (SAH) [2]. Adenosine tightly binds to SAH which, studies have suggested, confers protection to adenosine from the actions of adenosine deaminase, in addition to forming a pool of cytosolic adenosine.

Adenosine deaminase (ADA), adenosine kinase (AK) and membrane transport are responsible for the inactivation and removal of adenosine from tissues. All three pathways are widely distributed in mammalian tissues. ADA acts as an enzyme that degrades adenosine into inosine and ammonia, whereas AK catalyzes the formation of AMP from adenosine. ADA is markedly found in endothelial cells, vascular smooth muscle and the heart, and with its high affinity for adenosine, when cytosolic adenosine concentrations are high; ADA is a major pathway of adenosine degradation [1].

During resting conditions, AK is the predominant pathway. Its higher affinity for adenosine results in near maximum saturation of adenosine kinase, which indicates that during resting conditions, a high level of AMP production is occurring. The last form of removal of adenosine, membrane transport, is achieved through two mechanisms of nucleoside transport; the equilibrative bi-directional facilitators and the concentrative, inwardly directed Na^+/nucleoside co-transporters. Membrane transport into cells is required for both ADA and AK pathways and is a required association for adenosine metabolism [1].

The metabolism of AMP to adenosine is followed by activation of a multitude of G-protein coupled receptors [3]. A further source for nucleotide stores is the diet, and the body also possesses many mechanisms for the absorption and subsequent incorporation into the tissues [6].

Inosine is a direct metabolite of adenosine, and in the microvasculature it further converts to hypoxanthine, xanthine, and subsequently uric acid and reactive oxygen species. During reperfusion both adenosine and inosine are released from the ischemic cells by way of ENT1, facilitating the conversion of adenosine and inosine and so forth. As substrates for xanthine oxidase, both metabolites hypoxanthine and xanthine catalyze the formation of superoxide radicals on reperfusion [1].

Nucleosides, nucleotides and nucleobases are all inherently linked. Their role within the body is important for many biological processes. Biological molecules such as nucleobases are components of deoxyribonucleic acid (DNA) and ribonucleic acid (RNA). The nucleobases guanine, adenine, cytosine and thymine, collectively known as purines and pyrimidines, are the foundation of all nucleosides and nucleotides [7] (Figure 1.2). Nucleotide formation occurs when the nucleoside is mono-phosphorylated, di-phosphorylated or tri-phosphorylated.

This conversion between nucleobases, nucleosides and nucleotides is constantly occurring throughout biological processes. These interconverting biological molecules are important in biological processes including serving as direct sources of metabolic energy, as well as structural and regulatory functions [8]. Nucleotide pools are utilized for DNA and RNA formation; the building blocks of NTP and dNTPs. Further important biological processes include formation of nucleoside triphosphates (ATP, GTP, CTP and UTP) in which ATP and GTP play large roles in the supply of energy, and cell signaling by way of cyclic AMP and cyclic GMP [9] (Figure 1.3). It is unclear as to which sources contribute most to the nucleotide stores, however, it is believed that production and salvage mechanisms and by-products of cellular turnover, are sufficient to maintain cellular function.
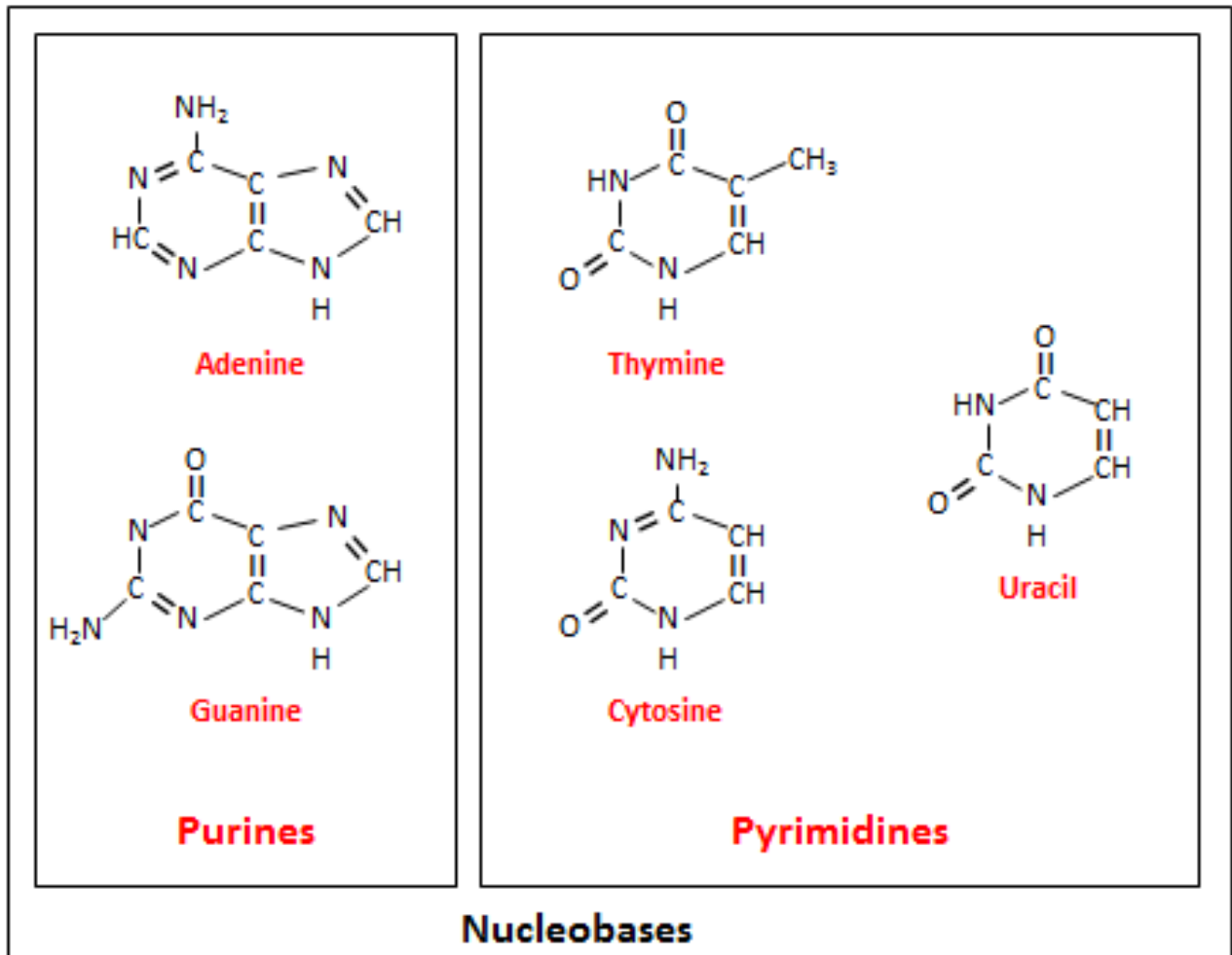
Figure 1.2: Structures of Purines and Pyrimidines. The nucleobases adenine, guanine,

thymine and cytosine are collectively known as purines and pyrimidines.
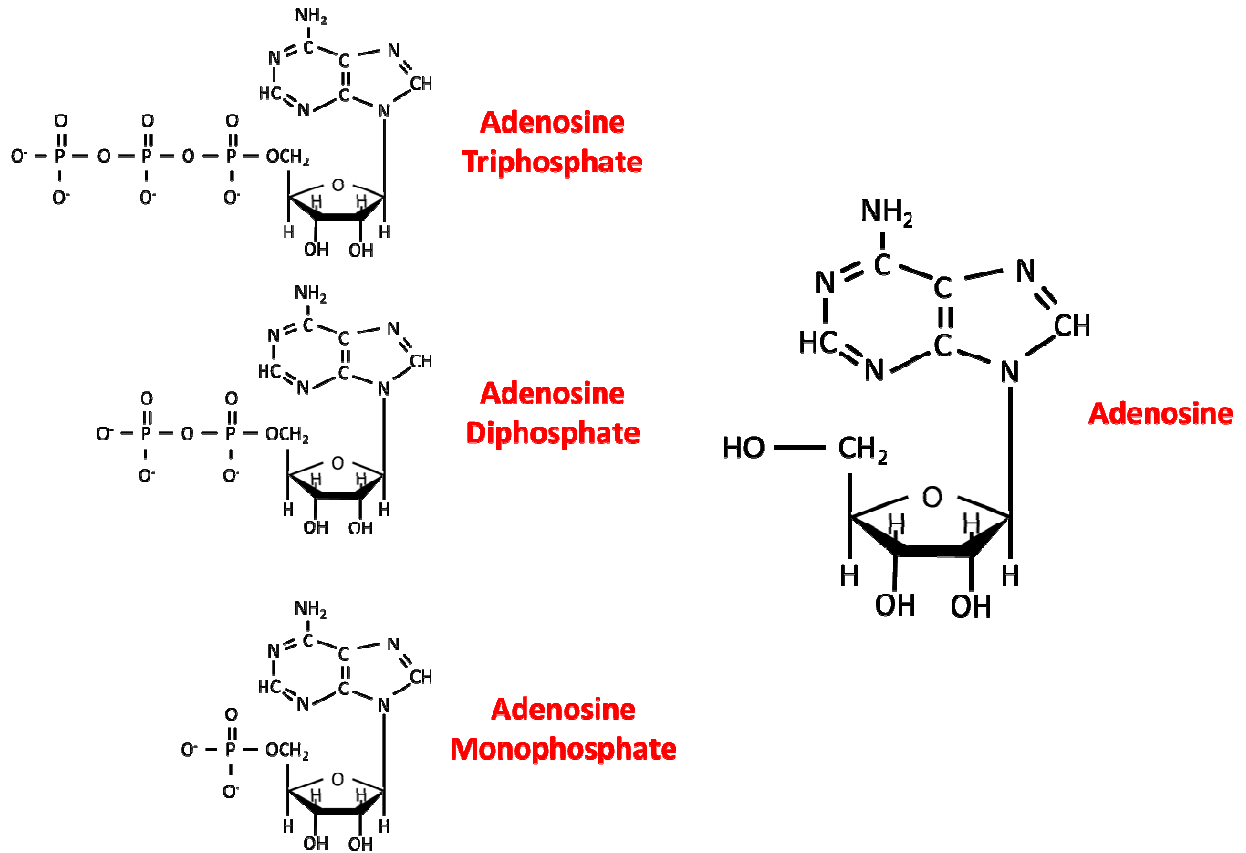
Figure 1.3: Structures of Adenosine, AMP, ADP and ATP.

Biological molecules such as nucleobases are components of deoxyribonucleic acid (DNA) and ribonucleic acid (RNA). The nucleobases are collectively known as purines, guanine and adenine, and pyrimidines, cytosine and thymidine, are the foundation of all nucleosides and nucleotides. Adenosine has been identified as a purine that is important in cell signaling via purine receptors. Purine receptors are broken down into two main families: (1) P1 receptors (adenosine receptors) which are important in cell signaling; and (2) P2 receptors. P2 receptors recognize nucleoside triphosphates, and are further divided into two unique receptor families: (1) G protein-coupled receptors (GPCR) and (2) ligand-gated ion channels [9].

The cellular signaling by adenosine is mediated by specific GPCR. Like other GPCRs, the adenosine receptors possess seven transmembrane domains of hydrophobic amino acids with the N-terminal lying extracellular and the C-terminal within the cytoplasm. Ligand binding occurs within the three dimensional arrangement of the α-helical transmembrane domain [10]. Four subtypes have been identified within the adenosine receptor family. Subtypes are based on various molecular, biochemical and pharmacological factors: (1) A_1; (2) A_{2A}; (3) $A_{2B;}$ and (4) A_3 [11].

The A_1 receptor is most widely recognized of the four subtypes. It functions through inhibitory G proteins to inhibit adenylate cyclase, causing a decrease in the second messenger cyclic adenosine monophosphate (cAMP), affecting cAMP-dependent protein kinases. This results in a decrease in phosphorylation of various proteins. The inhibition of adenylate cyclase by way of A_1 receptors also restricts the activities of other agents that act via adenylate cyclase activity [1].

The A_1 receptor has additional signaling properties which cause the activation of phospholipase C (PLC), resulting in downstream cascade effects of up-regulation of inositol 1,4,5-trisphosphate (IP_3), diacylglycerol (DAG) and increased mobilization of Ca^{2+} from the sarcoplasmic reticulum[1].

The distribution of A_1 receptors varies between tissues. High levels of A_1 receptors can be found throughout the central nervous system (CNS), and are important in reducing oxygen consumption during events of hypoxia or ischemia, resulting in a neuroprotective effect [1]. A_1 receptors are also found within the kidney and within heart tissues; affecting filtration rate, renin secretion and neurotransmitter release within the kidney, and mediating cardiac depression within the heart. The A_1 receptors also affect blood vessel tone although the effects are rare in comparison to others in the P1 receptor family due to decreased receptor distribution [1].

A_{2A} receptors activate adenylate cyclase with the coupling of the G protein G_s (stimulatory). When the A_{2A} receptors are activated, cAMP increases, which affects many downstream signaling pathways, including the initiation of protein kinase A (PKA) pathway and inhibiting the mitogen-activated protein (MAP) kinase pathway [12]. The results of the activation of A_{2A} receptors are in stark contrast to that of A_1 receptors.

The A_{2A} receptors can be found in the vascular smooth muscle, the CNS, platelets, immune tissues and endothelium. These receptors, along with A_{2B}, are the main adenosine receptors that are expressed within the vasculature and are associated with vasodilatory effects [13]. The distribution of A_{2A} receptors seems to be variable between blood vessels, mediating vasodilation in some while not present in others; receptors in the pulmonary arteries appear to be

A_{2B} whereas those in the smaller arteries appear to be A_{2A} subtype. Oftentimes, when no effect can be seen through A_{2A} receptor activation, relaxation is mediated through the A_{2B} receptor [9].

A_{2B} signaling pathway involves stimulation of adenylate cyclase and activation of PLC and IP_3. This receptor possesses a lower affinity for adenosine than the A_{2A} receptor. Although found ubiquitously throughout the body of most species, the abundance of this receptor is actually minor; and for receptor activation and subsequent response to occur, a large quantity of adenosine must be present [9].

A_3 receptors, which are found in the plasma membrane of myocytes, have a similar effect as that of the A_1 receptors, inhibition of adenylate cyclase, although receptor agonists typically have higher affinity at the A_3 receptor than compared to the A_1 [14,15]. Similar to A_{2B}, the distribution is widespread however; controversy still shrouds its physiological role. Frequently the adenosine receptor family overlaps in tissue distribution resulting in multiple subtypes being expressed by the same cell. Expression such as this allows for adenosine to act on, and fine tune, multiple signaling pathways allowing independent receptor regulation [9] (Figure 1.4).

The adenosine receptors have been identified in the heart and vasculature as well as other locations in the body, the A_1 receptors having been described previously as having many of the cardioprotective functions of adenosine associated with it such as mediating the chronotropic, dromotropic and negative inotropic effects. A_{2A} and A_{2B} mediate the vasodilation that is produced by adenosine and may also have an impact on the cardioprotection along with A_3 and A_1 [16]. Studies done by Zhan *et al.* (2011) found that for a maximal A_1 cardioprotective effect, i.e. beneficial A_1 mediated post-ischemic function and decreased infarct size, more than one

receptor subtype must also be involved, thus supporting the theory that cardioprotection is

mediated by interactions between receptor subtypes [17].
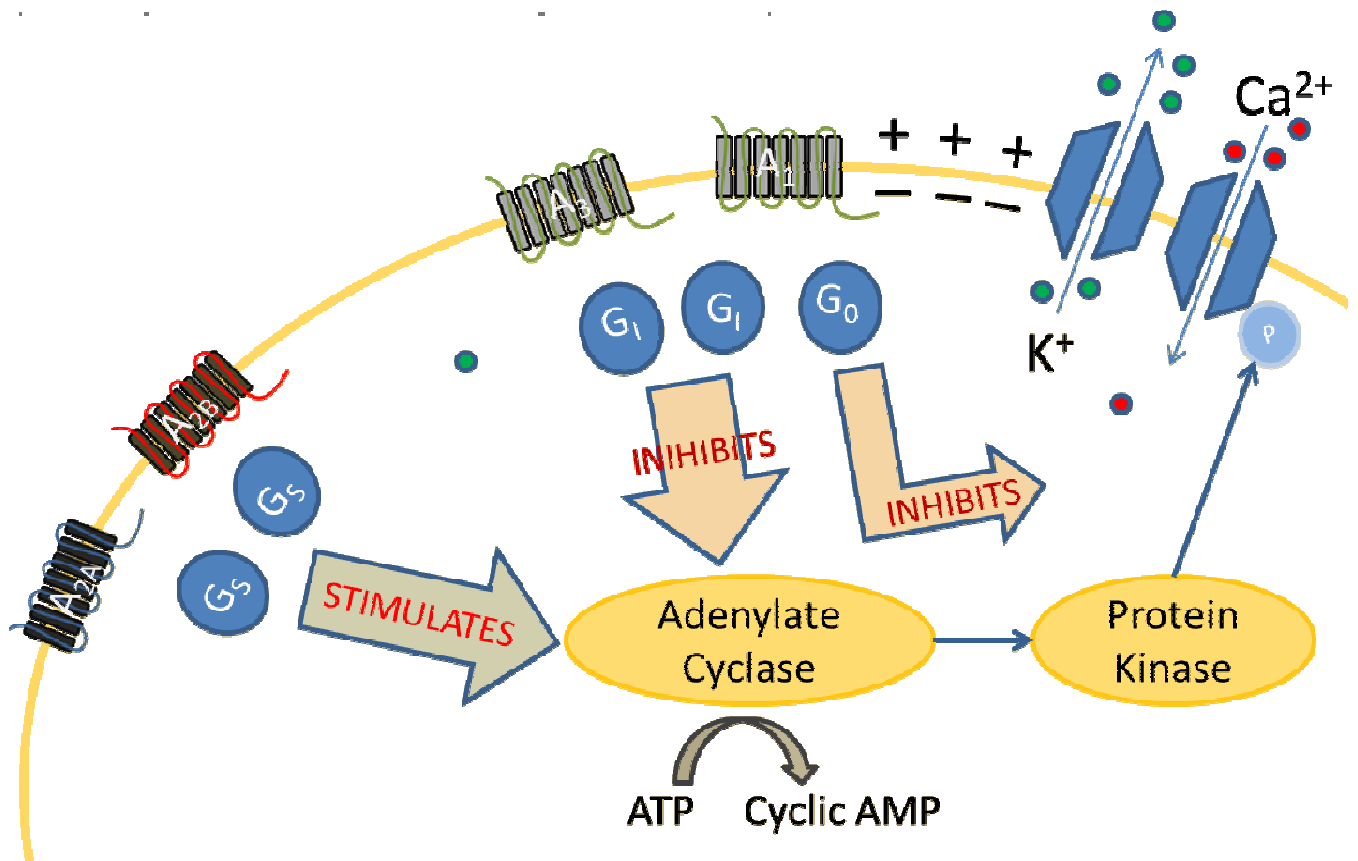
Figure 1.4: The Adenosine signaling pathway. Adenosine receptor activation results in adenylate cyclase and cAMP up-regulation or down-regulation. Up-regulation results in hyper-polarization, reduced intracellular calcium, and subsequent vaso-relaxation. Down-regulation results in the opposite effect.

1.2 Adenosine Transporters: ENTs and CNTs

As nucleosides are hydrophilic molecules they require a specialized transport protein to cross cell membranes [8]. In mammalian cells there are two mechanisms of nucleoside transport, the equilibrative bi-directional facilitators (ENTs) and the concentrative, inwardly directed Na^+/nucleoside co-transporters (CNTs) which are found primarily in specialized epithelial tissues, including but not limited to the liver, kidney and small intestine [7].

ENTs are found ubiquitously throughout the body as they are present in most, potentially all, cell types. They are required for the transport of the hydrophilic nucleosides across cell membranes [7]. The ENT family, also known in humans as SLC29, consists of four transport proteins in human cells, ENT1, ENT2, ENT3, and ENT4 (hENT1/2/3/4 to specify human origin).

ENT1 and ENT2 are two of the major nucleoside uptake mechanisms of mammalian cells [8]. Located predominantly in the plasma membranes of cells, they are found throughout the body. ENT1 and ENT2 are distinguished functionally on the increased sensitivity of ENT1 to *S*6-(4-nitrobenzyl) mercaptopurine riboside (NBMPR, nitrobenzylthioinosine) and by the ability of ENT2 to transport nucleobases [7]. Much less is known about ENT2 than ENT1 due in large part to ENT2 being present in conjunction with ENT1. These transporters are driven solely by the concentration gradient of nucleoside permeants [18]. Alternatively, ENT3 is thought to be a previously identified low affinity transport system for nucleosides in lysosomes, while not much is known about ENT4 subcellular distribution [8].

In a study done by Barnes *et al.* (2006), levels of hENT4 mRNA were found in many adult and fetal tissues with particularly high levels of abundance in the adult heart, intestine, liver, pancreas, lymph nodes, kidney and the bone marrow [19]. ENT4 efficiently transports

adenosine but it is sensitive to extracellular pH levels [19]. Optimally, physiological pH of 7.4, ENT4-mediated adenosine transport activity is nearing zero. Within acidic pH levels of 5.5 its activity increases, suggesting that during ischemic conditions and subsequent acid build-up, ENT4 may play an important role in the regulation of extracellular adenosine concentrations [19].

Concentrative nucleoside transporters (CNT) are proteins encoded by three SLC28 genes (SLC28A1, SLC28A2, and SLC28A3), which represent CNT1, CNT2 and CNT3 respectively [20]. They function by promoting nucleoside transport into the cells against the concentration gradient by using the plasma membrane sodium ion gradient to generate energy while serving as transporters for adenine and other permeants, although selectivity for permeants are variable across CNT subtypes, and act as nucleoside drug import pumps [20]. CNT1 prefers pyrimidine nucleosides, CNT2 the purine nucleosides and CNT3 is involved in both substrates translocation.

1.3 ENT Inhibitors

The endogenous purine, adenosine is transported across cell membranes by the nucleoside transporters which are the major regulators of adenosine extracellular concentrations. Adenosine is the focus because it is the nucleoside that exhibits the highest affinity for facilitated diffusion by this system [21].

The specificity of transport inhibitors has been measured using techniques in which the disappearance of adenosine from cell suspension and whole blood is quantified. Currently, there are reasonably selective adenosine uptake inhibitors for ENT1.

NBMPR is a nucleoside analogue. It is the most specific ENT1 inhibitor that is currently known and as such, its introduction has led to an increased ability to characterize the nucleoside

transporter due to its high level of potency and specificity. It is selective for ENT1, and varies little between models with a K_i in erythrocytes of $10^{-9} - 10^{-7}$ and 10^{-9} in rat tissue, although rats only have ENT2 mediated uptake therefore often report higher values [22,23].

There are many other well-known inhibitors of ENT, all with different specificities and limitations. Dipyridamole is an inhibitor of both ENT1 and ENT2 (equilibrative, insensitive) nucleoside transporters [24]. With a K_i value of $10^{-9} - 10^{-7}$ M it is an effective inhibitor however in addition to uptake inhibition it also is involved in phosphodiesterase inhibition which affects uptake [22]. Unlike NBMPR which has a similar affinity for ENT1 across species, dipyridamole sensitivity varies between rat, mouse and humans [25]. Oral treatments with dipyridamole have been shown to effectively increase concentrations of plasma adenosine and protect against ischemia-reperfusion injury in the forearm skeletal muscles of healthy individuals [26,27].

Dilazep and draflazine are two additional inhibitors, both of which have been studied extensively. Draflazine has been a focus of study in cardiac tissue protection against damage resulting from ischemia. Draflazine is known to have an enhancing effect on extracellular adenosine concentrations and is relatively ineffective in the inhibition of secondary ENT (ENTs 2-4) subtypes that a cell may possess [28]. Dilazep has similar potency to NBMPR as an inhibitor of ENT1 transport however it also has ENT2 inhibiting effects. However, dialzep is 2-3 orders of magnitude more effective when inhibiting ENT1 than ENT2 depending on the model [22]. Dilazep is also able to inhibit adenosine uptake ex vivo but results in weak inhibition upon oral consumption [22]. Similar to dipyridamole, it is a useful tool in increasing plasma adenosine concentrations but its non-specific inhibition makes it difficult to measure the specific effects of the ENT1 [22].

Currently there are only three known compounds that have a higher affinity for ENT2 when compared to ENT1. They include 2-chloroadenosine, 2-fluoroadenosine and, soluflazine which is a draflazine analogue however, their affinity for ENT1 is too low to serve as a probe [28].

1.4 Mouse Model

A whole body ENT1-null mouse was developed by Doo-Sup Choi *et al* (2004) by the inactivation of the Slc29a1 gene on a C57BL/6J x 129X1/SvJ background [29,30]. Targeting vector pKSloxPNT-mod was used to target and eliminate 425 of 1,380 base pairs within the protein coding region of the Slc29a1 gene which encodes ENT1 [29,30]. Subsequently, exons 2 and 4 were deleted [30]. The complete null allele was confirmed and heterozygous Slc29a1 mice which were phenotypically normal were mated to produce the ENT1$^{-/-}$ mouse as well as wild type littermate pairs (Figure 1.5).

Upon initial study of these mice, there were no anomalies reported. The ENT1$^{-/-}$ mice showed a lower body weight when compared to littermate pairs. Otherwise there were no abnormalities in brain development, or spontaneous mortality rates [29].

The initial studies utilized these mice in an effort to identify the role of adenosine transport through ENT1 in the CNS in relation to alcohol consumption [29]. These studies found that ENT1$^{-/-}$ mice had lower response to ethanol however consumed greater amounts than their wild type littermates [29]. In addition, the ENT1$^{-/-}$ mouse exhibited reduced anxiety as measured through an elevated plus maze test [29]. The behavior witnessed was compared to decreased stimulation of A_1 receptors by endogenous adenosine as opposed to a defect in the A_1 receptor family [29].

Work has been done within the Hammond laboratory using microvascular endothelial cells from the ENT1$^{-/-}$ mouse to assess the mechanisms of transport and metabolism of nucleosides and nucleobases [31]. Further work done within the Hammond laboratory has also lead to a novel finding in which ENT1 is seen to take a part in the regulation of calcification of soft tissue. Warraich *et al.* (2013) predicted that the ENT1$^{-/-}$ mouse model may be useful in investigating and evaluating therapeutics for the prevention of mineralization in diffuse idiopathic skeletal hyperostosis (DISH) [32]. DISH has been characterized by the ectopic calcification of spinal tissue and in mice lacking ENT1, development of calcified lesions similar to those found in DISH were observed.

In addition, collaborators within the Coe laboratory at York University were able to establish a link between ENT1 and cardioprotection when they induced an ischemic event and measured infarct size. Significantly less myocardial infarction was found in the ENT1$^{-/-}$ when compared with the wild type littermates [33].
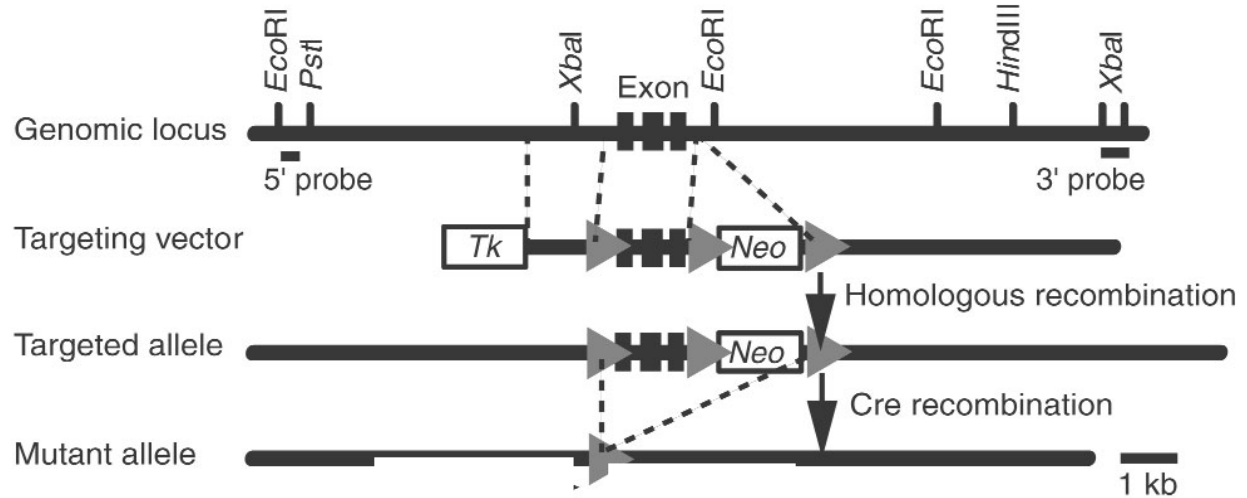
Figure 1.5: The generation of ENT1-null mouse.

Permission to use copyrighted material: from Choi *et al.* 2004. The organization of the gene

encoding mouse ENT1, the targeting construct, and the allele resulting from homologous

recombination are shown. The targeted exons (2–4) are represented by boxes. The *loxP*

sequences and the recognition sites for Cre recombination are presented by gray arrows.

1.5 Cardiovascular System

The cardiovascular system is composed of the heart and the pulmonary and systemic circulatory systems. The heart is a structure composed of muscle which pumps blood throughout the body into the two circulatory systems. The lungs are supplied with blood via pulmonary circulation, and the systemic circulatory system transports the blood to and from the tissues and organs within the body.

The heart pumps blood from venous to arterial, and is divided into left and right halves which are further divided into atria and ventricles. Deoxygenated blood is received through the right half of the heart, collected from peripheral tissues. It is then pumped into the pulmonary arteries, which then enters the pulmonary circulation. Oxygenated blood then leaves the pulmonary circulation to re-enter the heart through the pulmonary vein and subsequently be pumped out of the heart to disseminate to peripheral tissues via the aorta. The arteries which feed the peripheral tissue decrease in size as they extend further from the heart.

1.5.1 Tunica Intima, Tunica Media and Tunica Adventitia

Blood vessels throughout the body differ in size and complexity in terms of wall structure and as such are divided into six different groups: arteries, arterioles, capillaries, lymphatic vessels, veins and venules. All are composed of the same wall structure, the inner layer tunica intima, middle layer tunica media and the outer layer tunica adventitia, except for capillaries and post-capillary venules which have no tunica media [34].

The inner layer, tunica intima is comprised of an endothelial layer which is only a single cell layer thick. Tunica media is composed of circularly arranged smooth muscle cells. This layer is particularly well developed in arteries, where the ability to constrict and dilate is essential to

control blood pressure. Collagen and elastic fibrils comprise the tunica adventitia although in the veins it is mostly smooth muscle. This layer of the vessel wall is the most prominent in veins. In larger vessels, the walls require perfusion via small blood vessel and the vasa vasorum within the adventitia layer because both the adventitia and the media layers are too thick to be supplied with oxygen and nutrients by way of diffusion from the lumen [34](Figure 1.6).
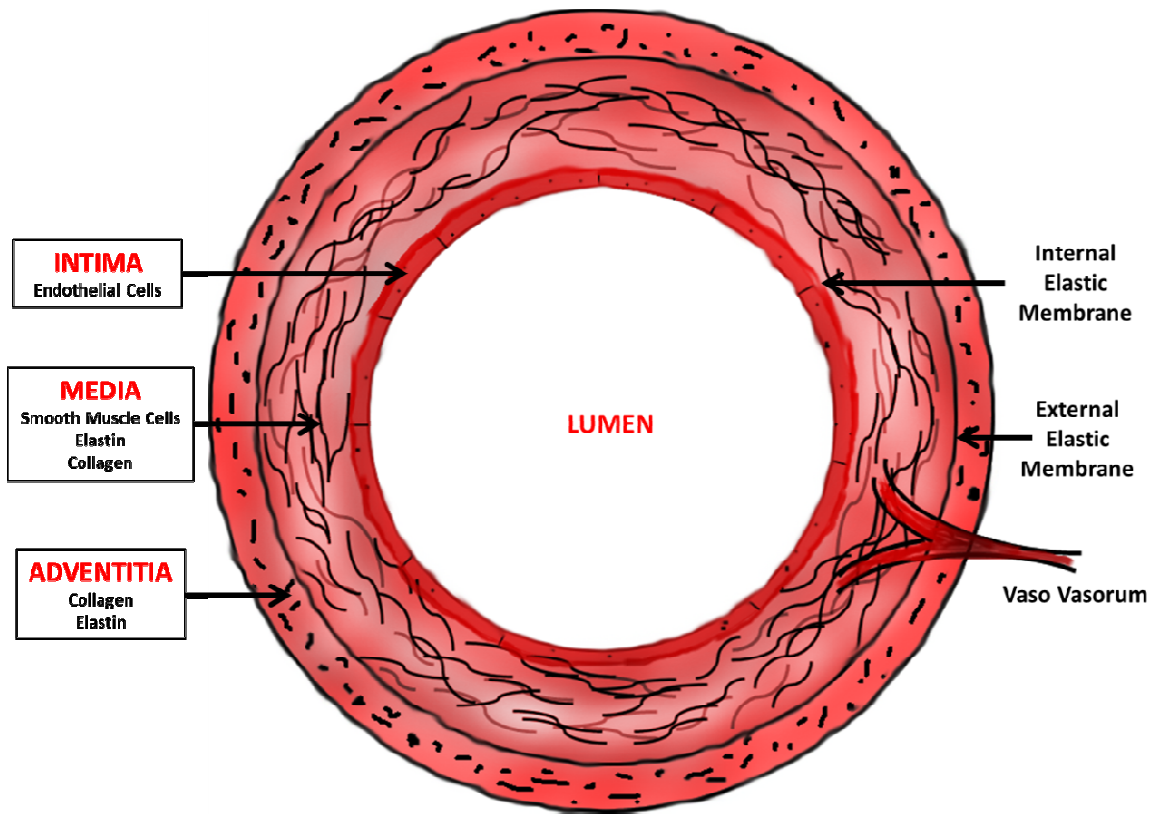
Figure 1.6: Blood vessel wall organization. Figure shows the three layer of an artery. Surrounding the lumen is the tunica intima made up of a layer of endothelial cells. The tunica media, the bulk of the arterial wall is formed by smooth muscle cells, elastin and collagen. Finally the outer layer, the tunica adventitia, is made of collagen and elastin as well as fibroblasts.

1.5.2 Aorta

The aorta is the largest vessel in the body. It transports oxygenated blood to every organ in the body from the left ventricle of the heart. The anatomy of the aorta can be divided into seven sections; (1) the aortic valve, (2) the aortic root, (3) the ascending aorta, (4) aortic arch, (5) the descending thoracic aorta, (6) the abdominal aorta, and (7) the thoracoabdominal aorta. The vessel extends from the upper left side of the heart, forms an arch and descends [35].

The descending thoracic aorta is the most posterior position of the aorta and supplies the spinal cord as well as the thymus and the lymph nodes with the mediastinal branches of the aorta. The aorta also has intercostal arteries that supply the intercostal spaces, and these can be seen when removing the connective tissue from the aorta upon dissection [34].

As mentioned previously, the aorta itself is also made up of different wall layers. The inner layer is the intima, the middle layer the media and the outer layer the adventitia, all of which have well defined roles in development, homeostasis and pathogenic degradation. The media is made up of elastic lamella that alternates with layers of muscle cells [36]. Composed of elastin, collagen and vascular smooth muscle cells this layer provides viscoelasticity. There are discrepancies in cellular origin within the aorta that result in differences in extracellular matrix microfibril density and vascular smooth muscle cell reactivity. Consequently, analysis on the aorta must be done on isolated sections.

1.5.3 Carotid Arteries

The carotid arteries supply nutrients and oxygenated blood to the head and neck regions. The carotids are located on either side of the neck, the right common carotid branching from the brachiocephalic artery and the left common carotid branching directly from the aorta. The

internal carotid and external carotid arteries are both branches from the left and right common carotids. The internal carotid supplies the brain and eyes while the external supplies the throat, neck glands, tongue, mouth, scalp, face, and the meninges.

1.6 Hypoxia

Hypoxia is defined as a reduction in normal tissue oxygen tension levels. In other words, a decrease in the partial pressure of oxygen molecules dissolved within the blood plasma [37]. Hypoxic conditions have increased probability of occurring in vascular diseases, pulmonary diseases and cancers and lead to a variety of responses and production of growth factors. There is an initial shift from aerobic to anaerobic metabolism in which the method by which glucose is metabolized moves from the oxygen-dependent tri-carboxylic acid cycle to the oxygen-independent metabolic pathway, also known as glycolysis. The process of glycolysis also has a secondary effect by which the pH is lowered by lactic acid generation. Haemoglobin production is increased in the renal cells and angiogenesis is induced by a large number of genes, including but not limited to angiopoietin-2, cyclooxygenase-2, hepatocyte growth factor, nitric oxide synthase, Tie-2 (an angiopoietin receptor), vascular endothelial growth factor (VEGF)-A, VEGF receptor-1 and placental growth factor (a member of the VEGF sub family).

VEGF along with other factors including insulin-like growth factors and hepatocyte growth factors activate the protein tyrosine kinase receptor signaling pathway and subsequent myocardial hypertrophy [38]. These VEGF are crucial in embryogenesis and angiogenesis. There are three different VEGF receptors, VEGFR1, VEGFR2 and VEGFR3; VEGFR1 being a positive regulator of monocyte and macrophage migration, VEGFR2 involved in normal and pathological vascular endothelial cell, and VEGF3 playing a large role in lymphatic endothelial

23

cell development as well as function [39]. These VEGFR collectively induce cell migration, survival as well as proliferation [39].

Another hypoxia induced factor is nitric oxide (NO) which is the active moiety of the endothelium-derived relaxing factor (EDRF) [40]. As a key regulator of vascular homeostasis, under basal conditions, low levels of NO are produced by the endothelium to regulate vascular tone [41]. NO is released from endothelial cells into adjacent vascular smooth muscle cells (VSMC). The diffusion of NO into VSMC results in the activation of soluble guanylyl cyclase and the subsequent increase in the production of 3,5-cyclic guanosine monophosphate (cGMP). Following this, the primary mechanism of NO mediated vasorelaxation occurs [42]. The cGMP induced inhibition of voltage gated Ca^{2+} channels and the activation of protein kinases also results in vasorelaxation following the decreased cystolic Ca^{2+} concentrations and subsequent inhibition of calcium-calmodulin myosin light chain kinase complex formation. In addition to hypoxic conditions, the synthesis of NO by nitric oxide synthase (NOS) occurs in response to a wide variety of mechanical stimuli as well as biochemical stimuli such as adenosine. Stimulation of the cAMP pathway leads to subsequent stimulation of NO synthesis [43]. Inhibition studies on NO have yielded detrimental effects in the vasculature including pathological vasoconstriction, tissue ischemia and hypertension.

Further effectors in the vasodilatory response include prostaglandins, and lipid compounds that are derived from fatty acids as well as others [44]. E-type prostaglandins are widely produced in the body and their receptors are part of the receptors classified as GPCRs. Prostaglandin E_1 (PGE_1) has vasodilatory properties and has been revealed to up-regulate VEGF as well as endothelial NOS. Prostaglandin E_2 (PGE_2) has also been shown to induce VEGF by

means of hypoxia-inducible factor 1α (HIF1α) which leads to the mechanistic downstream signaling discussed previously [45].

1.7 Vascular Protection and Preconditioning

In the United States, acute myocardial infarction (AMI) is the leading cause of death with approximately 1 million occurring annually [46]. Adenosine has been known to play an important role in the regulation of coronary circulation, therefore impacting the ischemic period that occurs during an AMI. In the heart it has many functions including depression of the activity of the sinus and atrio-ventricular nodes, depression of atrial contractility and reduction of the contractile response to catecholamines [14]. ENTs affect the concentrations of adenosine available to adenosine receptors. Adenosine is dependent on nucleoside transporters to exit the cell. Adenosine interacts with receptors to accomplish a wide variety of effects including reduction in apoptosis, increased angiogenesis and vasodilation.

The cellular signaling by adenosine is mediated by specific GPCRs. A_{2A}, specifically, simulates adenylyl cyclase production by coupling to G proteins. This activation increases cAMP which affects many downstream signaling pathways including the activation of PKA pathway and inhibition of the MAP kinase pathway.

Four types of receptors, A_1, A_{2A}, $A_{2B,}$ and A_3, previously described and discussed, have been identified in the heart and vasculature as well as other locations in the body, the A_1 receptors having been previously described as having many of the cardioprotective functions of adenosine associated with it. A_{2A} and A_{2B} mediate the vasodilation that is produced by adenosine and may also have an impact on the cardioprotection along with A_3 and A_1 [16]. The A_1 receptors are participants in the protective effects of adenosine when dealing with ischemia

and reperfusion as the receptor mediates the chronotropic, dromotropic and negative inotropic effects [14]. Adenosine mediates these effects through the inhibition of neutrophil aggregation, adherence to, and injury of endothelial cells as well as platelet aggregation [14]. In addition, as a metabolite of ATP, adenosine is able to minimize ATP's depletion during the ischemic event and increase ATP stores during reperfusion by means of glycolysis stimulation [14]. Finally, with adenosine's vasodilation properties, the oxygen supply/demand ratio can be normalized [14]. Adenosine's vasodilatory activity is mediated through the activation of GPCR which stimulate cAMP and subsequent cAMP dependent PKA downstream. PKA then phosphorylates numerous K^+ channels, resulting in vasodilation.

Cardioprotection is the reduction of myocardial infarction by rescuing cardiomyocytes at risk. There are various therapies aimed at reducing the incidence of myocardial infarction. The differing therapies focus on the idea of the reduction of myocardial infarction by rescuing injured cardiomyocytes from death [38]. When an ischemic event occurs, a number of naturally occurring substances and proteins are up-regulated and released to act on injured cardiomyocytes activating cell survival signaling pathways [38]. Two cardioprotective responses have been established; the former occurring shortly after the ischemic event and the latter occurring within several days [47]. The second response involves an up-regulation of factors such as adenosine and VEGF, and the release from vascular tissues. Adenosine, specifically with A_{2B} receptors, has been shown to stimulate VEGF production under normal as well as hypoxic induction [48].

The cardioprotective effects of adenosine have been shown in hearts exposed to short periods of ischemia. During these short ischemia periods, it has been observed that the release of adenosine protects the heart against injury sustained in future prolonged ischemic events and subsequently causes a decrease in infarct size [16]. The activation of adenosine receptors prior to

ischemia is known as one of the possible preconditioning pathways and confers cardioprotection by reducing infarct size, lethal arrhythmias and contractile dysfunction [47].

1.8 Vascular Disorders

Vascular dysfunction is a disorder in which there is poor function of the blood vessels; the function being disrupted and as a result, impaired blood flow arises. With the disruption in blood flow, the vasculature has difficulty getting oxygen and nutrients to the cells and waste removal does not proceed as efficiently.

Myocardial damage, during and after the infarction, involves reactive oxygen species (ROS) [49]. Myocardial infarction is most often seen after an atherosclerotic plaque in a coronary artery has ruptured, eroded or ulcerated. This is followed by acute thrombosis of the vessel and the inhibition of blood flow [49]. The physiology behind the vasculature involves the perfusion, or blood flow, through tissues or organs. This circulation is determined primarily by the dynamics of the blood flow, the actual anatomy of the circulatory system and the different regulatory mechanisms that control heart and blood vessels. The blood flow is related to the pressure and resistance.

A reduction in blood supply to tissues resulting in a shortage of oxygen and glucose required for cellular metabolism is known as ischemia. The primary method of intervention of an ischemic heart is reperfusion in hopes of myocardial salvage and patient survival. The depletion of ATP stores due to the ischemic effect elevates adenosine leading to the accumulation of inosine as well as other adenosine metabolites. Adenosine has been known to play an important role in the regulation of coronary circulation [14].

1.9 Rationale, Objectives and Hypotheses

Given the prevalence of heart disease in the North American population it is expected that myocardial infarction will remain one of the leading causes of death for the foreseeable future. The World Health Organization (WHO) has estimated that cardiovascular disease will claim the lives of nearly 23.6 million people by the year 2030, as the population becomes increasingly elderly [49]. There is considerable evidence indicating a beneficial effect of adenosine following an AMI. Adenosine is important in the regulation of vascular tone, and ENT1 is a regulator therefore, with the change in ENT1 expression and activity there will be an impact on the mechanisms of vasodilation that are dependent on adenosine. The research done by Figueredo *et al.* (1999) was able to demonstrate the sustained cardioprotection against ischemia-reperfusion with chronic ethanol exposure, ethanol down-regulation of the transporter [50]. Ethanol has been observed to be an inhibitor of nucleoside transport, subsequently increasing adenosine in the extracellular spaces in *in vitro* studies [29]. There have been numerous accounts of increased vasodilation both within human and animal models [51].

Rose *et al.* (2009) completed research into cardioprotection within the heart and the conclusions suggest that the loss of ENT1 results in significantly smaller myocardial infarct size when compared with the littermate pairs [33]. Since then, Rose *et al.* (2011) have further addressed adenosine and inosine levels within the intracellular and extracellular spaces of cardiomyocytes and found extracellular adenosine increases as the cells are taken from normoxia to hypoxia, and similar results are found upon examination of the intracellular space when looking at inosine [52]. The effects seen in these previous studies suggest that a similar form of protection will exist in the vascular system.

In addition, studies done on cardioprotection in ecto-5'-nucleotidase (CD73) and ectonucleoside triphosphate diphosphohydrolase 1 (CD39) null mice have also found that these mice develop larger infarcts than their wild type counterpart [53]. A CD73 or CD39 null mouse is unable to break down ATP, ADP and AMP to adenosine therefore there would be a decrease in extracellular adenosine, and subsequent adenosine receptor activation. Further studies in these mouse models were done in which extracellular adenosine levels were increased via intra-arterial infusion resulting in increased cardioprotection by ischemia preconditioning [54]. Increases in phosphohydrolysis of ATP, ADP and AMP are a key factor in cardioprotection during a hypoxic challenge. Without CD73 and CD39, in other words, without large quantities of extracellular adenosine, the cardioprotective effects seen from adenosine were severely reduced. Hypoxia is believed to enhance cellular ATP production and release while also hydrolyzing adenine nucleotides, thereby increasing adenosine production [55]. Depending on the temporal relationship with onset of hypoxia and ATP release, it is also possible that the loss of ENT1 initially results in an inadequate release of adenosine resulting in a delayed response to the hypoxic event. Loss of ENT1 may also result in higher levels of extracellular adenosine thereby causing a theoretical increase in cardiovascular protection.

As mentioned previously, studies conducted by Choi *et al.* (2004) as well as Warraich *et al.* (2012) have also yielded evidence of morphological changes within the ENT1-null mice that has resulted from the loss of ENT1 [32]. Ectopic mineralization on spinal tissue has led to the examination of the parallels of this phenotype with the human disease known as DISH. An 8.7% decrease in body weight, as well as decreased fat as observed during the initial characterization of this mouse line also leads us to question what else may be changing within the vascular tissue, and the mouse model as a whole.

Hypothesis #1: Loss of ENT1 will lead to a vascular phenotype due to disruption of the normal purinergic homeostatic mechanism which is critical to vascular regulation.

A working hypothesis was also formulated to examine a specific potential vascular characteristic.

Hypothesis #2: Loss of ENT1 will result in an increase in interstitial adenosine levels leading to compensatory changes in the vasculature that would mimic preconditioning.

To explore these hypotheses specific observations were outlined:

1) Determine the baseline vascular characteristics of the ENT1 $^{-/-}$ mouse versus the ENT1$^{+/+}$ mouse.

2) Examine the aorta looking for structural differences between the ENT1 $^{-/-}$ and ENT1$^{+/+}$ mouse.

3) Examine the vascular tissue in response to hypoxic conditions.

Chapter 2:

Materials and Methods

2.1 Animal Protocol

ENT1$^{+/+}$, ENT1$^{-/-}$ and Charles River mice strain C57BL/6 were utilized in our studies. The ENT1$^{-/-}$ mice were generated through the targeted deletion for exons 2 to 4 of the gene encoding ENT1 by a cre-loxP targeting strategy [29]. The ENT1$^{-/-}$ were then bred with C57BL/6 mice as previously described by Chen *et al.* (2007) [30]. Maintenance of the mouse colony occurred through the breeding of ENT1$^{+/-}$ (F1 generation) to obtain ENT1$^{+/+}$ and ENT1$^{-/-}$ (F2 generation) littermates. The care was in accordance with policies and guidelines outlined by the Canadian Council on Animal Care. The mice were used in accordance with the protocols approved by the Animal Use Subcommittee of the University of Western Ontario. Mice were housed under a 12 hour light/dark cycle and allowed unlimited access to rodent chow and drinking water. Male mice were utilized for this study to reduce the influences of hormonal cycles on the vascular functions that are being studied between mice. Mice were euthanized at 3-4 months of age (12-19 weeks).

2.2 Assessment of Vascular Reactivity in Aortas

The vascular reactivity was assessed in aortic rings in accordance with previously published methods [38,56]. ENT1$^{+/+}$ and ENT1$^{-/-}$ mice were anaesthetized with pentobarbital sodium (540 mg/kg ip), the chest wall was opened and the thoracic aorta was removed and transferred to a Petri dish containing Krebs physiological salt solution (KPSS) at 4˚C. The composition (mmol/L) of KPSS was NaCl 118.0, NaHCO$_3$ 25.0, d-glucose 11.1, KCl 4.72, CaCl$_2$2H$_2$O 2.56, NaH$_2$PO$_4$2H$_2$O 1.13, MgCl$_2$6H$_2$O 1.12, (-) ascorbic acid 0.114, and disodium EDTA 0.0297. Connective tissue and blood were removed carefully and four ring segments (2mm in length) from each aorta were cut and mounted in KPSS with an applied tension of 0.5 g,

to simulate physiological pressure, in organ baths individually gassed with 95% O_2 and 5% CO_2 and maintained at 37˚C. The rings were equilibrated for 30 minutes before being maximally constricted with potassium chloride (KCl, final bath concentration, 100 mM) to assess viability. Additional pre-treatments of NBMPR (1 μM) or dimethyl sulfoxide (DMSO) (5 μL) were used as controls for KCl viability. Tissues were incubated in treatment 15 minutes prior to KCl. KPSS in the organ bath was changed three times after each treatment (Figure 2.1, i.).

DMT (Danish Myo Tecnhnology) Myograph 620M was used to measure the tension generated. The unit consists of four single vessel myographs in a rack paired with a separate electronic unit. The data were rendered through a computer using PowerLab 4/30 (ADInstruments) and LabChart 7 Pro software (ADInstruments, Australia) recorded the waveform. (Figure 2.1)

2.2.1 Vasoconstrictor Dose-Response:

Following a previously described tissue viability test, aortic rings were then exposed to increasing doses of phenylephrine (PE, 1 nM – 30 μM), prostaglandin F2α (PGF2α, 10 nM – 30 μM) or serotonin (1 nM – 30 μM). The reason we are testing these receptor mediated vasoconstrictors rather than using KCl is because KCl works via cell depolarization. The addition of extracellular KCl results in a shift in resting membrane potential ultimately resulting in the release of calcium stores, KCl addition is not a natural occurrence and therefore cannot extrapolated to in vivo studies. The receptor mediated approach targets a specific subset of receptors and the mechanism of contraction results in signaling pathways that vary between receptor types. The contraction resulting from PE, PGF2α and serotonin administration was quantified by means of measuring directly the contraction generated. The receptor mediated

contraction responses were expressed as a percentage of the initial KCl maximum contraction. This preliminary test was done to establish a consistent vasoconstrictor to be used for subsequent dose-responses under various experimental conditions (Figure 2.1, ii.)

2.2.2 Vasodilator Dose-Response:

Vasodilation was tested to establish adenosine mediated vasoreactivity and to test whether the A_{2A} receptor is responsible for vasodilation observed (Figure 2.1, iii.). Following the previously described tissue viability test, aortic rings were then incubated in the presence of PGF2α (concentration 80% of maximum, dose range 1 μM – 10 μM) alone or with PGF2α and SCH58261 (100 nM). SCH58261 is a selective antagonist for the A_{2A} receptor. Following the incubation period an adenosine dose-response assay was carried out (100 nM – 1 mM). PGF2α was added 10 minutes before adenosine and increasing adenosine concentrations were added every two minutes thereafter. The relaxation resulting from adenosine administration was quantified by means of measuring directly the maximum PGF2α tension generated and the resultant vasodilation that occurred as a result of adenosine administration. The adenosine mediated relaxation responses were expressed as a percentage of the initial PGF2α maximum contraction.

2.2.3 Phenylephrine Dose-Response following tissue exposure to Hypoxia:

A dose-response assay was conducted following hypoxia to test whether a vascular protection effect was occurring (Figure 2.1, iv.). Following a previously described tissue viability test, aortic rings were then incubated in the presence of adenosine (30 μM – 300 μM) for 30 minutes, NBMPR (1 μM) for 15 minutes, or NBMPR (1 uM) for 15 minutes followed by adenosine (300 μM) for 30 minutes. Aortic rings were then exposed to hypoxic conditions (95%

$N_2 - 5\%$ CO_2) for 60 minutes. NBMPR and/or adenosine were left in solution during hypoxia. Following hypoxic treatment KPSS was then changed three times and organ bath was switched back to normoxic (95% $O_2 - 5\%$ CO_2) conditions and tissue was incubated for an additional 30 minute period. Aortic rings were then exposed to increasing doses of phenylephrine (PE, 1 nM – 30 μM). The contraction resulting from PE administration was quantified by means of measuring directly the contraction generated. The PE-mediated contraction responses were expressed as a percentage of the initial KCl maximum contraction.

2.3 Length Tension Curve:

Tissue was equilibrated at room temperature (22˚C) in KPSS. Following the equilibrium period tissue was stretched an additive 50 microns every two minutes until tension generated reach a maximum and plateaued. As mentioned previously, the data were rendered through a computer using PowerLab 4/30 (ADInstruments) and LabChart 7 Pro software (ADInstruments,Australia) recorded the waveform.
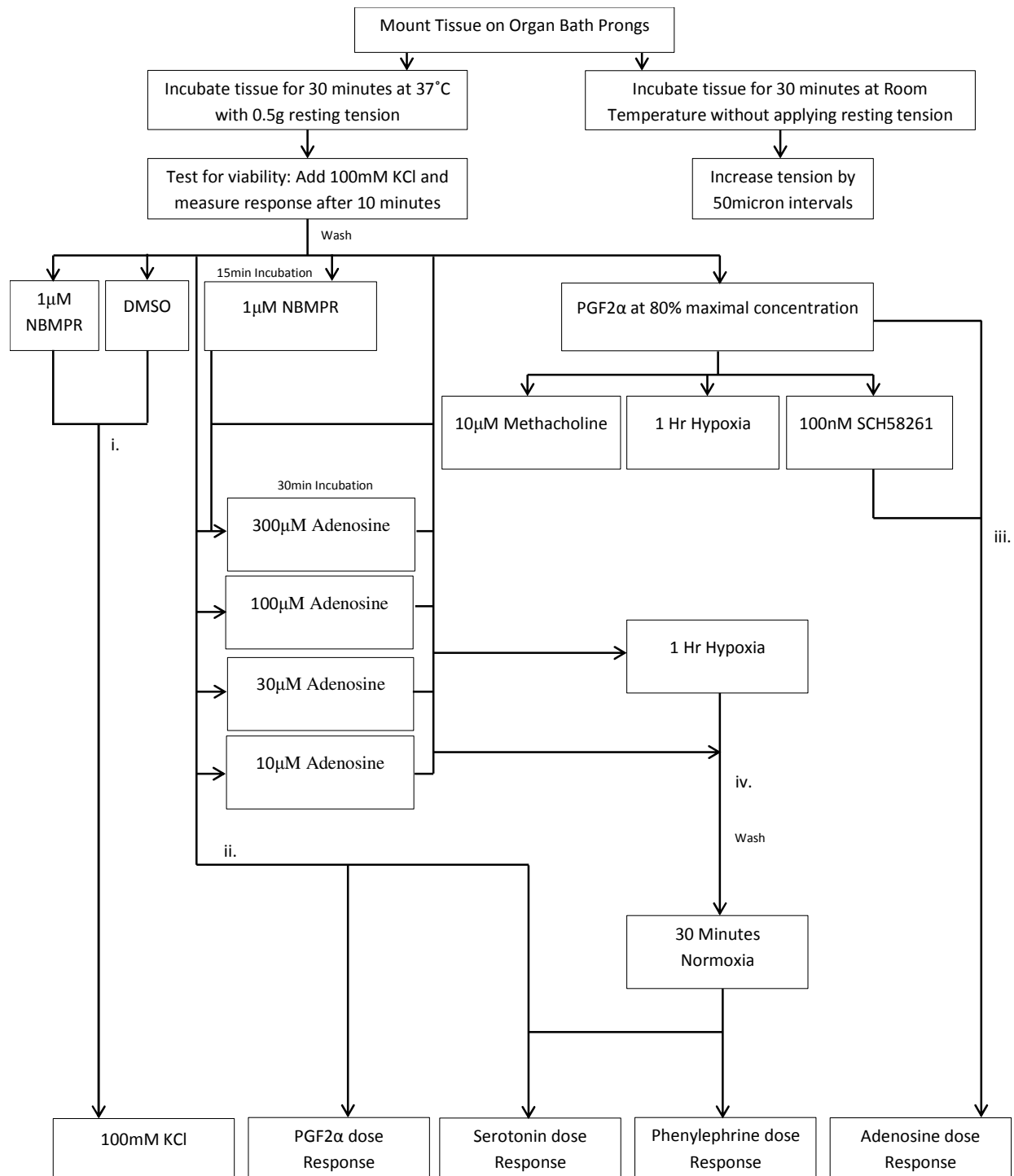
Figure 2.1: Assessment of vasculature reactivity flowchart. All previous methods involving vascular reactivity as measured through DMT Myograph M620M are outlined.

2.4 Histological:

Aortas or carotid arteries were dissected under pressure, using gravity perfusion. Excised from three ENT1$^{+/+}$ and three ENT1$^{-/-}$ mice of 3 – 4 months of age, the vessels were fixed in 10% neutral buffered formalin. Following standard histological processing, samples were embedded in paraffin and cut into 5 μm-thick serial sections. The aortic and carotid tissues were sectioned in the coronal plane, mounted on glass slides and baked at 45˚C for 48 hours. The Molecular Pathology Laboratory at Robarts Research Institute (London, Ontario) processed the samples prior to being embedded in paraffin. Sectioning was carried out by Diana Quinonez of the Hammond lab. Samples were then stained with hematoxylin and eosin (H&E) or Alizarin Red counterstained with H&E, which I carried out. Following staining protocol the sections described previously were dewaxed in xylene and rehydrated via consecutive immersion in decreasing concentrations of ethanol to aid in the visualization of the cell nuclei. Shur/Mount xylene-based liquid mounting media (Durham, NC) was used.

2.5 Metabolic Cages:

Oxygen consumption, carbon dioxide production, respiratory exchange ratio, food and water intake, sleep bouts, and physical activity were simultaneously measured in ten 3 – 4 month old mice by using the Comprehensive Lab Animal Monitoring System (CLAMS) interfaced using Oxymax software (Columbus Instruments, Columbus, OH). Mice were individually housed in the metabolic chambers and temperature was maintained at 24±1˚C. The mice were given free access to the standard rodent chow and water on a flow rate of 0.5 L/min. Metabolic chambers were maintained on a 12 hour light and 12 hour dark cycle with measurements being taken every 10 minutes for 48 hours following a habituation period of 16 hours.

Volume of oxygen consumption (VO_2) and carbon dioxide production (VCO_2)

measurements were determined based on concentrations of gases supplied to the chambers as

compared to concentrations of gases leaving the chambers and normalized to body mass

(mL/kg/h). Respiratory exchange ratio (RER), a measure of metabolism substrate choice

(carbohydrate vs. fat), was calculated from VCO_2/VO_2. An RER of 0.7 is indicative of high fat

oxidation whereas high carbohydrate oxidation is shown by an RER of 1.0. Intense exercise or

the synthesis of fat from carbohydrates is indicated by an RER that exceeds 1.0. Energy

expenditure/heat (EE) (kcal/h) was calculated from RER and VO_2 and corrected for body weight.

The observed RER derives a caloric value (CV) which is then used with the VO_2 to calculate

heat. Heat = CV x VO_2 where CV = 3.815 + 1.232 x RER.

Total activity and ambulatory activity were obtained using the Opto-M3 Activity Monitor

and Oxymax software algorithms (Columbus Instruments, Columbus, OH). Infrared photo beam

breaks were monitored as counts on the X- and Y-axis and consecutive beam breaks were

assessed as ambulatory movements.

Food and water intake were obtained by using the Oxymax software algorithms

(Columbus Instruments, Columbus, OH). Feed data is a measurement of how much food is

consumed. Drinking is measured when the Volumetric Drinking Monitor detects the mouse

licking a specifically designed sipper tube quantifying the volume of liquid made available to the

test animal.

Sleeping bouts were calculated based on sampling intervals taken every ten seconds. The

mouse is considered sleeping if it fails to break the beams over the course of several sampling

intervals.

2.6 Haemodynamics:

Heart rate and blood pressure were determined using the CODA-6 non-invasive tail-cuff machine (Kent Scientific Corporation, Torrington, CT, USA,). Where needed, anaesthesia was induced using 1.5% isoflurane in O_2. Anaesthetized animals were kept on a heated pad to prevent loss of body temperature. Animals were subjected to five acclimatization rounds (no data collection) followed by two separate acquisition cycles of 15 measurements each. There was a 60 second rest between acquisition cycles. The tail cuff deflated over a period of 20 seconds during data acquisition.

2.7 Quantitative Real Time PCR:

At 3 – 4 months of age, littermate-paired wild type and ENT1$^{-/-}$ mice (N=3 for each genotype) were dissected to thoracic aortas inclusive of endothelial layer. Tissues were placed directly in 1 mL of PureZOL RNA isolation Reagent (Life Technologies, Wilmington, DE) and homogenized using a Dounce homogenizer. Total RNA was extracted using the Aurum Total RNA Fatty and Fibrous Tissue Kit (Mississauga, ON), using kit protocol and quantified using a NanoDrop 2000 spectrophotometer (Thermo Scientific, Mississauga, ON). For each sample, 210 ng RNA was reverse transcribed into cDNA using Superscript II Reverse Transcriptase (Life Technologies). Gene expression patterns were determined by real-time PCR using the Bio-Rad CFX384 system. PCR reactions were run in triplicate, using 5 μM forward and reverse primers (primer sequences in Table 2.1) with 2X SsoFast EvaGreen Supermix (Bio-Rad, Mississauga, ON). The PCR program started with an initial 3 min at 95˚C for denaturing followed by 95˚C for 10 s denaturing and 30 s annealing/elongation (temperatures provided in Table 2.1), for a total of 40 cycles. Gene transcript levels were determined relative to Beta Actin.

The primers were designed using PrimerBank and Integrated DNA Technologies targeting the sequence specific to the gene of interest, always producing amplicons between 75 and 175 base pairs in length. Optimization for primers was determined using 5-fold serial dilutions of cDNA that was synthesized from a mix of wild type heart, muscle, kidney, brain and intervertebral disc as well as aorta cDNA at a range of temperatures between 56-62˚C to optimize the annealing and elongation temperatures. Optimization was done in collaboration with Sumeeta Warraich of the Hammond laboratory. The specificity of the primers was determined by melt curve analysis.

Primer Sequence Table 2.1:

Gene Name	Primer Sequence (5' to 3')	Annealing/Elongation Temperature (^{o}C)
Beta Actin	Fwd – GGCTGTATTCCCCTCCATCG Rev – CCAGTTGGTAACAATGCCATGT	60
Catalase	Fwd – TGGCACACTTTGACAGAGAGC Rev – CCTTTGCCTTGGAGTATCTGG	60
Ak	Fwd – CTCAGTGGTTGATTCAGGAGC Rev – CAGCCTTACGCTTCAGGATCT	60
Ada	Fwd – ACAATCAGAAGACCGTGGTGGCTA Rev – TCTTTACTGCGCCCTCATAGGCTT	60
ENT1	Fwd – CAAGTATTTCACAAACCGCCTGGAC Rev – GAAACGAGTTGAGGCAGGTGAAGAC	56

2.8 Statistical Analysis:

Data points are represented as means ± standard error of the mean (SEM). Curves were fitted using the software Graphpad Prism 5.03. Statistical analysis was performed using a two-tailed student's *t*-test or a Two-way ANOVA with Bonferroni post-tests to compare replicates where appropriate. The minimum level of significance was set at $P<0.05$ on a two-sided test. (Prism 5.03; GraphPad Software Inc., San Diego, CA).

Chapter 3:

Results

3.1 Mouse full body analysis shows decreased weight and differences in metabolic activities.

Prior to reports of ectopic mineralization, the previous studies in the ENT1-null mouse model have yielded findings of no spontaneous mortality and showed a normal phenotype with no gross anatomical abnormalities. Body weight had been found to be approximately 8.7% lower in the ENT1^{-/-} mouse and spontaneous mortality rates were similar between genotypes [29]. Warraich *et al.* (2012) had then found that ENT1 plays a role in bio-mineralization which they linked to diffuse idiopathic skeletal hyperostosis (DISH) [32].

In the present study, upon examination of the mouse litters at 3 – 4 months of age we also noticed the variance in body weight compared to the ENT1^{+/+} littermates. The ENT1^{-/-} mouse was 25.3 ± 1.0 g and was significantly smaller than the 29.3 ± 0.8 g of ENT1^{+/+} mice (N=10; **$P<0.01$ Student's t-test) (Figure 3.1, Panel **J**). To further analyze the cause of the weight difference, metabolic cages were used to examine food and water consumption along with respiratory exchange ratio, the amount of energy expended, the volume of oxygen consumed, carbon dioxide released, as well as the amount of movement seen over a 24 hour period during the light and dark cycles and the percentage of time spent sleeping (N=10; $P<0.05$ Student's t-test). During the dark cycle we observed significantly higher water consumption (Figure 3.1, Panel **H**), ambulatory movement (Figure 3.1, Panel **D**) and total movement (Figure 3.1, Panel **E**) in the ENT1^{-/-} when compared to the ENT1^{+/+} ($p<0.05$). In addition, significant decrease was seen when analyzing the respiratory exchange ratio (Figure 3.1, Panel **C**) and the energy expenditure (Figure 3.1, Panel **F**). The RER value which is closer to 0.7 (0.9, $P<0.05$) in the ENT1^{-/-}, when compared to ENT1^{+/+}, is oxidizing more fat than carbohydrates. No significant differences were seen in volume of oxygen consumed (Figure 3.1, Panel **A**), volume of carbon

dioxide released (Figure 3.1, Panel **B**), food consumption (Figure 3.1, Panel **G**) or % of time

spent sleeping (Figure 3.1, Panel **I**).
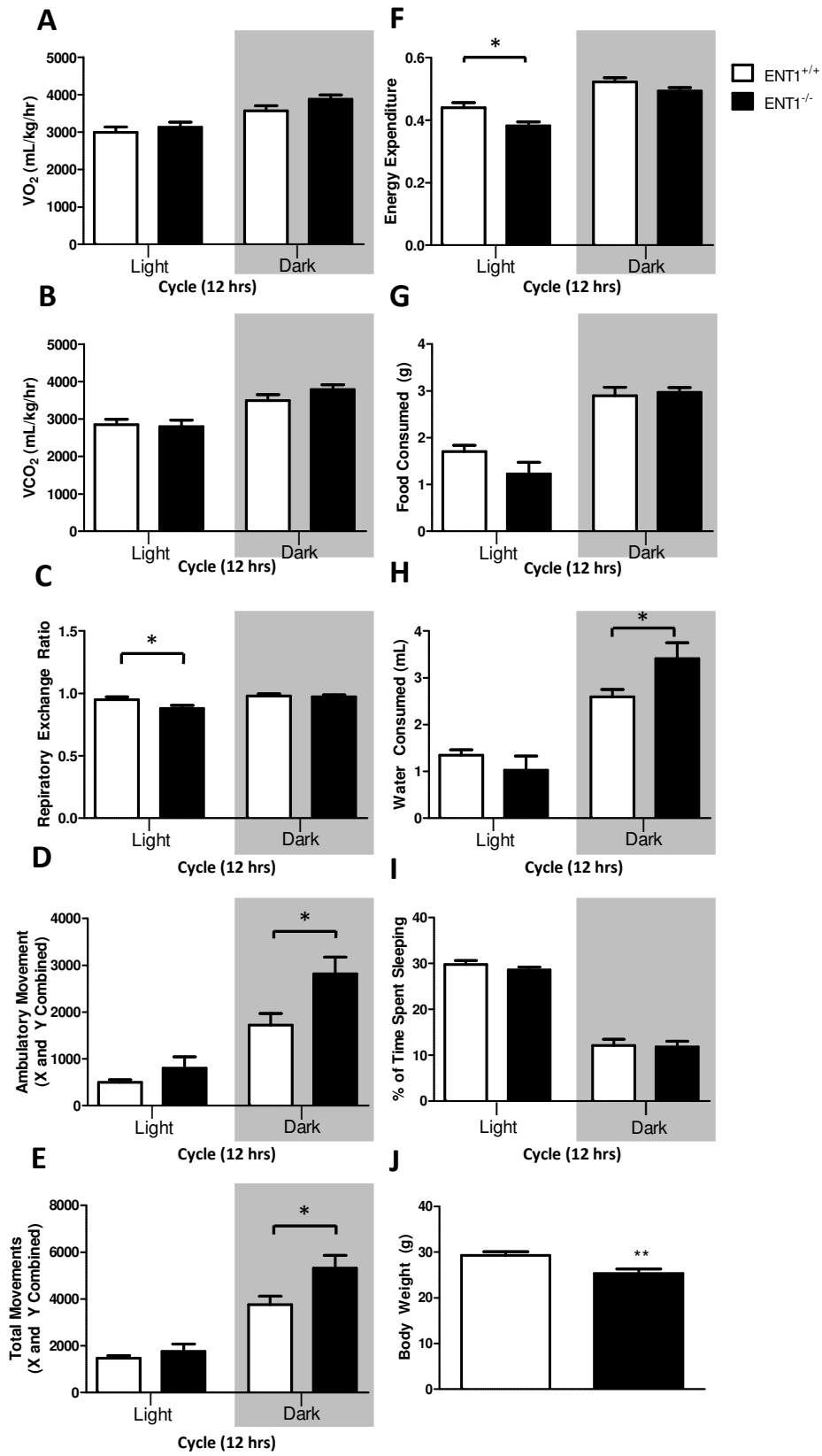
Figure 3.1. Metabolic analysis of ENT1$^{+/+}$ and ENT1$^{-/-}$ mice using metabolic chambers as described previously in the methods. VO$_2$ consumption (Panel **A**), VCO$_2$ production (Panel **B**), Respiratory Exchange Rate analysis (Panel **C**), Ambulatory Activity per hr (Panel **D**), Total Activity per hour (Panel **E**), Energy Expenditure (Panel **F**), Food Consumption (Panel **G**), Water Consumption (Panel **H**), Body Weight (Panel **J**). N=10. % of time spent sleeping (Panel **I**). N=8. *Significant difference for 3 – 4 month old mice studies. (Student's t test for unpaired experimental parameters,* $P<0.05$, **$P<0.01$)

3.2 Haemodynamics

Further analysis of the baseline vascular characteristics led us to measure the heart rates of conscious and anaesthetized 3 – 4 month old ENT1$^{+/+}$ and ENT1$^{-/-}$ mice (Figure 3.2, Panel **A**) were not significantly different although anaesthetized mice showed a trend towards increased heart rate (p=0.06, N=5). Anaesthetized ENT1$^{+/+}$ mice hearts beat 517.0 ± 13.0 beats per minute (N=5) which was less than the ENT1$^{-/-}$ counterparts at 563.5 ± 16.9 beats per minute. The heart rate in awake ENT1$^{+/+}$ mice was 676.5 ± 16.5 beats per minute (N=10) which is comparable to the ENT1$^{-/-}$ rate of 675.4 ± 12.5 beats per minute (N=11) (Figure 3.2, Panel **A**). In conscious mice (Figure 3.2, Panel **B**), the ENT1$^{-/-}$ mouse had significantly higher blood pressure compared to the ENT1$^{+/+}$ counterparts. Systolic: 129.9 ± 5.4 mm/Hg, 149.5 ± 3.5 m/Hg; diastolic: 100.8 ± 5.3 mm/Hg, 115.8 ± 2.6 mm/Hg; and mean arterial pressure (MAP): 110.1 ± 5.3 mm/Hg, 126.7 ± 2.8 mm/Hg as observed from ENT1$^{+/+}$ (N=10) and ENT1$^{-/-}$ (N=11) respectively. In anaesthetized mice (Figure 3.2, Panel **C**), the ENT1$^{+/+}$ mouse blood pressure had no significant differences compared to ENT1$^{-/-}$ counterparts. Systolic: 101.5 ± 13.2 mm/Hg, 101.9 ± 8.6 mm/Hg; diastolic: 72.9 ± 12.1 mm/Hg, 69.0 ± 9.5 mm/Hg; and mean arterial pressure: 82.1 ± 12.4 mm/Hg 79.7 ± 9.2 mm/Hg as observed from ENT1$^{+/+}$ (N=5) and ENT1$^{-/-}$ (N=5), respectively. These results were not expected as previous studies in the ENT1 mouse model found these mice to have an anxiolytic phenotype.
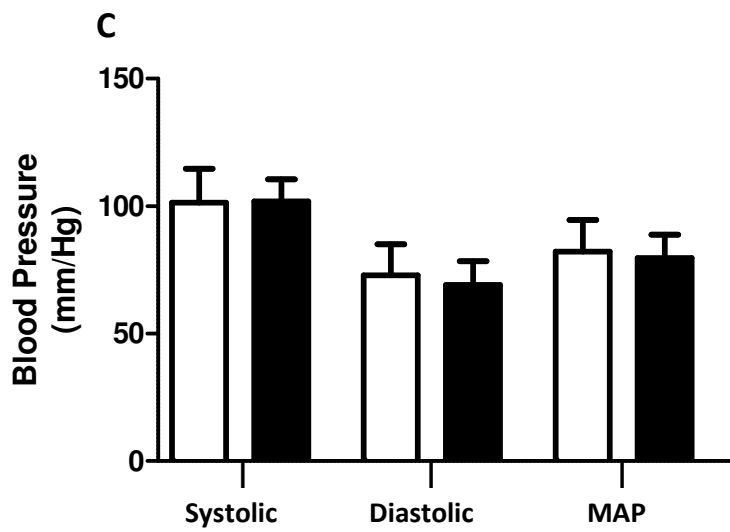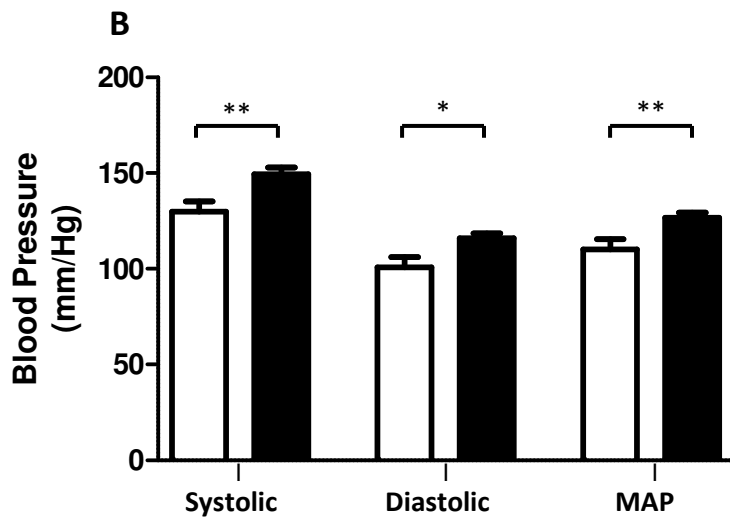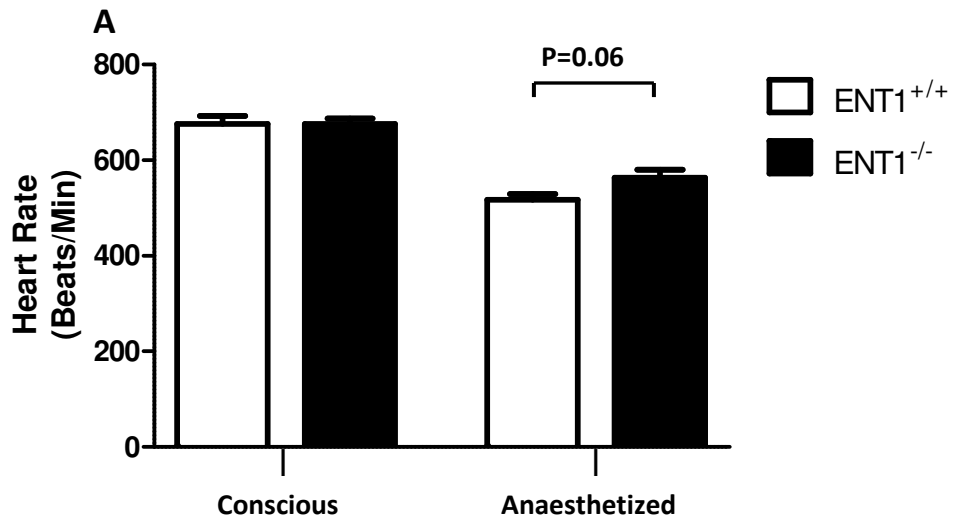
Figure 3.2. 3 – 4 month old mice were analyzed with a CODA-6 non-invasive tail-cuff machine as described previously in the methods. Heart rates of conscious and anaesthetized ENT1$^{+/+}$ and ENT1$^{-/-}$ mice were determined (Panel **A**). Systolic, Diastolic and Mean Arterial Pressure were determined for conscious mice (Panel **B**) and isoflurane anaesthetized mice (Panel **C**). Conscious mice were N=10 for ENT1$^{+/+}$ and N=10 for ENT1$^{-/-}$ and anaesthetized mice were N=5. *Significant difference for 3 – 4 month old mice blood pressure and heart rate studies. (Student's t test for unpaired experimental parameters,* P<0.05, **P<0.01)

3.3 Visualization of isolated tissues with Haematoxylin and Eosin staining.

Aortic and carotid tissues from 3 – 4 month old male ENT1$^{+/+}$ and ENT1$^{-/-}$ mice, stained with H&E did not appear significantly different from each other (Figure 3.3). The tissues were analyzed based on layers of elastin and nuclei organization within the arterial walls. ENT1$^{-/-}$ aortic (Panel **A**) and carotid (Panel **B**) vessel walls were comparable to the ENT1$^{+/+}$. Vasculature wall thickness (Figure 3.4, Panel **A**) and lumen circumference (Figure 3.4, Panel **B**) were also analyzed for morphological differences. The width of the aorta, measured in microns, was not significantly different in the ENT1$^{-/-}$ 28 ± 1 microns (N=6) when compared with the ENT1$^{+/+}$ counterparts of 30 ± 2 microns (N=6, $P<0.05$). Similarly the carotid arteries were not significantly different in width with ENT1$^{+/+}$ 18 ± 2 microns (N=4) and ENT1$^{-/-}$ 16 ± 2 microns (N=4, $P<0.05$). The lumen circumference of the aorta, measured in microns, was significantly different in the ENT1$^{-/-}$ 2064 ± 36 microns (N=6) when compared with the ENT1$^{+/+}$ counterparts of 2320 ± 71 microns (N=6, **$P<0.01$). The carotid arteries were not significantly different in circumference with ENT1$^{+/+}$ 1153 ± 19 microns (N=4) and ENT1$^{-/-}$ 1105 ± 51 microns (N=4, $P<0.05$). The decrease in lumen circumference was not expected however it does corroborate the findings of increased blood pressure.

3 Month ENT1$^{+/+}$ **3 Month ENT1$^{-/-}$**

A Thoracic Aorta
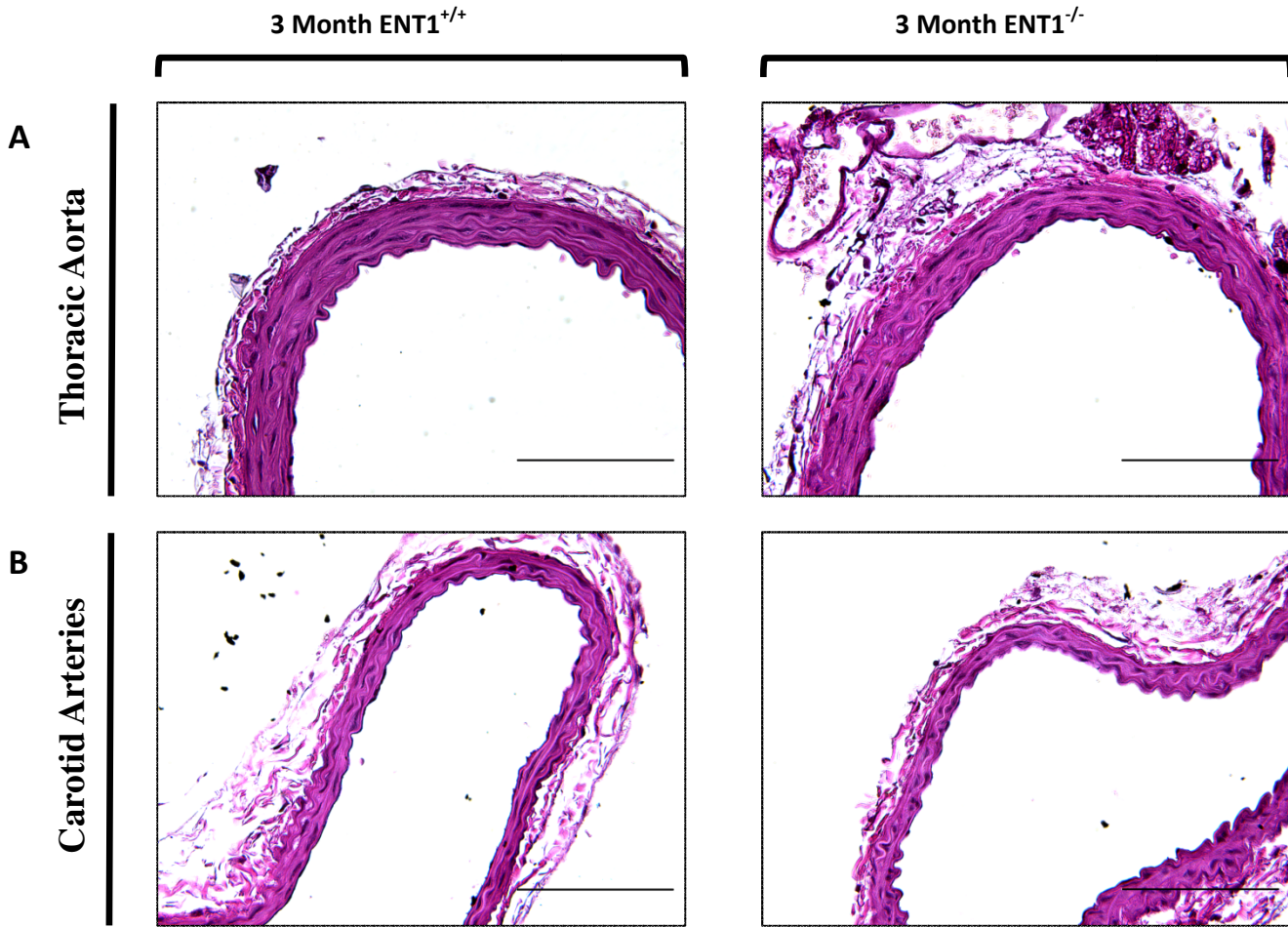
B Carotid Arteries

Figure 3.3. Histological appearance of thoracic aorta (Panel A), and carotid arteries (Panel B) in 3 – 4 month-old ENT1$^{+/+}$ and ENT1$^{-/-}$ mice. Layers of elastin as well as nuclei arrangement were analyzed. Samples were sectioned in the transverse plane and stained with haematoxylin and eosin (H&E). Images are representative of three animals of each genotype at 3 – 4 months of age. Scale bars represent 100 μm.
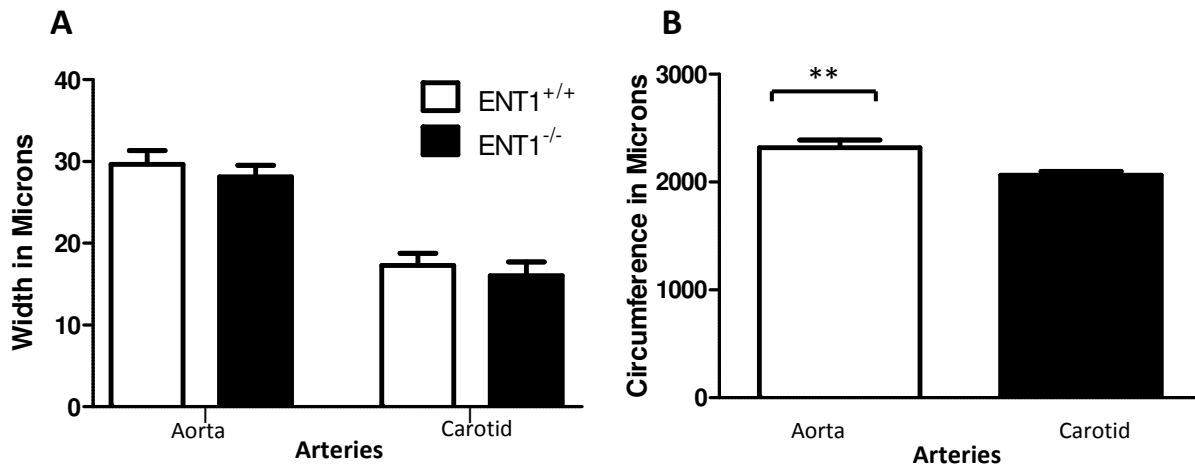
Figure 3.4. Measurement of ENT1$^{+/+}$ and ENT1$^{-/-}$ aortas and carotids looking at vascular wall thickness (Panel A) and lumen circumference (Panel B). Tissues were perfusion fixed with paraformaldehyde. Each point represents the mean ± SEM from six experiments in aortas and four experiments in carotids in ENT1$^{+/+}$ and ENT1$^{-/-}$ mice. *Significant difference between circumference of ENT1$^{+/+}$ and ENT1$^{-/-}$. (Student's t test for unpaired experimental parameters, **P<0.01)

3.4 Visualization of isolated tissues with Alizarin Red counterstained with Haematoxylin

Aortic ring slices from 3 – 4 month old male mice, stained with Alizarin Red and counterstained with Haematoxylin, did not appear significantly different from each other (Figure 3.5). ENT1$^{+/+}$ and ENT1$^{-/-}$ thoracic aorta (Panel **A**) were analyzed for calcification of the tissues to determine whether the mineralization phenotype previously described in Warraich *et al.* (2012) would not have an effect on vascular studies to be carried out in mouse line [32]. Positive and negative controls were used to ensure consistency of staining method (Panel **B**). Positive control shows bone from a post-natal mouse at day zero of development and negative control is a mouse heart at 3 – 4 months of age. The positive control has large areas of red which is the anthraquinone dye reacting with the calcium cations to form a chelate. The negative control, mouse heart, has very small amounts of red indicating lower levels of calcium. The areas of interest had no apparent calcium rich areas and a positive signal was not visualized.

A Thoracic Aorta

ENT1$^{+/+}$

ENT1$^{-/-}$

B Control

Positive Control
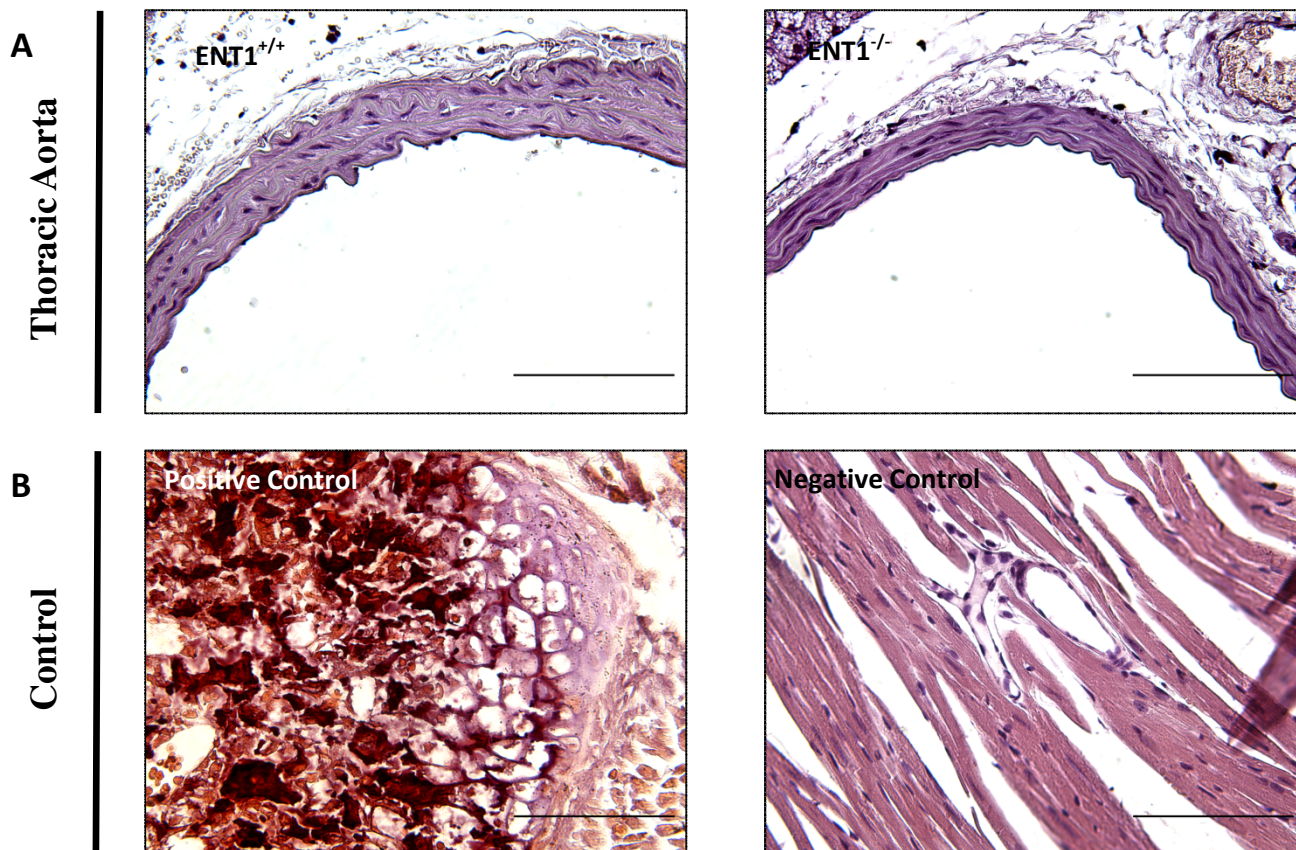
Negative Control

Figure 3.5. Histological appearance of thoracic aorta (Panel A), and positive and negative controls (Panel B). Positive control is bone from a post-natal day zero mouse and the remainer are 3 – 4 month old mice. Layers of elastin as well as nuclei arrangement. Samples were sectioned in the transverse plane and stained with alizarin red and counterstained with alizarin red and counterstained with haematoxylin. Images are representative of three animals of each genotype at 3 – 4 months of age. Scale bars represent 100 µm.

3.5 Aortic vascular wall is stiffer in ENT1$^{-/-}$ than ENT1$^{+/+}$

Length-tension curves were carried out in which 3 – 4 month old male mice vessels were stretched at intervals of 50 microns. There was a significant difference between ENT1$^{+/+}$ and ENT1$^{-/-}$ mice in which the length-tension curves of ENT1$^{-/-}$ aortas are increased (Figure 3.6, Panel **A**, *$P<0.05$). No significant difference was seen in the ENT1$^{-/-}$ and ENT1$^{+/+}$ carotid arteries (Figure 3.6, Panel **B**, $P<0.05$). The increase in vessel stiffness within the aorta was not expected but is consistent with the increased blood pressure observed in the conscious ENT1$^{-/-}$.
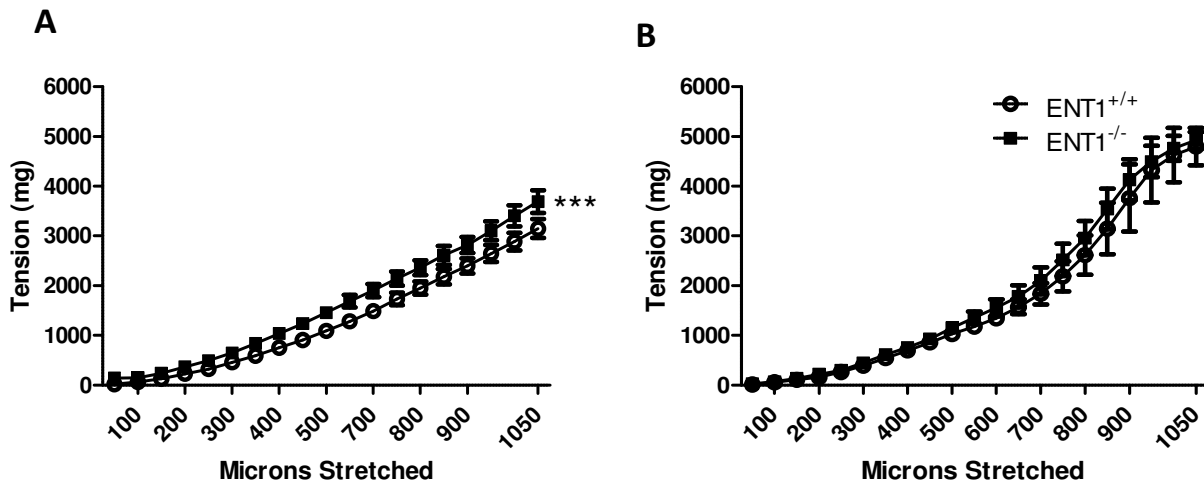
Figure 3.6. Length-Tension curves of ENT1$^{+/+}$ and ENT1$^{-/-}$ aorta (Panel A) and carotid arteries (Panel B). The effect of stretching vascular tissue in intervals of 50 microns on the tension generated in 3 – 4 month old mice. Tissues were incubated for 30 minutes at 22˚C in KPSS buffer with no resting tension. Each point represents the mean ± SEM from seven experiments on aortas (Panel **A**) and three experiments on carotid arteries (Panel **B**) in ENT1$^{+/+}$ and ENT1$^{-/-}$ mice. *Significant difference between microns stretched and resultant tension in ENT1$^{+/+}$ and ENT1$^{-/-}$ aorta. (Two-Way ANOVA for unpaired experimental parameters, ***$P<0.001$)

3.6 Potassium Chloride induced depolarization resulted in significantly greater generated tension in ENT1$^{-/-}$ vascular tissues

A number of vasoconstrictors were tested to determine if there were any tissue receptor specific differences or increased sensitivities in the aortas and carotid arteries between genotypes. Initial viability tests were done using 100 mM of KCl tested aortic rings at applied resting tensions of 500 mg, 750 mg and 1000 mg, and carotid arteries were tested at 500 mg of tension (Figure 3.7). In this model, when vascular rings were exposed to 100 mM KCl, a generated contraction of more than 200 mg was considered viable.

The KCl induced depolarization was significantly higher in both the aortas and carotids of ENT1$^{-/-}$ mice. The aortas of 3 – 4 month old ENT1$^{-/-}$ mice resulted in vasoconstriction significantly more at 500 mg and 750 mg of resting tension, and were trending towards significance at 1000 mg of resting tension (P=0.062). The KCl-mediated vasoconstriction was significantly higher in the ENT1$^{-/-}$ mice at 750 mg and 1000 mg resting tension, and trending towards significance at 500 mg resting tension for the mice at 6 months of age (P=0.067). Vasoconstriction in the carotid arteries showed the same trend with increased tissue depolarization and greater generated contraction in the ENT1$^{-/-}$ mice (P<0.01). Increased tissue depolarization as a result of KCl is an entirely novel finding and was completely unexpected.

To replicate the conditions seen in the ENT1$^{-/-}$ mice in the ENT1$^{+/+}$ mice, aortic rings were incubated in 1 μM of NBMPR (the high affinity selective inhibitor of ENT1) following which 100 mM KCl was applied. As previously described, the control KCl treatment produced significantly greater vasoconstriction in ENT1$^{-/-}$ tissue than compared to the ENT1$^{+/+}$ counterparts (P<0.05) but when incubated with NBMPR the ENT1$^{+/+}$ tissues level of

depolarization remained consistent between control and experimental parameters whereas the

ENT1$^{-/-}$ tissue trended (P=0.059) towards a large decrease in vasoconstriction (Figure 3.8). The

contraction between ENT1$^{-/-}$ control and NBMPR test groups was not significant, neither was the

difference between ENT1$^{+/+}$ and ENT1$^{-/-}$ NBMPR treatment groups. We had expected to mimic

the ENT1$^{-/-}$ response by inhibiting ENT1 with NBMPR, thus the change in ENT1$^{-/-}$ response in

the presence of NBMPR was not expected.
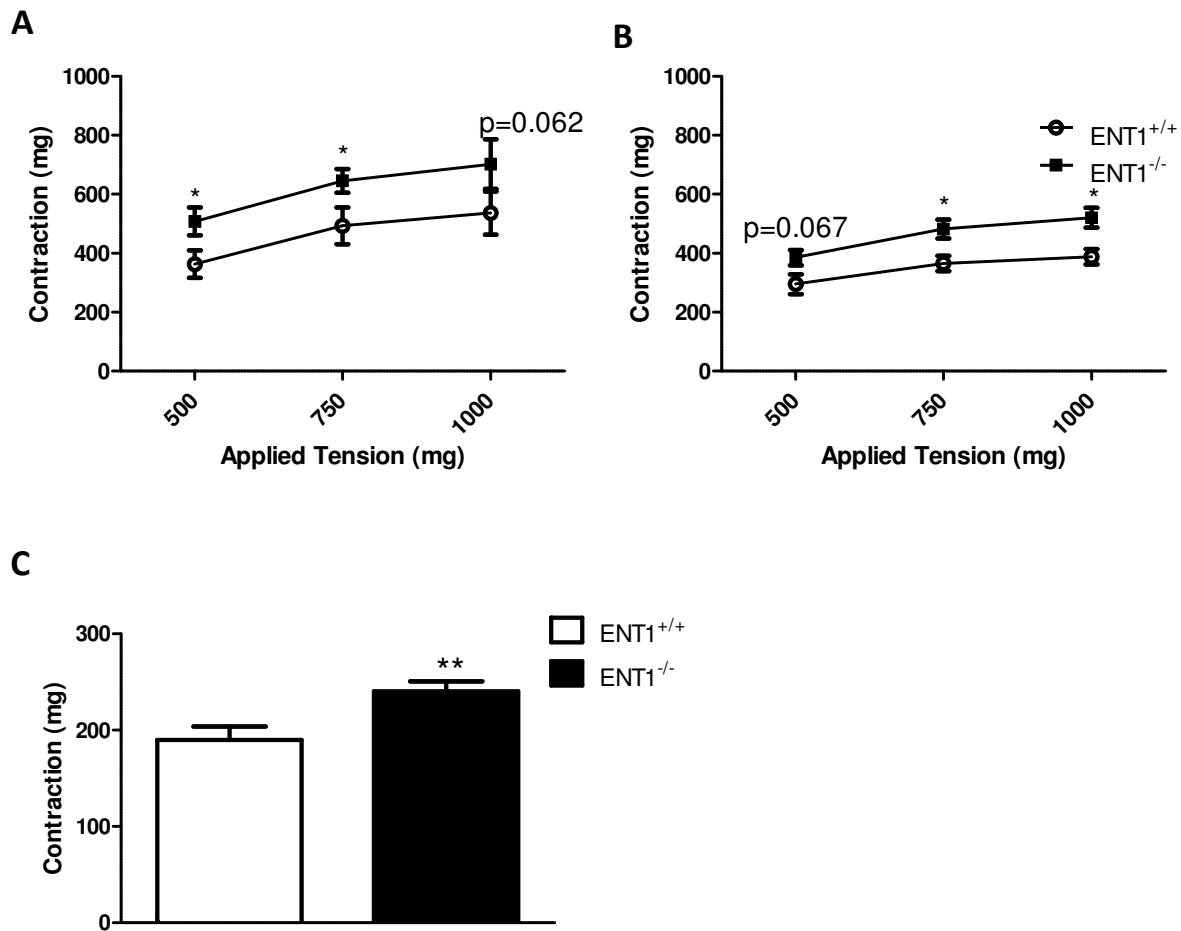
Figure 3.7. Treatment of ENT1$^{+/+}$ and ENT1$^{-/-}$ aortas and carotids with KCl. Effects of KCl on contraction by tissue depolarization in 3 – 4 month old mice (Panel **A** and Panel **C**) and 6 month old mice (Panel **B**). Tissues were incubated for 30 minutes at 37°C in KPSS buffer at resting tensions of 500 mg, 750 mg and 1000 mg. Following equilibration period, 100 mM KCl was administered to assess tissue viability. Each point represents the mean ± SEM from six experiments (Panel **A**), five experiments (Panel **B**) and 7 ENT1$^{+/+}$ and 11 ENT1$^{-/-}$ (Panel **C**). *Significant difference in both age groups for KCl studies. (Student's t test for paired experimental parameters,* $P < 0.05$, **$P < 0.01$)
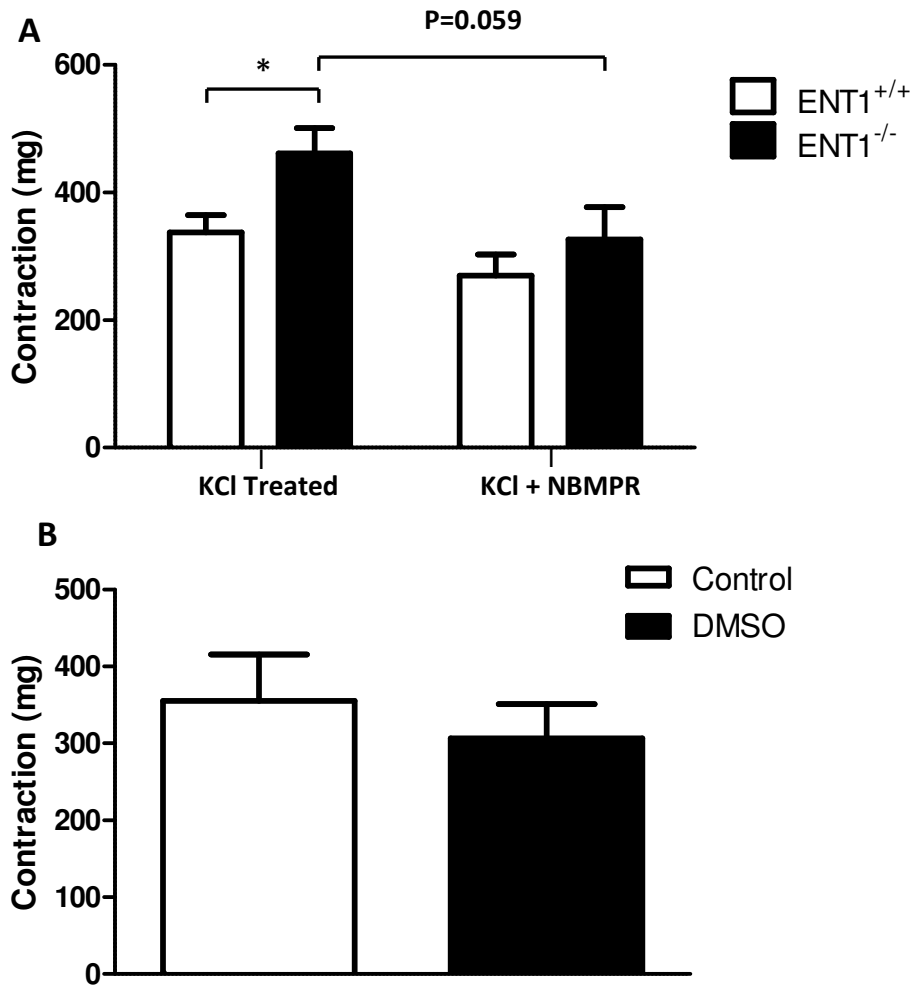
Figure 3.8. KCl and NBMPR treatment of ENT1$^{+/+}$ and ENT1$^{-/-}$ aortas. Effects of KCl on contraction by tissue depolarization in 3 – 4 month old mice and the effects of KCl (100 mM) on contraction when in the presence of: ENT1 blocker NBMPR (Panel **A**) or DMSO (Panel **B**). Tissues were incubated for 30 minutes at 37°C in KPSS buffer at resting tensions of 500mg. Each point represents the mean ± SEM from seven experiments (KCl treated) and six experiments (KCl + NBMPR) in ENT1$^{+/+}$ and ENT1$^{-/-}$ mice. *Significant difference between KCl ENT1$^{+/+}$ and ENT1$^{-/-}$. ENT1$^{+/+}$ aortas were tested with DMSO (N=4) only to ensure the DMSO had no effect on the tissues. No significant difference was seen between the control and DMSO experimental group. (Student's t test for paired experimental parameters, *P<0.05)

Receptor-mediated vasoconstrictors phenylephrine, PGF2α and serotonin were applied to aortic rings at resting tensions of 500 mg. In addition, the aorta was tested with 750 mg and 1000 mg of resting tension with phenylephrine and the carotid arteries were tested with phenylephrine at resting tensions of 500 mg. The purpose of testing multiple vasoconstrictors was to establish a baseline receptor mediated contraction that could be compared across all future experiments. Establishment of the vasoconstrictor was essential to carry out the hypoxia experiments outlined in the objectives. All tests were carried out in 3 – 4 month old mice. Initial vasoconstriction testing with PGF2α (Figure 3.9, Panel **A**), serotonin (Figure 3.9, Panel **B**) and phenylephrine (Figure 3.9, Panel **C**) yielded no significant differences between the $ENT1^{+/+}$ and $ENT1^{-/-}$ mice with serotonin EC_{50}s $6.37x10^{-7}$ for $ENT1^{+/+}$ and $5.80x10^{-7}$ for $ENT1^{-/-}$, and phenylephrine EC_{50}s $9.07x10^{-8}$ for $ENT1^{+/+}$ and $5.70x10^{-8}$ for $ENT1^{-/-}$. A V_{max} was not obtained for PGF2α therefore an EC_{50} could not be calculated. No significant difference was seen in the phenylephrine dose-response on the carotid arteries (Figure 3.9, Panel **D**), with EC_{50} of $1.08x10^{-7}$ for $ENT1^{+/+}$ and $1.51x10^{-7}$ for $ENT1^{-/-}$. The phenylephrine dose-response curves appeared to be trending towards a significant difference. To tease apart the results, a phenylephrine dose-response was carried out at 1000 mg of resting tension (Figure 3.10) and analyzed using a Two-Way ANOVA. Phenylephrine dose-response while at 1000 mg of resting tension yielded an EC_{50} of $5.67x10^{-8}$ in the $ENT1^{+/+}$ and $1.49x10^{-8}$ in the $ENT1^{-/-}$ mouse. No significant difference was seen between the $ENT1^{+/+}$ and $ENT1^{-/-}$ (N=3, P<0.05). The lack of significant differences between experimental groups is what was expected.
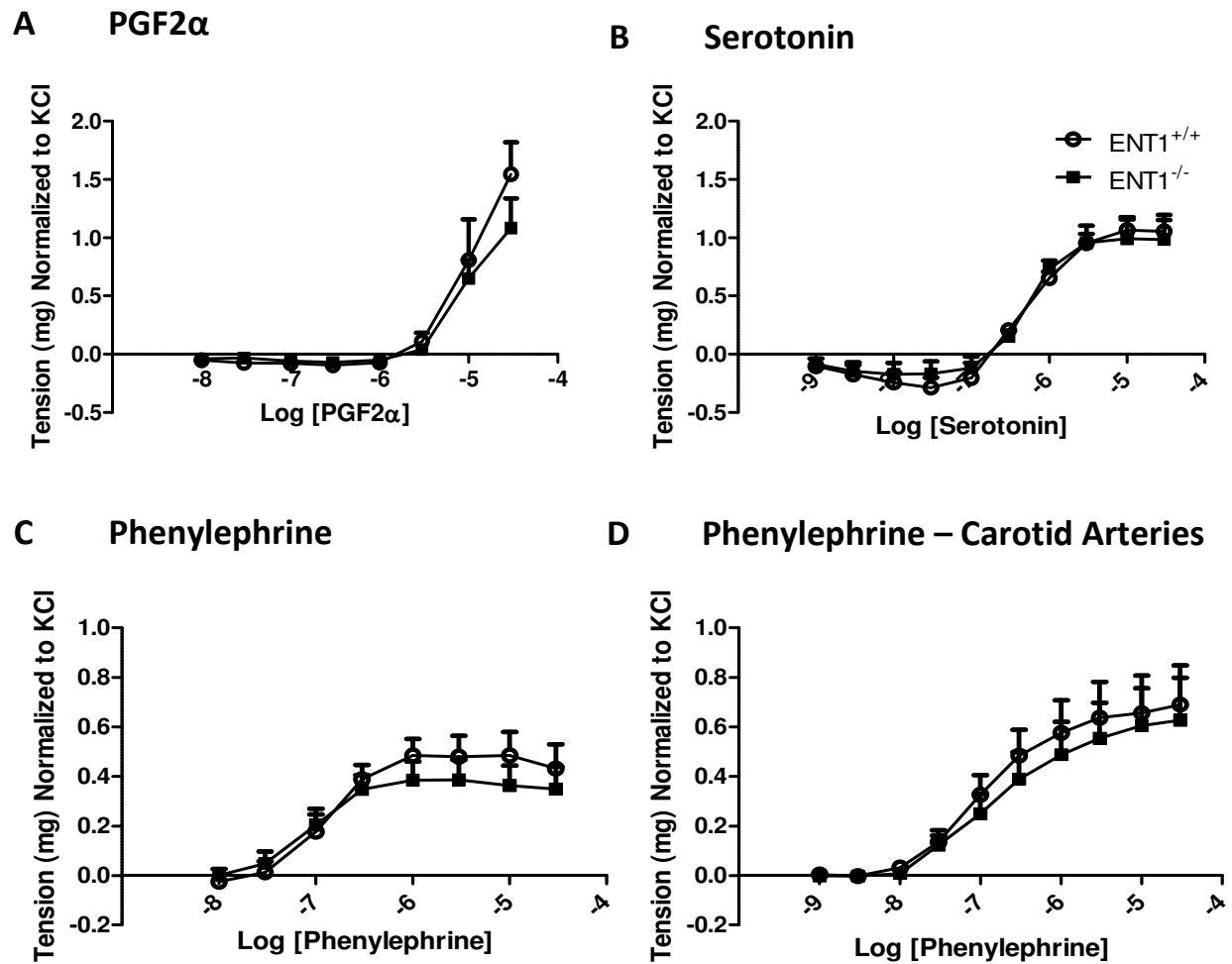
Figure 3.9. Dose-Response curves of ENT1$^{+/+}$ and ENT1$^{-/-}$ aortas (Panels A, B and C) and carotid arteries (Panel D). Effects of PGF2α (Panel **A**), Serotonin (Panel **B**) and Phenylephrine (Panel **C** and **D**) on receptor mediated contraction in 3 – 4 month old mice. Tissues were incubated for 30 minutes at 37˚C in KPSS buffer at resting tensions of 500 mg after which they were depolarized with 100 mM KCl. Each point represents the mean ± SEM from five experiments (Panel **A**), three experiments (Panel **B**), six experiments (Panel **C**) and six experiments (Panel **D**) in ENT1$^{+/+}$ and ENT1$^{-/-}$ mice. No significant difference between ENT1$^{+/+}$ and ENT1$^{-/-}$. (Two-Way ANOVA for paired experimental parameters, P<0.05)
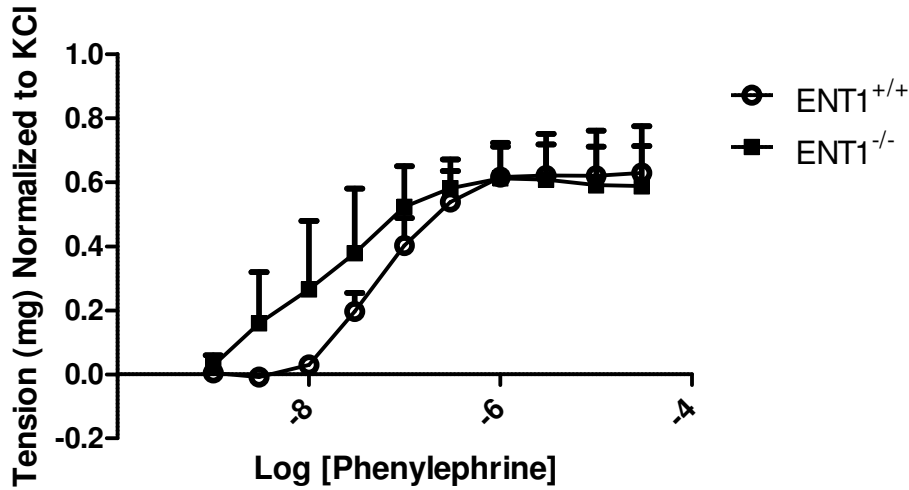
Figure 3.10. Dose-Response curve of ENT1^{+/+} and ENT1^{-/-} aortas with 1000mg of resting tension applied. Phenylephrine on receptor mediated contraction in 3 – 4 month old mice. Tissues were incubated for 30 minutes at 37˚C in KPSS buffer at resting tensions of 1000mg after which they were depolarized with 100 mM KCl. Each point represents the mean ± SEM from three experiments in ENT1^{+/+} and ENT1^{-/-} mice. *No significant difference between ENT1^{+/+} and ENT1^{-/-}. (Two-Way ANOVA for unpaired experimental parameters, $P<0.05$)

3.7 ENT1$^{-/-}$ mice had variable response to hypoxic conditions when compared to ENT1$^{+/+}$

In accordance with the outlined objectives, the ENT1$^{-/-}$ vasculature was compared to the ENT1$^{+/+}$ under hypoxic conditions. Phenylephrine was applied to aortic rings at resting tensions of 500 mg (Figure 3.11). All tests were carried out in 3 – 4 month old mice. The mice were compared between genotypes under various conditions. As previously stated, under control conditions the phenylephrine dose-response yielded an EC$_{50}$ of 9.07×10^{-8} (SEM=2.28×10^{-8}) in the ENT1$^{+/+}$ and EC$_{50}$ of 5.70×10^{-8} (SEM=2.13×10^{-8}) in the ENT1$^{-/-}$ mouse. Under hypoxia with no other experimental conditions, the EC$_{50}$ was 7.97×10^{-8} (SEM=3.68×10^{-8}) in the ENT1$^{-/-}$ and EC$_{50}$ was 6.13×10^{-8} (SEM=1.97×10^{-8}) in the ENT1$^{+/+}$ mouse (Figure 3.11 Panel **A** and Table 3.1). Treatment with adenosine at concentrations 10 μM, 30 μM, 100 μM and 300 μM, yielded EC$_{50}$s of 1.41×10^{-8} (SEM=1.88×10^{-8}), 3.62×10^{-8} (SEM=5.83×10^{-5}), 3.53×10^{-8} (SEM=2.35×10^{-8}), 7.19×10^{-8} (SEM=2.91×10^{-8}), respectively in the ENT1$^{+/+}$ mice. These treatments were used as controls for the adenosine treated hypoxia experiments.

Treatment with adenosine prior to hypoxia was carried out in both ENT1$^{+/+}$ and ENT1$^{-/-}$ mice. All treatments were followed with a 30 minute normoxic period then a phenylephrine dose response. Ten μM concentrations of adenosine yielded EC$_{50}$ values of 6.16×10^{-8} (SEM=8.30×10^{-8}) in the ENT1$^{+/+}$ and 1.89×10^{-8} (SEM=9.80×10^{-9}) in the ENT1$^{-/-}$. At 30 μM, ENT1$^{+/+}$ and ENT1$^{-/-}$ yielded EC$_{50}$ values of 1.17×10^{-7} (SEM=5.05×10^{-8}) and 5.82×10^{-8} (SEM=2.68×10^{-8}), respectively. One hundred μM and 300 μM concentrations of adenosine yielded EC$_{50}$ values of 7.38×10^{-8} (SEM=2.39×10^{-8}) and 1.16×10^{-7} (SEM=3.08×10^{-8}) in the ENT1$^{+/+}$ and 6.05×10^{-8} (SEM=5.29×10^{-8}) and 7.38×10^{-9} (SEM=1.21×10^{-8}) in the ENT1$^{-/-}$ respectively. The ENT1$^{-/-}$ aortic tissue had significantly less vasoreactivity at all concentrations of adenosine except for 100 μM. A significant difference was seen between the pretreatment with 30 μM (*$P<0.05$), 100 μM (*$P<0.05$) and 300 μM (***$P<0.001$) on ENT1$^{+/+}$ and the pretreatment followed by hypoxia

ENT1$^{+/+}$. The 100 μM concentration resulted in significantly smaller generated tension than the adenosine control whereas the 30 μM and 300 μM concentrations resulted in significantly more contraction in response to phenylephrine. Treatment with ENT1 blocker NBMPR prior to hypoxia yielded an EC$_{50}$ of 1.72x10^{-8} (SEM=1.33x10^{-8}) and treatment with NBMPR followed by 300 μM adenosine and subsequently hypoxia, yielded an EC$_{50}$ of 3.10x10^{-8} (SEM=9.14x10^{-9}) within the ENT1$^{+/+}$. Treatment with ENT1 blocker NBMPR prior to hypoxia on the ENT1$^{-/-}$ aortic tissue yielded an EC$_{50}$ of 1.39x10^{-8} (SEM=9.30x10^{-8}). The NBMPR alone compared to adenosine plus NBMPR resulted in a significantly lower dose-response (***$P<0.001$) in the ENT1$^{+/+}$. Between genotypes, the ENT1$^{-/-}$ also generated diminished contraction when compared to the ENT1$^{+/+}$ (**$P<0.01$). The diminished response in the ENT1$^{-/-}$ was not expected as previous evidence has shown ENT1$^{-/-}$ mice to be cardioprotected.

Table 3.1. **Phenylephrine Dose-Response EC_{50}s of ENT1$^{+/+}$ and ENT1$^{-/-}$ aortas under different experimental conditions.** Effects of an hour of hypoxia on aortic tissue after pre-treatment with increasing doses of Adenosine (10 – 300 μM) and NBMPR (1 μM), on phenylephrine induced contraction (1 nM – 30 μM).

Treatment	Genotype	EC_{50}	SEM	T_{max} (%)
Control	+/+	9.07×10^{-8}	2.28×10^{-8}	49.0
	-/-	5.70×10^{-8}	2.13×10^{-8}	38.4
Hypoxia	+/+	6.13×10^{-8}	1.97×10^{-8}	43.9
	-/-	$7.97 \times 10^{-8}**$	3.68×10^{-8}	32.5
Control + 10 μM Adenosine	+/+	1.41×10^{-8}	1.88×10^{-8}	39.6
Control + 30 μM Adenosine	+/+	3.62×10^{-8}	5.83×10^{-5}	31.2
Control + 100 μM Adenosine	+/+	3.53×10^{-8}	2.35×10^{-8}	41.1
Control + 300 μM Adenosine	+/+	7.19×10^{-8}	2.91×10^{-8}	45.6
10 μM Adenosine + Hypoxia	+/+	6.16×10^{-8}	8.30×10^{-8}	49.9
	-/-	$1.89 \times 10^{-8}***$	9.80×10^{-9}	27.7
30 μM Adenosine + Hypoxia	+/+	$1.17 \times 10^{-7}*$	5.05×10^{-8}	61.2
	-/-	$5.82 \times 10^{-8}**$	2.68×10^{-8}	40.2
100 μM Adenosine + Hypoxia	+/+	$7.38 \times 10^{-8}*$	2.39×10^{-8}	36.4
	-/-	6.05×10^{-8}	5.29×10^{-8}	43.7
300 μM Adenosine + Hypoxia	+/+	$1.16 \times 10^{-7}***$	3.08×10^{-8}	65.8
	-/-	$7.38 \times 10^{-9}**$	1.21×10^{-8}	20.4
NBMPR + Hypoxia	+/+	$1.72 \times 10^{-8}***$	1.33×10^{-8}	44.3
	-/-	$1.39 \times 10^{-8}**$	9.30×10^{-8}	29.6
NBMPR + 300 μM Adenosine + Hypoxia	+/+	3.10×10^{-8}	9.14×10^{-9}	67.7

*T_{max}(%) = maximum tension developed, expressed as a percentage of the pretreatment of 100 mM KCl. Values are a mean ± SEM of N=6 for control, N=6 for hypoxia, N=3 for 10 μM, 100 μM and 300 μM Adenosine controls (30 μM Adenosine with Control is only N=2), N=4 for 10 μM, 30 μM, 100 μM and 300 μM Adenosine in Hypoxia, N= 4 for NBMPR in hypoxia and N=4 for NBMPR + 300 μM Adenosine in hypoxia. Note: (*) indicates significance between treatments within the ENT1$^{+/+}$ genotype. (Two-Way ANOVA for unpaired experimental parameters, *$P<0.05$, **$P<0.01$, ***$P<0.001$).

A

Control ENT1$^{+/+}$
Control ENT1$^{-/-}$
Hypoxia ENT1$^{+/+}$
Hypoxia ENT1$^{-/-}$

B

Control 10 μM Adenosine ENT1$^{+/+}$
Hypoxia 10 μM ENT1$^{+/+}$
Hypoxia 10 μM ENT1$^{-/-}$

C

Control 30 μM Adenosine ENT1$^{+/+}$
Hypoxia 30 μM Adenosine ENT1$^{+/+}$
Hypoxia 30 μM Adenosine ENT1$^{-/-}$

D

Control 100 μM Adenosine ENT1$^{+/+}$
Hypoxia 100 μM Adenosine ENT1$^{+/+}$
Hypoxia 100 μM Adenosine ENT1$^{-/-}$

E

F
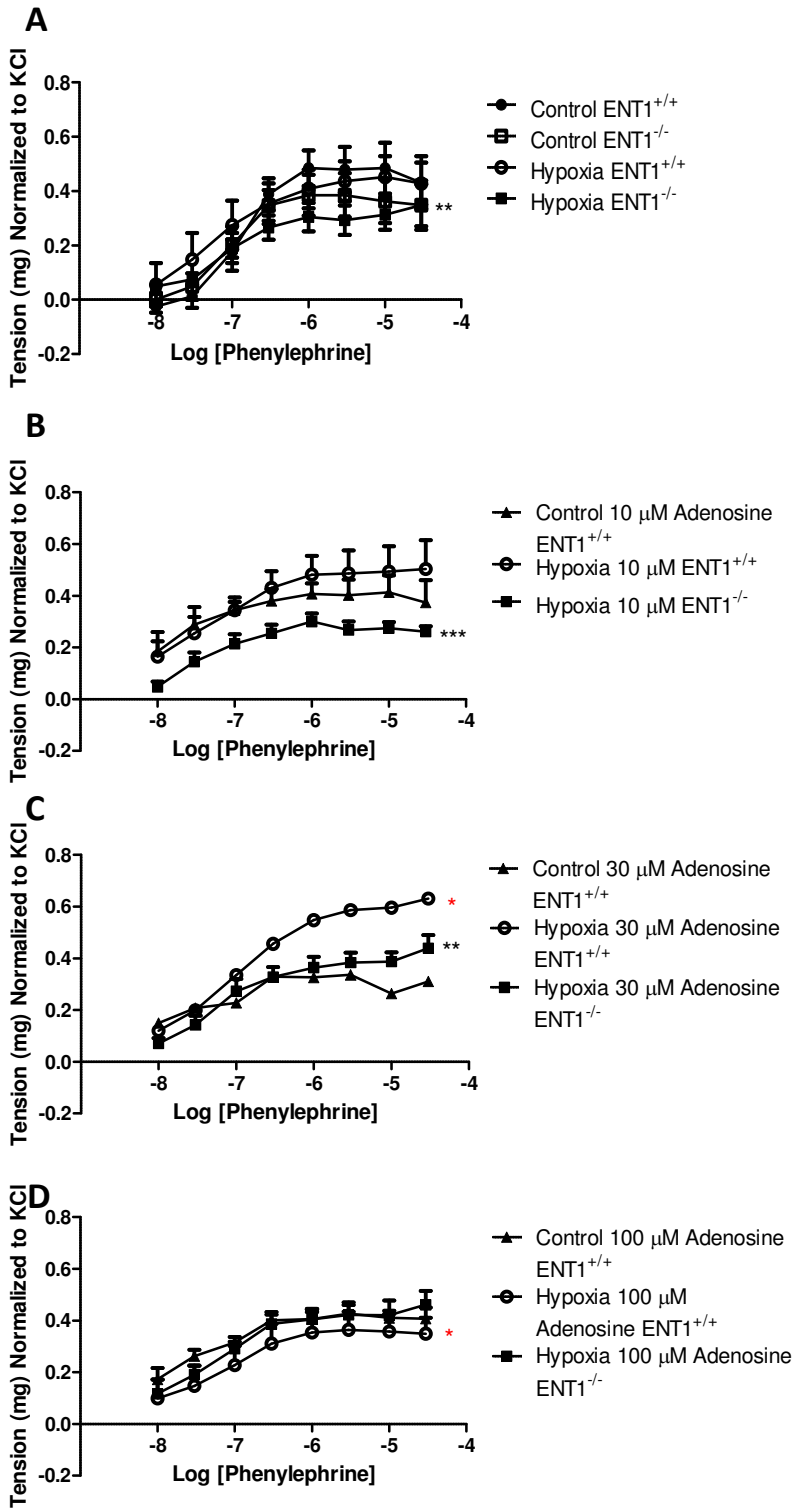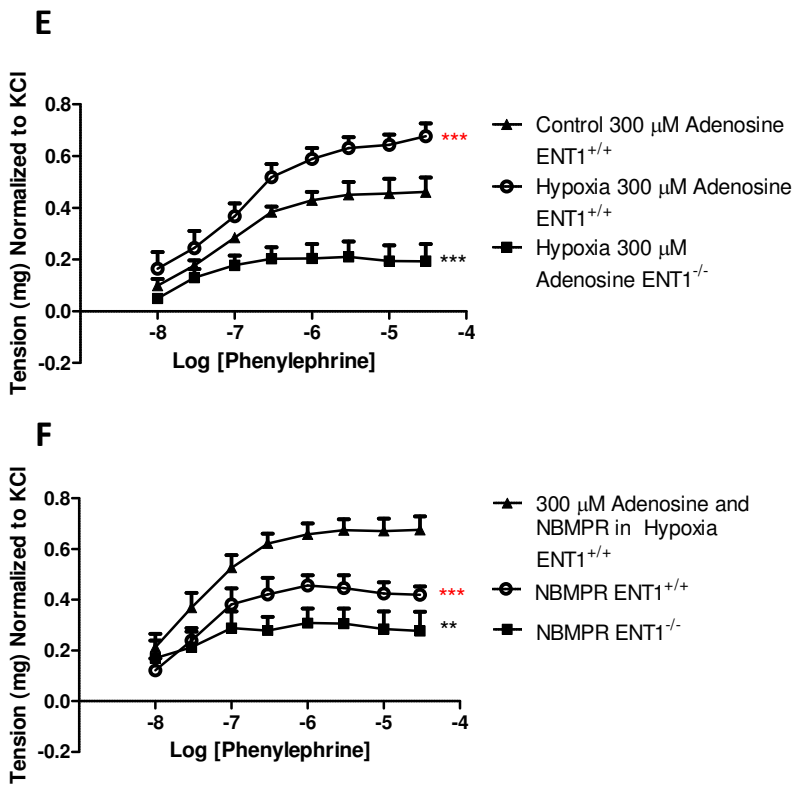
Figure 3.11. Phenylephrine Dose-Response Curves following Hypoxia. Normoxia vs. Hypoxia (Panel **A**), 10 μM adenosine experiments (Panel **B**), 30 μM adenosine experiments (Panel **C**), 100 μM adenosine experiments (Panel **D**), 300 μM adenosine experiments (Panel **E**), NBMPR with and without 300 μM adenosine experiments (Panel **F**). Tissues were incubated for 30 minutes at 37˚C in KPSS buffer at resting tensions of 500 mg after which they were depolarized with 100 mM KCl. Hypoxic conditions were introduced to the organ bath on all experimental groups except for control and lasted 60 minutes. In treatment groups with Adenosine, treatment was administered 30 minutes before hypoxic period. Groups treated with NBMPR were administered 15 minutes prior to either adenosine treatment or hypoxia. Each point represents the mean ± SEM with N=6 for control, N=6 for hypoxia, N=4 for 10 μM, 30 μM, 100 μM and 300 μM Adenosine in Hypoxia, N= 4 for NBMPR in hypoxia and N=4 for NBMPR + 300 μM Adenosine in hypoxia.*Significant difference between genotypes. Note: (*) indicates significance between treatments within the ENT1$^{+/+}$ genotype. (Two-Way ANOVA for unpaired experimental parameters, *P<0.05, **P<0.01, ***P<0.001).

PGF2α was then used to test whether there was a release of adenosine from the aorta and carotid arteries during the hypoxic event allowing us to examine the vascular tissue as it responded to hypoxic conditions (Figure 3.13) . The ENT1$^{+/+}$ and ENT1$^{-/-}$ vessels were vasoconstricted within PGF2α at 80% maximal and allowed to plateau. Tissues were then exposed to one hour of hypoxia. The initial plateau period prior to hypoxia was then compared to the final generated contraction. The aortas measured a contraction of 99.4 ± 20.8 mg in the ENT1$^{+/+}$ and 115.2 ± 9.8 mg in the ENT1$^{-/-}$(N=6).The carotid arteries measured a contraction of 110.2 ± 18.2 mg in the ENT1$^{+/+}$ and 75.1 ± 12.1 mg in the ENT1$^{-/-}$(N=5). Neither the aortas (Figure 3.13, Panel **A**) nor the carotids (Figure 3.13, Panel **B**) had significantly different levels of vasodilation following the hypoxic challenge (P<0.05).
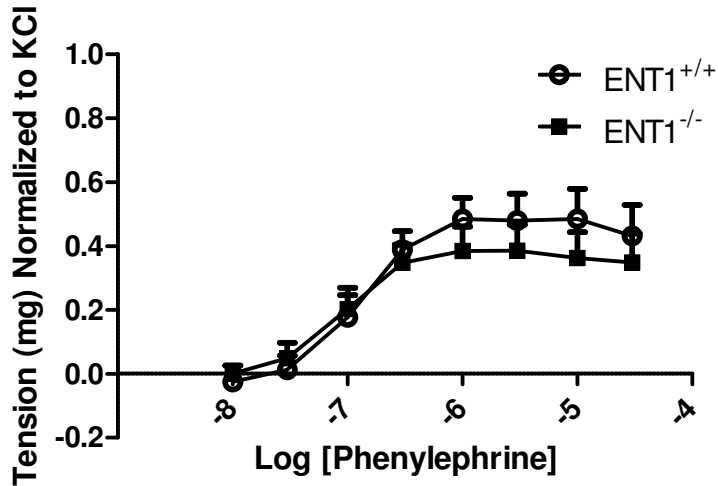
Figure 3.12. Phenylephrine Dose-Response Curves of ENT1^{+/+} and ENT1^{-/-} in carotid arteries under hypoxic conditions. Tissues were incubated for 30 minutes at 37˚C in KPSS buffer at resting tensions of 500mg after which they were depolarized with 100mM KCl. Hypoxic conditions were introduced to the organ bath and lasted 60 minutes. Afterwards, tissues were then incubated in normoxic conditions for 30 minutes followed by a phenylephrine dose-response. Each point represents the mean ± SEM with N=6. No Significant difference between treatment groups. (Two-Way ANOVA for unpaired experimental parameters, *P<0.05)
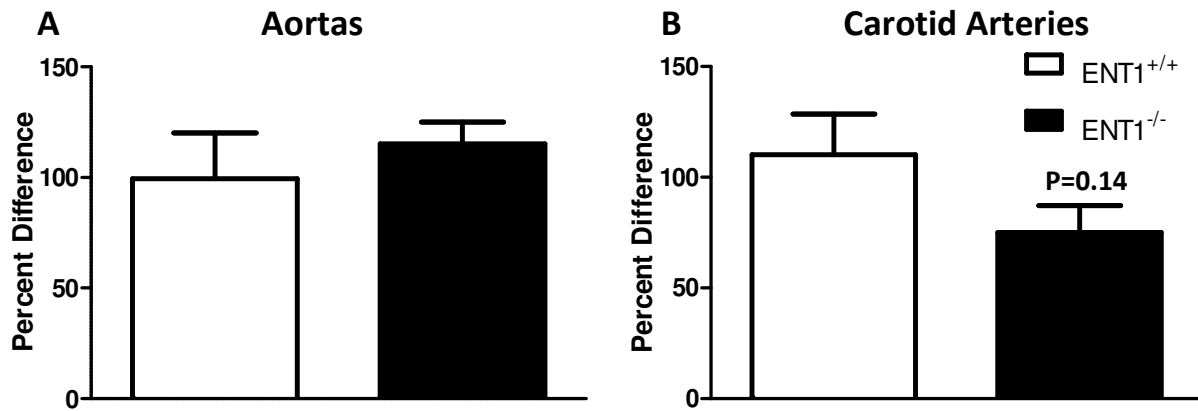
Figure 3.13. Hypoxia induced vasodilation in ENT1$^{+/+}$ and ENT1$^{-/-}$ aortas (Panel A) and carotid arteries (Panel B) after preconstriction with 80% of maximum PGF2α. Tissues were incubated for 30 minutes at 37°C in KPSS buffer at resting tensions of 500 mg after which they were depolarized with 100 mM KCl to test for viability. Results were then normalized to PGF2α and converted to a percentage. Each point represents the mean ± SEM from six experiments (Panel **A**) and five experiments (Panel **B**). (Student's t test for unpaired experimental parameters, *P<0.05)

3.8 Vasodilatory effects variable between ENT1$^{+/+}$ and ENT1$^{-/-}$ mice

Three – four month old male mice were compared between genotypes to identify the effects seen between the ENT1$^{+/+}$ and ENT1$^{-/-}$ when adenosine is applied in increasing concentrations alone and in the presence of the A$_{2A}$ blocker SCH58261. The vasodilation measured in the aorta during the experiments with only adenosine (Figure 3.14, Panel **A**) showed a significantly greater response in the ENT1$^{-/-}$ (***$P<0.001$, N=5) when compared to the ENT1$^{+/+}$ vessel. The carotid arteries did not however show any significant difference in vasodilation between genotypes (N=5, Figure 3.8, Panel **B**). Ten µM methacholine was used to ensure the endothelium was still intact. No significant difference was seen between ENT1$^{+/+}$ and ENT1$^{-/-}$ in either aorta or carotid arteries (Figure 3.14, Panel **C**) ($P<0.05$). The A$_{2A}$ blocker SCH58261 also yielded no significant difference between the ENT1$^{+/+}$ and ENT1$^{-/-}$ 3 – 4 month old mice in either the aortas (N=15, Figure 3.10, Panel **A**) and carotid arteries (N=4, Figure 3.15, Panel **B**). The resultant increase in adenosine vasodilation in the absence of SCH58261 was what was expected with the loss of ENT1.
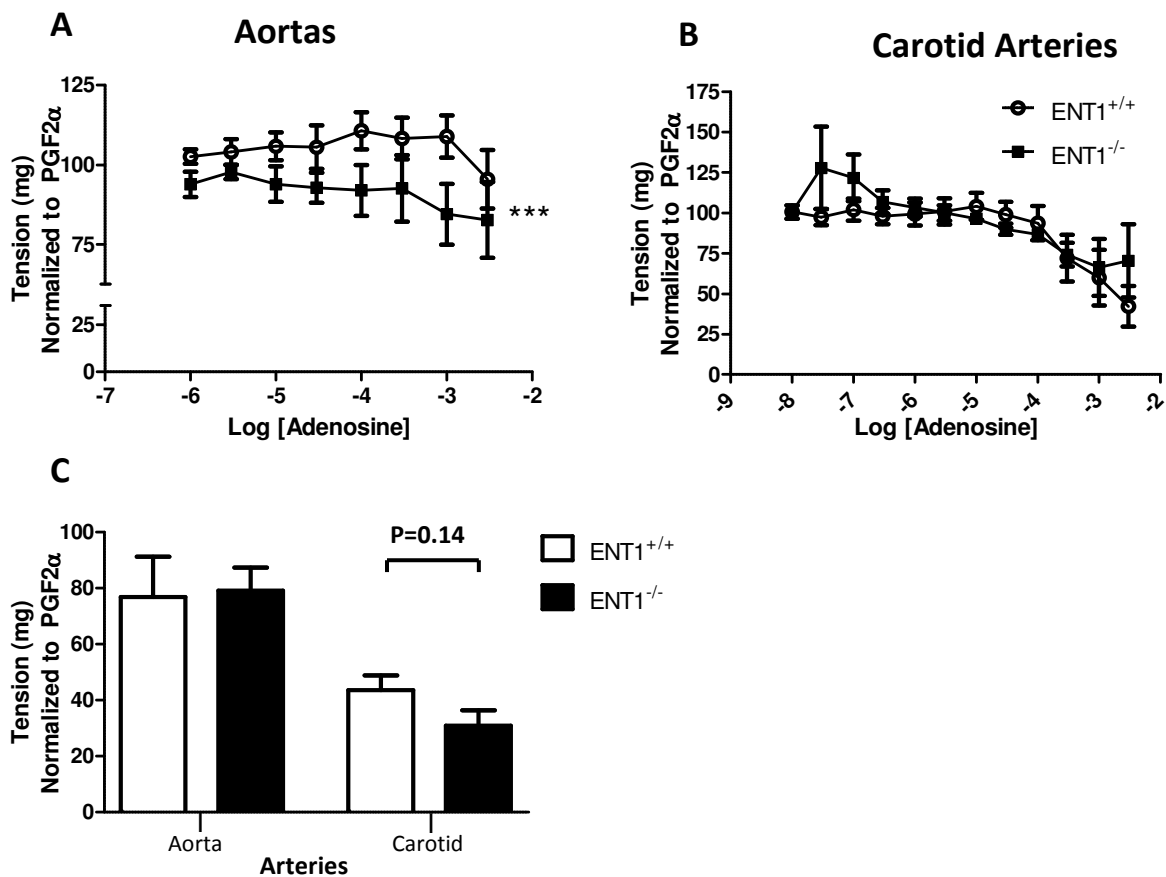
Figure 3.14. Dose-Response of adenosine in ENT1^{+/+} and ENT1^{-/-} aortas (Panel A) and carotid arteries (Panel B) analyzing vasodilatory effects after preconstriction with 80% of maximum PGF2α. Presence of endothelium was established via a 10 μM methacholine dose in ENT1^{+/+} and ENT1^{-/-} aortas and carotid arteries (Panel **C**) after preconstriction with 80% of maximum PGF2α. Tissues were incubated for 30 minutes at 37°C in KPSS buffer at resting tensions of 500 mg after which they were depolarized with 100 mM KCl to test for viability. Results were then normalized to PGF2α and converted to a percentage. Each point represents the mean ± SEM from five experiments Panel **A** and **B** are six experiments in arotas, five experiments in ENT1^{+/+} and four experiments in ENT1^{-/-} carotid arteries (Panel **C**). *Significant difference between vasodilation of ENT1^{+/+} and ENT1^{-/-} aortas. (Student's t-test for unpaired experimental parameters, Two-Way ANOVA for unpaired experimental parameters, ***P<0.001)
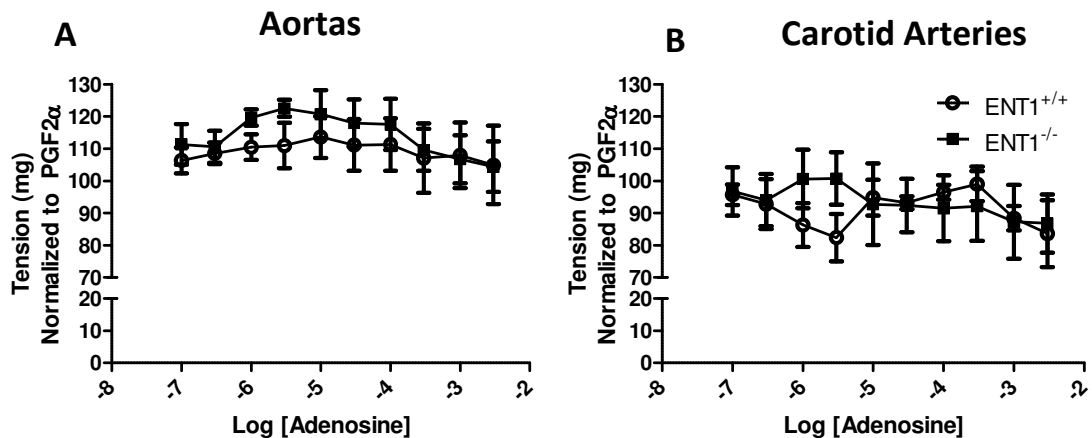
Figure 3.15. Dose-Response of adenosine in ENT1$^{+/+}$ and ENT1$^{-/-}$ aortas (Panel A) and carotid arteries (Panel B). Vasodilation as a result of adenosine was measured after tissue was pre-incubated with 0.1uM of A$_{2A}$ blocker SCH58261 for 15 minutes and pre-constriction with 80% of maximum PGF2α. Tissues were incubated for 30 minutes at 37˚C in KPSS buffer at resting tensions of 500 mg after which they were depolarized with 100 mM KCl to test for viability. Results were then normalized to the PGF2α maximum tension generated and converted to a percentage. Each point represents the mean ± SEM from four experiments in aortas (Panel **A**), three experiments in carotid arteries (Panel **B**). (Two-Way ANOVA for unpaired experimental parameters, P<0.05)

3.9 Expression of target genes *Ada, Ak* and *Catalase*, in the descending thoracic aorta found no significant differences between genotypes

Gene expression was important to understand what was changing on a molecular scale and to directly examine the hypothesis and understand what is being disrupted in the normal purinergic homeostatic mechanism. Gene expression data were not significantly different between genotypes for *catalase*, *Ak* or *Ada* in 3 – 4 month old mice. The ENT1$^{+/+}$ and ENT1$^{-/-}$ aorta expression data were calculated relative to beta actin expression (beta actin was within 1 ct value). *Ada* expression in ENT1$^{+/+}$ was 1.01 ± 0.12 (N=3) and ENT1$^{-/-}$ was 1.01 ± 0.12 (N=3). *Ak* expression in ENT1$^{+/+}$ was 1.12 ± 0.32 (N=3) and ENT1$^{-/-}$ was 1.03 ± 0.19 (N=3). *Catalase* expression in ENT1$^{+/+}$ was 1.04 ± 0.20 (N=3) and ENT1$^{-/-}$ was 1.05 ± 0.23 (N=3). *ENT1* expression was not present in the ENT1$^{-/-}$ which was not surprising and within the ENT1$^{+/+}$ was 0.96 ± 0.48 (N=5).
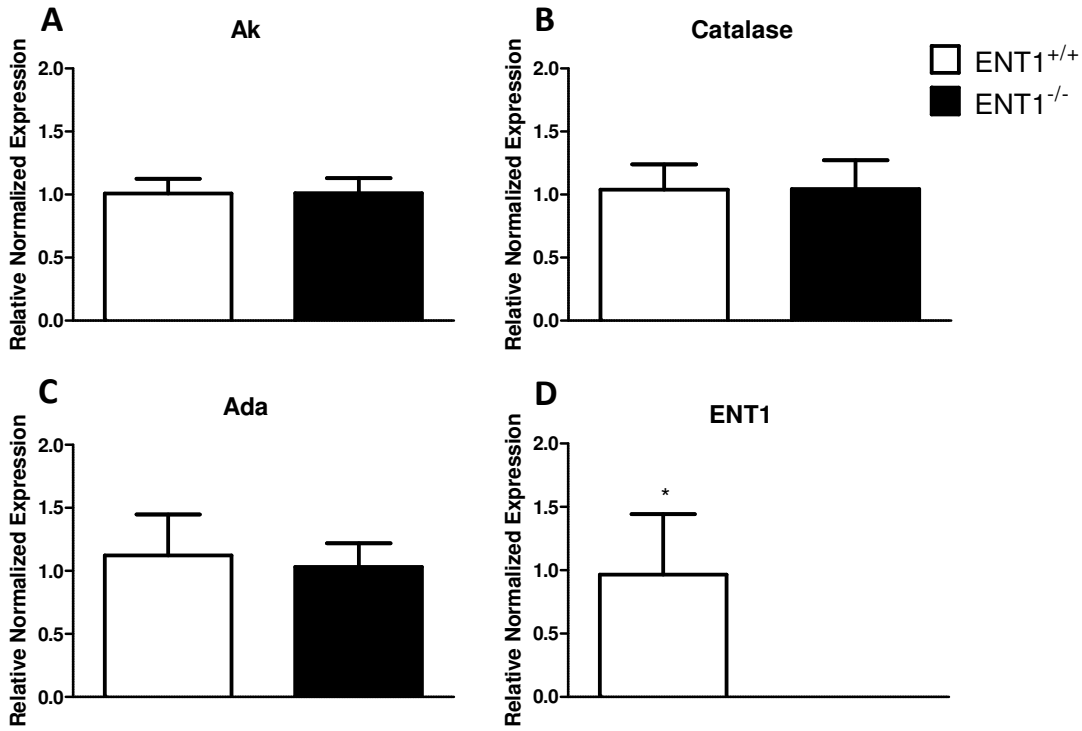
Figure 3.16. Relative Gene Expression of ENT1$^{+/+}$ and ENT1$^{-/-}$ aortas. Results were normalized to Beta Actin. Each point represents the mean ± SEM from three experiments (Panel **A** – **C**) and five experiments (Panel **D**). (Student's t-test for unpaired experimental parameters)

Chapter 4:

Discussion

Cardioprotection via purinergic signaling has been examined extensively across many animal models. Studies examining the effects of ecto-5□-nucleotidase (CD73) and ectonucleoside triphosphate diphosphohydrolase 1 (CD39) on extracellular adenosine production and signaling; and subsequent cardioprotection via ischemic pre-conditioning are well documented [54]. The goal of the current study was to establish a link between adenosine transport across cell membranes and vascular protection.

Prior to this thesis, there has been work done within the ENT1-null mouse model designed by Choi *et al.* (2004) [29]. This mouse model has made research on cardiac tissues, analysis of the spine and skeletal phenotype and a look at neurophysiology possible within a full body knock-out. The mouse line was initially characterized to assess the role of adenosine transport within the central nervous system [29], particularly looking at behavioural aspects and analyzing the ENT1$^{-/-}$ propensity for greater ethanol consumption. The observed behaviour was linked to the decrease of A_1 receptor stimulation presumably due to reduced extracellular adenosine. Work done within the Hammond laboratory by Warraich *et al.* (2012) found evidence of calcified lesion within the spinal tissue of the ENT1$^{-/-}$, a phenotype which may be linked to diffuse idiopathic skeletal hypertosis (DISH) in humans [32]. As yet, this finding remains relatively new and DISH patients have not been examined for mutations in ENT1. This finding led to a preliminary investigation of the vasculature, looking for evidence of calcium deposits although no evidence of increased cardiovascular disease has been witnessed in subjects with DISH.

Other work within the Hammond laboratory has been done using microvascular endothelial cells from the ENT1$^{-/-}$ mouse to assess the mechanisms of transport and how nucleosides and nucleobases are metabolized [31]. It was found that there was no change in the

79

ENT2 or equilibrative nucleobase transporter subtype 1 (ENBT1) expression in cells from ENT1$^{-/-}$ mice [57]. However, an increase in adenosine deaminase (ADA) and adenosine A_{2A} receptors was observed in the ENT1$^{-/-}$ cells when compared to the wild type, indicating an adaptive response due to loss of the transporter [31].

Collaborators at York University found evidence of cardioprotection within this null mouse model when examining infarct size differences between the ENT1$^{-/-}$ and their wild type counterparts. The wild type possessed a larger infarct area following an hypoxic challenge, which further fueled an interest in examining the vascular protective properties of ENT1 loss or inhibition [33].

The inability of the ENT1$^{-/-}$ mouse tissue to release adenosine through the transporter may lead to generation of reactive oxygen species (ROS) through the enhanced intracellular metabolism of adenosine. The increased activation of ADA results in inosine production and stimulation of the xanthine oxidase pathway (Figure 4.1).

4.1 ENT1$^{-/-}$ mouse vasculature has morphological and phenotypic differences

To assess whether the disruption of the transporter had any morphological effects on the vasculature, paraformaldehyde was used to fix the aorta and carotids of 3 – 4 month old male mice and stained with haematoxylin and eosin (H&E) as well as alizarin red counterstained with haematoxylin (Figure 3.3, Figure 3.5), to visualize the structure and to determine whether calcium was present in any quantities within the vascular tissues.

H&E is a stain in which the haematoxylin is used to stain acidic structures such as the nuclei of cells, as the dye itself is basic, while eosin, which is an acidic dye, stains the basic structures which include the cytoplasm, collagen, and muscle fibers. Alazarin Red uses an

anthraquinone dye to react with calcium cations to form a chelate. Counterstain of haematoxylin was used to provide contrast to any visualized red. It has been observed that ENT1 has a role in the regulation of soft tissue calcification as observed in the ENT1$^{-/-}$ mice [32].
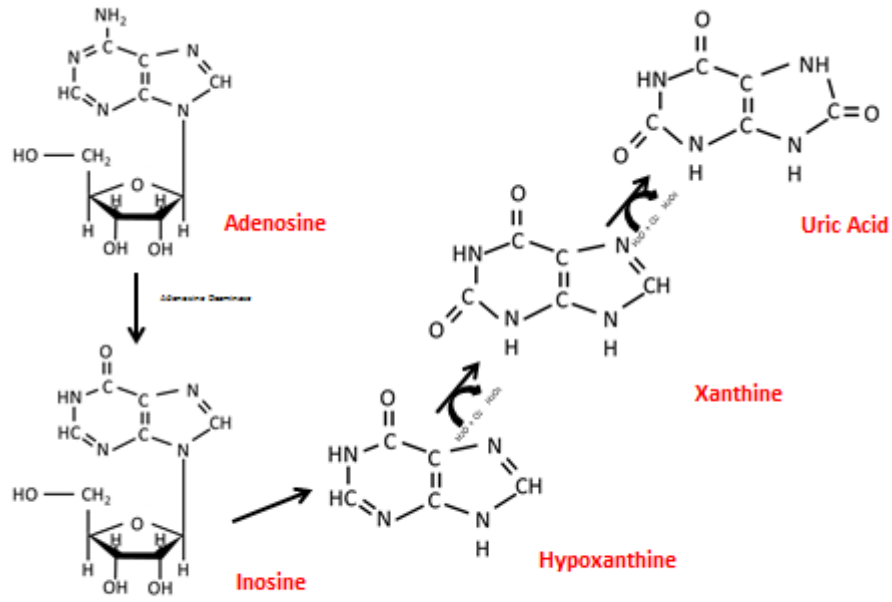
Figure 4.1 Adenosine deaminase and xanthine oxidase pathway.

The examination of the vertebral discs found that an above average amount of mineralization was occurring at 6 – 8 weeks of age in the ENT1$^{-/-}$ male mice. Therefore, to ensure the calcification discovered previously in this mouse model was localized to the vertebral discs, the present study using Alizarin Red was carried out on the vasculature of the aorta. Previous studies had found that aberrant mineralization occurred within 6 – 8 weeks of age however the aortas were negative for alizarin red staining which suggests that calcium is not present within the vasculature at 3 – 4 months of age. Finding calcium within the vasculature would have been entirely novel, and any findings alluding to its presence would impact all studies done within the vasculature in this line of mice. Typically, arterial calcification involves the accumulation of calcium phosphate crystals within the arterial walls. The presence of calcification in the medial layer is known as Monkeberg's sclerosis; a form of atherosclerosis. An underlying disease state in the vasculature of the ENT1$^{-/-}$ model such as atherosclerosis would have widespread consequences on the vascular studies [58].

The staining of the aorta and carotid arteries with H&E yielded no apparent changes in nuclei organization nor did the amount of elastic fiber layers indicate any gross morphological changes. More or fewer nuclei could indicate a greater or lesser degree of cell replication which in turn could affect cell ATP production, enzyme modulation and protein synthesis. The presence of more, or degraded and fragmented elastic fibers could have an equally varied effect. During the cardiac cycle the elastin provides reversible extension and having more or less would affect the ability of the vasculature to expand or contract. Elastic lamellae in unloaded arteries appear wavy as opposed to when they are under pressure, at which point they are straightened [59]. Tissues were excised under pressure, using gravity perfusion, to mimic the appearance under

physiological conditions. With increased elastic capabilities due the requirement of pumping blood throughout the body, it is not surprising that arteries have more elastic fibers than veins.

In studying arterial stiffness by stretching the aorta and carotid arteries, while measuring tension, we observed stiffening within the aorta of ENT1$^{-/-}$ mouse walls (Figure 3.6) although none was seen in the carotid arteries. This could imply the beginnings of arterial damage that has not yet reached the peripheral arteries in its progression. Arterial stiffness is an important precursor to cardiac mortality. Increased vascular stiffness is found in patients with hypertension as well as a score of other diseases and this increased stiffness is the beginning of an increased mechanical load on the heart [60,61].

Further analysis of the vascular tissues found that the lumen circumference in the ENT1$^{-/-}$ had an approximate decrease of 11% however wall thickness was unchanged. The narrowing of the lumen can have many implications on the overall flow rate of the system, including increasing the velocity of the flow as well as the pressure. A decrease in lumen circumference will result in a decrease in the volume flow rate. The increase in pressure that results from a smaller lumen in an artery, especially within a major artery as the aorta is significant because it places an increased load on the heart requiring the heart to pump harder to increase the pressure of the circulating blood, in order to maintain sufficient blood flow to the peripheral vasculature and the tissues they supply. Blood pressure analysis of the mice in a conscious state (Figure 3.2) were consistent with these findings and confirmed that there is an increase in systolic, diastolic and mean arterial pressures.

Elevation of the blood pressure puts a strain on the heart affecting cardiovascular health. Chronic elevation of the blood pressure is a disease of the heart, termed hypertension. High

arterial blood pressure can lead to a shortened life span or death from myocardial infraction or stroke, whereas mild increases may have no lasting effects on cardiovascular health [62]. Due to previous studies done by Chen *et al.* (2007) in which the activation of adenosine receptors in the brain, linked to the loss of ENT1 and the ability to transport adenosine into and out of the cell resulting in anxiolytic phenotype, it was thought that blood pressure would in fact decrease [30,63,64]. However a review of anxiety and cardiovascular disease was published in which a comparison of various studies done across the world found instances in which higher levels of anxiety symptoms were associated with lower blood pressure, and studies in which high anxiety did not lead to any increased risk of hypertension [65,62]. Further, the mice were examined while they were anaesthetized with isoflurane and no differences were found between the ENT1$^{-/-}$ and ENT1$^{+/+}$. It is important to note that, while the mice were anaesthetized, the mean arterial pressure dropped significantly in both genotypes with a 28% decrease in the ENT1$^{+/+}$ and a 37% decrease in the ENT1$^{-/-}$ mice.

Decreases in blood pressure while sleeping are known as nocturnal dipping. These changes occur normally and are associated with a decrease in sympathetic output. The sympathetic nervous system (SNS) is responsible for the fight-or-flight response in which there is a release of adrenal catecholamines [66]. A decrease in sympathetic output, that is greater in the ENT1$^{-/-}$, suggests a difference between sympathetic regulation. Release of epinephrine or norepinephrine, or differential abundance of adrenergic receptors can result in variations in sympathetic output between genotypes. Any changes among the three alpha$_1$-, three alpha$_2$- or three beta-receptors could potentially result in the differences observed. In the context of this study, the SNS impacts heart rate acceleration, capacity and resistance of peripheral vessels and contractility [67]. In a heart failure model, the SNS is activated to restore cardiac output. This

mechanism is explained via the stimulation of pacemaker cells, the cells that create the rhythmic electrical impulses that innervate the heart, by the sympathetic nervous system. Endocrines such as norepinephrine and epinephrine increase the ion flow rate through channels. Increased cation entry increases the rate of pacemaker cell depolarization leading to a downstream effect of increased attainment of threshold levels and subsequent action potential firing. Increased action potential firing leads to increased heart rate. Heart rate measurements yielded no change between genotypes. Beyond the expected decrease while anaesthetized, no obvious sign of impairment or increased cardiac output was observed. Trends towards higher heart rate in the ENT1$^{-/-}$ were apparent but not statistically significant.

We observed that the ENT1$^{-/-}$ mice being studied possessed smaller body weights than ENT1$^{+/+}$ mice which is consistent with previous work done by Choi *et al.* (2004) in which a difference of 8.7% was seen in ENT1$^{-/-}$ mice aged 10 – 12 weeks [30]. In the present study, mice were 12 – 19 weeks old (3 – 4 months of age) and the difference between genotypes became even more significant at 13.6%. We then sought to explain this further by analysis of other metabolic factors.

Analysis of food consumed did not yield any significant differences indicating that under-eating is not a factor in apparent weight changes; however water consumption during active hours was higher in the ENT1$^{-/-}$ mice. We did find that during the active hours, an increased amount of ambulatory and total movement over a 12 hour period of time was present. The higher levels of activity seen in the ENT1$^{-/-}$ mice could account for the leaner bodies; however on closer examination we found that this may only be one contributing factor. The fasting respiratory exchange ratio of the ENT1$^{-/-}$ mouse was lower than that of the ENT1$^{+/+}$ indicating a propensity for more fat oxidation than carbohydrate. This trend was only witnessed in mice during the light

cycle, indicating that this state occurs during inactivity. During periods of high activity, respiratory exchange ratios between genotype were similar and closer to carbohydrate oxidation. Further analysis found that energy expenditure, also during fasting periods was lower, in the ENT1$^{-/-}$ mice. It is important to note that the ratio of brown to white fat is unknown within this mouse type and it is possible that a difference in fat storage may be present between genotypes.

A study done in 1991 (Zurlo *et al.*) found that increased body weight was associated with an increased respiratory exchange ratio; and this finding was considered independent of any energy expenditure, although another study published in 1992 (Seidell *et al.)* claims that both an increase in respiratory exchange ratio and a decrease in energy expenditure are predictive factors of weight gain [68,69]. Inability of the cells to transport adenosine into the cells would lead to increased fat oxidation in an attempt by the cell to increase ATP stores. Extracellular adenosine is transported into the cells to undergo ATP production. Without adenosine being replenished the cells may experience energy (ATP) deprivation and begin removing ATP from stored deposits, depleting the liver, fat and muscle tissues.

4.2 Assessment of potassium mediated depolarization

Potassium chloride was initially used as a means of testing tissue viability within the aorta and carotid arteries. The mode of action of KCl involves the establishment of a resting membrane potential due to a diffusion potential of potassium across the membrane thus resulting in smooth muscle contraction. Upon testing for viability within the tissue, we noticed that the ENT1$^{-/-}$ mice were producing a considerably higher degree of contraction when compared to the ENT1$^{+/+}$ mice (Figure 3.7) in both aorta and carotid arteries. This was analyzed at various resting tensions in the aorta and was not found to be significant at all tensions. Those that were not significant were

trending towards this same effect. This was a novel observation and we hypothesized that the depolarization of the tissue simulated distress resulting in the ENT1$^{+/+}$ tissue releasing adenosine from the cell, whereas the tissue was unable to release adenosine in the ENT1$^{-/-}$ due to the lack of transporter. ATP and adenosine are often characterized as distress signals and under specific circumstances, most notably necrotic cell death, there is a release of cellular adenine nucleotides resulting in an increase in adenosine stores [6]. The adenosine that is released in the ENT1$^{+/+}$ mice is able to act on the adenosine receptors causing a vasodilatory effect that is not seen in the ENT1$^{-/-}$. However when we tested this theory in the aorta using the selective ENT1 blocker NBMPR (Figure 3.8), rather than mimicking the effects seen in the experimental group, the ENT1$^{-/-}$ aortas responded much like the ENT1$^{+/+}$. In the presence of NBMPR the generated contraction as a result of KCl depolarization was 29% lower in the ENT1$^{-/-}$ than that of the contraction that was generated previously. The ENT1$^{+/+}$ also decreased by 20% in the presence of NBMPR. Neither experiment was significantly different from the KCl in the absence of inhibitor experiment, however, neither were they significantly different between genotypes following NBMPR treatment.

To ensure that the solvent, dimethyl sulfoxide (DMSO), in which the NBMPR was dissolved did not affect our results, the effects were tested on the ENT1$^{+/+}$ aortas and we found no significant effect. This result has led us to the prediction that it is not simply the lack of ENT1 that has resulted in the increased depolarization seen in these tissues but a byproduct of ENT1 removal through growth and development. We hypothesized that NBMPR at this concentration may be exhibiting a toxic effect on the ENT1$^{-/-}$ that we are not observing in the ENT1$^{+/+}$, once again as a result of long term ENT1 deficits. It is also possible that ENT1$^{-/-}$ now exhibits an alternate transporter that is affected by NBMPR. Unfortunately the hypothesis

regarding toxicity is not corroborated by the literature, and studies in which 100 μM of NBMPR was utilized to incubate human fibroblast cells, the NBMPR was found to be non-toxic [70]. It was then suggested that the increased arterial stiffening may account for this increased response; however there is little evidence to support this as well. This increased susceptibility to potassium chloride is a novel finding thus it follows that further experiments will be required to elucidate the cause.

4.3 Assessment of vasoreactivity to various receptor mediated agonists

To determine if any receptor mediated vasoconstriction or vasodilation differences were present in the aorta, and to find a vasoconstrictor to use for subsequent vasodilation and hypoxia studies, multiple agonists were used. The characteristics we sought for the ideal vasoconstrictor were a strong generated contraction that was able to plateau and remain stable. The chosen agonists are the most widely used in vascular tissue studies and allowed us to use other models as a benchmark by which to set up our experimental protocols.

Initially, examination of receptor mediated vasoconstriction was done with phenylephrine with the result of no significant difference between the $ENT^{+/+}$ and $ENT1^{-/-}$ mouse (Figure 3.9). The initial curves suggested trending towards significance. To further elucidate this trend, additional experiments at a resting tension of 1000 mg were carried out (Figure 3.10). The results, however, did not show any further trend at this tension. The phenylephrine mechanism of action utilizes α_1-adrenergic receptor signaling which is part of the G-protein coupled receptor superfamily. Phospholipase C activation increases inositol triphosphate resulting in an interaction with the calcium channels of the sarcoplasmic reticulum and increased Ca^{2+} within the cell. There have been numerous studies in which α1-adrenergic receptor agonists have been

tested for receptor desensitization. Decreased response to phenylephrine, and, in fact a large number of vasopressors has been reported in deep vessel tissue studies in which numerous animal models were subjected to moderate and extreme hypothermia. Studies have also been conducted in which the interaction of β-Arrestin 1 with G-protein coupled receptors can have a desensitizing effect, and recently in cirrihosis patients and rats this interaction was found to have direct bearings on the $G_{\alpha s}$ protein [71,72]. Therefore, it can be suggested that such an interaction may largely impact $G_{\alpha q}$ as well, although at the point of this paper, this question has yet to be answered as the dual functions of β-Arrestin and how they interact when all occur simultaneously, is still relatively unknown.

Since phenylephrine did not provide us with a satisfactory result, we next examined serotonin which acts on $5HT_2$ (5-hydroxytryptamine) type receptors [73]. Because $5HT_2$ receptors within the aorta are believed to up-regulate transforming growth factor (TGF)-β1 expression and the activity of phospholipase C (PLC), serotonin was a good potential constrictor for this project [74]. Phospholipase C catalyses the synthesis of inositol trisphophate (IP_3) (diacyglycerol), subsequently causing an increase in Ca^{2+} cytoplasmic concentrations as well as protein kinase C activation and substrate phosphorylation [75]. The contraction is caused by a release of Ca^{2+} from the sarcoplasmic reticulum. Ca^{2+} binds to calmodulin activating the myosin light chain kinase (MLCK) which phosphorylates myosin light chains with ATP. Cross-bridges are formed between myosin heads and actin filaments with this phosphorylation and the muscle contracts. The serotonin response was not maintained long enough between doses to confidently assess a dose-response and would not be useful for sustained generation of contraction to carry out a vasodilation dose-response.

Finally, PGF2α acts on the Prostaglandin F (FP) receptor stimulating $G_{\alpha q}$ and the hydrolysis and mobilization of inositol phospholipid hydrolysis leading to an increase in Ca^{2+}. The study by Davis *et al.* (1987) also confirmed that PGF2α induces rapid and concentration-dependent increases in Ca^{2+} that reach maximum within a 30 second time frame and maintained the contraction for a period of 8-10 minutes [76].

The results in the experiments dealing with phenylephrine, PGF2α and serotonin did not result in a significant difference in contraction between the $ENT1^{+/+}$ and $ENT1^{-/-}$ mice, however, they allowed me to characterize the $ENT1^{-/-}$ model further. We used PGF2α as a pre-constrictor for the subsequent adenosine vasodilation studies, as it maintains the most stable contraction of the three agonists I examined. Furthermore, in order to examine the validity of the $ENT1^{-/-}$ model by examining the ability of adenosine to relax the vascular tissue in the aorta and carotid artery, vasodilation studies in the presence and absence of A_{2A} blocker SCH58261 were undertaken.

With the loss of ENT1 it is suggested that the exogenous adenosine that is no longer able to be transported into the cells will now be free to act on adenosine receptors on the cell surface. Before testing with adenosine, methacholine was used to ensure that the endothelium was still intact as it is an endothelium dependent vasodilator, and is indicated by a tissue relaxation (Figure 3.15). Methacholine acts on the muscarinic receptors to stimulate nitric oxide synthesis and subsequent vasodilation. An intact endothelium is important to the vasodilation response. Downstream effects of adenosine receptor stimulation, as discussed previously, work in conjunction with cAMP and subsequent synthesis of nitric oxide by NOS, found within the endothelium. The endothelial layer must therefore be intact to elicit the entire vasodilation response [43].

Multiple studies have examined the distribution of adenosine receptors in the vasculature, particularly in the aorta and found that across most species the dominant form is the A_{2A}, and also present although at a lesser extent are the A_{2B} receptors. As previously mentioned, both receptors lead to a subsequent vasodilation within the tissue and it is this response that we are interested in characterizing; the difference in ENT1 expression effects on the receptor stimulation within the vasculature.

Using PGF2α as a pre-constricting agonist, a dose-response curve was carried out with adenosine and from the results, a clear vasodilation can be seen (Figure 3.15) that exceeds that of the ENT1$^{+/+}$, thus indicating an increase in receptor activation in the ENT1$^{-/-}$ aorta. The increase in extracellular adenosine due to the tissue's inability to transport the nucleoside results in the increased vasodilation that is observed in the ENT1$^{-/-}$ mice. Within the carotid arteries, the same phenomenon was not observed and could suggest differential distribution of the adenosine receptor subtypes. As not much is known of the level of receptor expression in the carotid arteries of mice, it is possible that a lesser amount of adenosine receptors are present overall and that at even low doses of adenosine, the receptors are saturated. Studies done by Li *et al.* (1998) utilizing endothelial cells from a human iliac artery and a porcine carotid artery found evidence of adenosine A_{2A} receptor stimulation and a marked increase of NO production as well as A_1 receptor stimulation which elicited a decrease in NO production so there is at least some level of vaso-regulation present [77]. Herlihy *et al.* (1976) also carried out vasodilation studies on vascular smooth muscle cells of hogs and dogs and adenosine application resulted in vasodilation [13].

Following the verification of a significantly higher degree of adenosine relaxation in the ENT1$^{-/-}$ aortas, we then sought to block the effects of the A_{2A} receptor using selective blocker

SCH58261. The higher degree of vasodilation observed in the ENT1$^{-/-}$ suggests a larger quantity of adenosine is acting on the adenosine receptors. This occurs because the tissue is unable to transport the adenosine from the extracellular into the cell of the ENT1$^{-/-}$. Our goal was to evaluate our theory that this vasodilation was via A$_{2A}$ receptor activation by using A$_{2A}$ blocker SCH58261. Minimal vasodilation was observed between genotypes, which contrasts what was seen in the previous study. This suggests that the A$_{2A}$ receptor is indeed responsible for adenosine mediated vasodilation in the aortas. Similarly, the carotid artery dilation was reduced with the SCH58261 treatment suggesting that at least some of the receptors in the carotid arteries responsible for vasodilation when adenosine is administered are the A$_{2A}$ receptors. This corresponds with the previously mentioned study completed on human and porcine carotid artery endothelial cells [77].

4.4 Assessment of vasoreactivity under test conditions of hypoxia in aorta and carotid arteries

Adenosine has been linked to cardioprotection as previously described, and furthermore, these mice have been studied extensively to examine the effects within the heart. To determine if the loss of ENT1 would attenuate damage when dealing with hypoxia in the vasculature to an increased degree than what is observed in the ENT1$^{+/+}$ as a result of higher levels of adenosine to act within the tissue, we exposed the tissues to periods of hypoxia within an organ bath. As previously discussed, hypoxic conditions along with mechanical and biochemical stimuli induce endothelium-derived relaxing factor (EDRF): NO. Adenosine receptor stimulation results in a downstream signaling cascade of cAMP and adenylate cyclase activating NOS.

Our studies with hypoxia involved analyzing vasoreactivity under various conditions including preconditioning with adenosine and in the presence of ENT1 inhibitor NBMPR. The goal was to measure the ability of the tissue to contract following the hypoxic challenge. For purposes of measuring vasoreactivity, phenylephrine was the agonist of choice as our previous studies with it proved to elicit a contraction that was not significantly different across genotypes; accordingly it would provide a valid baseline from which to establish experimental parameters.

The expectation was that in the ENT1$^{-/-}$ tissues, hypoxia would have less of a detrimental effect as evidenced by a smaller decrease in vasoreactivity when compared to the ENT1$^{+/+}$ group. The basis of this hypothesis is once again predicated on loss of ENT1 leading to an increase in adenosine mediated activation within the endothelium as there would be an increased quantity of adenosine in the extracellular space, resulting in purinergic signaling activation to increase cell survival, in other words preconditioning [52,78]. Our findings however do not support this hypothesis. What we found instead was that there was no significant difference in the hypoxic tissue when compared to the controls in either genotype which indicated that the hour of hypoxia was not a long enough period of oxygen deprivation to enlist permanent damage to the aortas or the carotids. Andresen *et al.* (2004) and Kim *et al.* (1993) used hypoxic periods of 30 minutes while in 1996, Kim *et al.* increased hypoxic period to 180 minutes [79,80,81](figure 3.11).

In previous studies in which cardiac tissue was exposed to hypoxic conditions, the importance of ENT1 in the cardioprotection of the whole heart against ischemia was verified [33]. However, the present study was not able to recreate these findings in the aorta model. In fact, it was only upon adding adenosine to the organ bath prior to the hypoxic event that we were able to witness any sort of effect within the tissues. Upon adding large amounts of adenosine (millimolar range) which is not physiologically relevant (adenosine is usually found in the

nanomolar - micromolar range), we were able to witness what appears to be preconditioning resulting in a vascular protective effect in all but one concentration in the ENT1$^{+/+}$ and at the two highest concentrations within the ENT1$^{-/-}$ mice.

This high quantity of adenosine was able to elicit a protective effect within the vasculature, which could indicate some level of A$_1$ and A$_3$ receptor expression is also present in the vasculature although perhaps not at a high enough quantity to elicit this type of response at a naturally occurring concentration of adenosine. This effect is not conclusive and may also be an unrealized consequence of A$_2$ receptor activation. The activation of A$_1$ and A$_3$ receptors has been shown to be responsible for the cardioprotective effect, and although there is evidence of the A$_{2A}$ and A$_{2B}$ receptors being of importance in the ischemia reperfusion model, possessing all receptors is required to elicit a similar outcome as has been seen in the studies done by Rose *et al.* (2009) [33]. It is not surprising therefore that although the tissue is from the same mouse the vascular protective effect we had hoped to see did not occur. It is reasonable to speculate that the A$_1$ receptor distribution was not abundant enough, if present at all, within the vascular tissue, to produce a similar response as what is witnessed in the heart. It is important to note that due to tissue handling, the vascular rings may not have a fully functional endothelium. Methacholine was used to elicit a vasodilation response to ensure the integrity of endothelium and the tissue was used only upon the generation of a strong response however the process of excising the tissue and removing the fatty tissue still results in some mechanical damage and a partially denuded artery can result in varying results.

In addition to the preconditioning effect of adenosine in both genotypes, hypoxia induced vasoreactivity was examined in the aorta. It is expected that adenosine release in ENT1$^{+/+}$ aortic segments should be higher than that in ENT1$^{-/-}$ aorta, ideally indicated by a higher degree of

relaxation, however, in both the carotid arteries and the aortas, neither result was significant nor did it appear as if much vasodilation occurred (Figure 3.13). Even if vasodilation had been observed, the possibility exists that another agent involved in vasodilation was at work, such a prostacyclin, bradykinin or NO, which would have been indicated by hypoxia vasoreactivity. It is also possible that the role of extracellular ATP breakdown as a source of adenosine is being underestimated which is resulting in the inability to distinguish between the two genotypes in terms of potential adenosine release.

In a tissue experiment it is expected that some fluctuations in contraction will occur past the point of what appears to be plateau thus the measurements over the course of an hour will vary. The possibility exists that the lack of significant difference between genotypes could be indicative of a down-regulation of CD73 or CD39 within the ENT1$^{-/-}$ which could have further effects within the cell. Reasons for a negative response could be potential release of other receptor agonist counteracting the suggested adenosine vasodilation. Marshall (2000) hypothesized that circulating constrictors such as catecholamines and vasopressin need to be overcome by the vasodilator, and the degree vasodilation varies depending on the level of hypoxia in that area [82].

4.5 Expression of target genes *Ada, Ak* and *Catalase*, in the descending thoracic aorta were not significantly different between genotypes

Adenosine formation can be carried out by dephosphorylation of AMP and can be removed via deamination in which the adenosine metabolite inosine is formed, or phosphorylation in which AMP is formed. Adenosine deaminase to form inosine is carried out by the enzyme adenosine deaminase (ADA). Similarly, adenosine kinase (AK) is responsible for phosphorylation to AMP. Due to relatively high levels of AMP, ADP and ATP compared to the

levels of adenosine within the tissue, AMP/adenosine substrate cycle changes have relatively little effect on the concentrations of AMP, ADP or ATP, however changes in the AMP/adenosine substrate cycle will have a large impact on the adenosine concentrations within the cell.

Previous work done by Rose *et al.* 2011 showed that blood serum concentrations of adenosine within the ENT1$^{-/-}$ mouse were significantly higher with almost double the concentration [52]. This change may suggest a decrease *Ak* expression and/or perhaps a decrease in *Ada* expression. ENT1$^{-/-}$ mice were observed to have increased extracellular adenosine compared to ENT1$^{+/+}$ mice indicating that some extracellular adenosine is being transported across the membrane in the ENT1$^{+/+}$ [52]. It therefore also follows that intracellular levels of adenosine in the ENT1$^{-/-}$ may be decreased as well. As such, a decrease in intracellular adenosine could result in a decrease in *Ak* or *Ada* expression. If intracellular adenosine concentrations are low, ADA may be down-regulated to conserve the adenosine stores and reduce activity of the xanthine oxidase pathway. As previously described, the xanthine oxidase pathway results in the generation of ROS, which can be detrimental to the cells. However, recent studies have also shown the benefits of xanthine oxidase in relation to disease states in which the ROS it generates are involved in an antimicrobial response, and currently not much is known about all the effects of xanthine oxidase [83]. It therefore would be plausible that *Ada* expression could be increased or decreased, although as the mice in the current study were not chronically ill with a microbial infection, it is more likely that *Ada* expression would have been down-regulated. AK on the other hand would more likely have been down-regulated in response to the decreased adenosine with less adenosine to convert to AMP. As previously described, AK is at maximum saturation during resting periods therefore, without a decrease in *Ak* expression, AK would be in excess. Neither of the proposed theories were corroborated as expression levels of *Ada* and *Ak* were

found to be unchanged in the aorta of ENT1$^{-/-}$ mice, and if there had been a down-regulation of *Ada* expression, the expected result would be a decrease in inosine concentration. Previous work carried out in cardiomyocytes of the ENT1$^{-/-}$ and ENT1$^{+/+}$ found inosine levels following a hypoxic challenge to be not significantly different, however this work has not been replicated in tissue [52].

Expression of *catalase* was also found to be unchanged in the aortas ENT1$^{-/-}$ mice. Catalase is an enzyme which is responsible for the protection of cells from oxidative damage via the conversion of hydrogen peroxide to water and oxygen. The formation of xanthine and hypoxanthine resulst in the production of ROS and it had been hypothesized that catalase would be up-regulated due to the increased production of ROS via the subsequent metabolite formation of inosine, xanthine and hypoxanthine from adenosine. The inability of adenosine to transport out of the cell would hypothetically result in the increased production of ROS and therefore a need for an increase in antioxidant activity.

Expression of *ENT1* was found to be non-existent in the aortas of ENT1$^{-/-}$ mice. The transporter is necessary for adenosine transport into and out of the cell and its loss, which is the focus of this study, would hypothetically result in increased activation of adenosine receptors on the outside of the cell, a mechanism which has been indicated in the cardioprotective effect seen in ischemic reperfusion therapy. However low extracellular adenosine production could result in the lack of positive correlation we are seeing between loss of the transporter and vascular protection. It is estimated that 30% of adenosine production in the endothelial cells is a result of ecto-5□-nucleotidase, and only 24% in smooth muscle cells [84]. Low levels of adenosine production in extracellular, relative to intracellular adenosine production; suggest that adenosine receptor stimulation may be attenuated by the efflux of adenosine. If these estimations are

correct, the ENT1$^{-/-}$ inability to transport adenosine outside of the cell may result in decreased adenosine receptor activation.

4.6 Summary and Conclusions

The studies carried out in this thesis were based on the pre-existing knowledge that connects adenosine and cardioprotection as well as the extensive research done within this mouse model in which an ischemic event within the heart has shown to exhibit a cardioprotective effect through alteration of purinergic signaling after exposure to a hypoxic challenge.

We hypothesized that: **Loss of ENT1 will lead to a vascular phenotype due to disruption of the normal purinergic homeostatic mechanism which is critical to vascular regulation.**

Working Hypothesis: Loss of ENT1 will result in an increase in interstitial adenosine levels leading to compensatory changes in the vasculature that would mimic preconditioning.

We explored this hypothesis with the following objectives:

1) To determine the baseline vascular characteristics of the ENT1$^{-/-}$ mouse versus the ENT1$^{+/+}$ mouse.

2) Examine the aorta looking for structural differences between the ENT1$^{-/-}$ and ENT1$^{+/+}$ mouse.

3) Examine the vascular tissue in response to hypoxic conditions.

We then characterized the ENT1$^{-/-}$ mouse vasculature looking specifically at morphological and functional differences.

Conclusion **4.1**: Mice lacking ENT1 demonstrate no morphological differences or calcium deposits in the vascular tissues of the aorta or carotid arteries. Although there is evidence that ENT1 has a role in the regulation of soft tissue calcification, no mineralization is present within the first four months [32].

Conclusion **4.2**: Mice lacking ENT1 possess an elevated blood pressure while conscious however no differences were seen while anaesthetized, nor were any differences seen in their heart rates. Mice lacking ENT1 had smaller lumens and increased aortic stiffness which was in line with the findings. The increased blood pressure could be the result of the narrowing of the lumen, resulting in increased vascular resistance.

Conclusion **4.3**: Mice lacking ENT1 were smaller in body weight and possessed a lower RER and EE while maintaining a higher level of activity during the dark cycle, all of which support prior evidence of leaner mice [29]. This indicates that adenosine signaling and transport plays a role in fat metabolism, accounting for the leaner appearances and lower body weight.

Within chapter four, we also sought to assess potassium mediated depolarization as well as receptor mediated constriction in both normoxic and hypoxic conditions.

Conclusion **4.4**: ENT1$^{-/-}$ had increased response to potassium chloride which indicates that there is either an increased responsiveness to depolarizing agent or a feedback response of adenosine on ENT1$^{+/+}$ tissue. The study indicated that the increased response is a result of increased responsiveness to depolarizing agents rather than a feedback response. The reason for this conclusion was based on the results of the study which clearly demonstrated that inhibition of the transporter did not result in increased depolarization. A more reasonable conclusion is that the

increased reactivity to KCl is a result of the increased arterial stiffness observed in the length-tension curves.

Conclusion **4.5**: Loss of ENT1 does not lead to any increased or decreased response in receptor mediated contraction, within the tested receptors, during normoxic conditions. It is reasonable to conclude that ENT1$^{-/-}$ mice do not possess differences in FP, 5-HT2 or α1-adrenergic receptor within the descending thoracic aorta, with respect to distribution or relative abundance in the tissue as compared to controls.

Conclusion **4.6**: Loss of ENT1$^{-/-}$ allowed for a greater vasodilation compared to control in aorta. This supports the theory that adenosine levels remain higher for a longer period of time at the receptors, due to the inability to transport across cell membranes.

Conclusion **4.7**: Blocking A$_{2A}$ receptor resulted in less vasodilation in the control and ENT1$^{-/-}$ of both the aorta and carotid arteries when compared to adenosine vasodilation in the absence of A$_{2A}$ blocker. This indicates that the main mechanism of vasodilation is via A$_{2A}$ receptors within the vasculature.

Conclusion **4.8**: Loss of ENT1 resulted in no contractile response changes in response to hypoxic conditions, nor did blocking the transporter result in any increased response to phenylephrine in the control mice. This indicates that the ENT1$^{-/-}$ mice are not vascular protected, and leads us to the hypothesis that perhaps intracellular adenosine generation and efflux plays a larger role in the preconditioning effect than previously speculated, hence the decreased reactivity following hypoxia in the ENT1$^{-/-}$ mice.

Conclusion **4.9**: Pre-treatment with adenosine in the control groups as well as the ENT1$^{-/-}$ mice results in increased reactivity post hypoxia, however the dose required to elicit this result in

ENT1$^{-/-}$ is higher than in mice possessing ENT1, again indicating that extracellular adenosine could play a more integral role in vascular protection than originally thought.

Conclusion **4.10**: *Ada*, *Ak* and *catalase* gene expression was not changed between genotypes indicating that the differences observed between the genotypes are not a result of decreased adenosine metabolites within the cell although the possibility exists that activity differences in enzymes are affecting metabolite production.

4.7 Significance of Research

Adenosine is an important signaling molecule in cardiovascular physiology, which has been the focus of many studies, and its effect in the protection against ischemia reperfusion injury is well documented. It is required for ATP and nucleic acid synthesis within the body which is important in cellular physiology however its effects in the mediation of ischemia reperfusion injury make it a significant factor in the mediation of cardiovascular health, and particularly significant in this research.

Numerous studies have been carried out in which manipulation of the upstream and downstream regulators of adenosine, such as CD39 and CD73, have resulted in a decreased cardioprotective effect due to the inability to synthesis adenosine. Studies in which adenosine transport into and out of the cell have been blocked using ENT inhibitors, such as NBMPR, have demonstrated an increased cardioprotective effect in the cells after a subsequent ischemic event. Work completed with this particular ENT1-null mouse model has yielded similar findings in the cardiac tissues.

Studies carried out by Rose *et al.* (2009) showed a decrease in infarct size in the ENT1$^{-/-}$ versus the mouse possessing the transporter [33]. The purpose of the study was to investigate the

mechanism underlying the protective effect of the loss of ENT1 within the vascular tissues of this mouse model. This study was unable to mimic the results seen in the cardiac tissue within the vasculature however, and in fact saw the opposite effects as would be expected. This result could be due to increased importance of extracellular adenosine levels rather than the release from the tissues themselves to initiate a vascular protection effect. In addition, hypoxia within the vasculature is not uniform and therefore responses to hypoxia are not entirely mediated in the same manner. Hypoxia-induced dilation factors are close to or produced near individual vessels based on oxygen depletion (Marshall, 2000) [82]. Our results varied greatly from the results we expected. Our expectations were based largely on the literature and the observations by Rose *et al.* which showed positive correlation between loss of ENT1 and cardioprotection [33,52]. The assumptions were also predicated on the vasculature possessing A_{2A} and A_{2B} receptors for which the extracellular adenosine could act on. However a relatively recent study (Zhan *et al.* 2011) that claimed the need for more than one receptor subtype, i.e. the need for all subtypes, A_1, A_{2A}, A_{2B} and A_3, to mediate a protective effect was not taken into account, but as mentioned in chapter 1, A_1 stimulation resulted in decreased infarct size and positive postischemic function [16]. The literature is not all encompassing and the vasculature is largely excluded from the discussion on hypoxia and protection. A recent study (Rath *et al.* 2012) found that ischemia reperfusion resulted in the reduction of NO-mediated relaxation but increased endothelium-derived hyperpolarizing factor (EDHF) mediated relaxation, however vascular hypoxic preconditioning was able to attenuate the reduction in NO-mediated relaxation as well as increase EDHF mediated relaxation. Further analysis of this study also found that transient receptor potential cation channels V4 (TRPV4) also directly affects the NO-dependent pathway

therefore participating in vascular protection [85]. This study is mentioned to illustrate the depth to which vascular protection is relatively unknown.

Studies of gene up-regulation and down-regulation could explain the effects of long term exposure to an ENT1 inhibitor such as NBMPR. The potential uses of ENT1 inhibitors in cardioprotection therapies require long term studies of the effects on the whole organism and this mouse model provides an avenue for the investigation of any "off-target" effects. Clinically, ENT1 inhibition has been considered as a potential treatment prior to ischemic reperfusion and these studies will help elucidate the effects of long term exposure within a mouse model.

The ENT1-null mouse model is a potentially useful model for understanding the long term consequences of chronic inhibition of adenosine transport. This model may also be useful for investigating the importance of intracellular versus extracellular adenosine during the process of ischemia-reperfusion. This study could lead to further discoveries of risk factors and assist in identifying limitations of use in other vascular tissues.

4.8 Limitations of Research and Suggestions for Future Studies

This study is the first analysis of the vascular system in these $ENT1^{-/-}$ mice and therefore there is still much to be done. Gene expression studies were undertaken to elucidate the regulation of adenosine within the vascular tissues (*Ada, Ak, ENT1, Catalase*) within the ENT1 mouse model however there are further genes of interest which could be further characterized such as xanthine oxidase, ecto-5□-nucleotidase and other ENT/CNTs and adenosine receptors.

Following gene analysis, protein detection of these gene products is important in developing the repertoire of information in studying and reaching conclusions in this type of research. We cannot make any conclusive statements about the mechanism of vasoreactivity

within these mice without conclusive data and therefore further observation is required. Additional studies of these mice at different ages is also necessary as there may be further up- or down-regulation of gene products over time which could lead to morphological changes within the tissues of these animals. From previous work done within the lab, it has been concluded that mineralization of the vertebral column resulting in lesions becomes apparent at the age of six months. This suggests the possibility that further along in development, that phenotype may lead to complications within the vasculature of the mice.

In addition to these approaches, tests can be done in which the hypoxic period is expanded. Hypothetically, an increased hypoxic period will result in increased damage to the vascular tissue. If we increase the period of hypoxia a more pronounced difference between the $ENT1^{+/+}$ and $ENT1^{-/-}$ may become apparent. Further experiments could also examine the use of inhibitors of adenosine formation or breakdown, such as the $5\square$-nucleotidase, adenosine deaminase or adenosine kinase. The scale of the experiments may also be increased in which whole organisms are subjected to hypoxic conditions and vascular tissues are tested. This could prove useful in the characterization of the differences of the effects seen in this study, which are clearly evident in the vasculature; thus providing the opportunity for comparative data on the protective effects on a larger scale. All testing was done on the aorta and in some cases the carotid arteries however, even slight changes to vessels such as the mesenteric arteries which supply the gut, can have a large impact on the functioning of the body.

In conclusion, all previous studies should be carried out in the peripheral vessels as well to access whether similar findings are present, and proposed future studies should elaborate on what this study has established. The proposed experiments will further clarify the mechanisms involved in the potassium mediated response and the apparent changes in vasoreactivity in the

mice lacking ENT1, and will ideally provide a model for examining vascular effects of

adenosine as well as downstream metabolites.

Chapter 5:

References

1. Tabrizchi, R., and S. Bedi, *Pharmacology of adenosine receptors in the vasculature.* Pharmacology & Therapeutics, 2001. **91**: p133-47.
2. Lasley, R.D., et al. *Evidence that cytosolic and ecto 5□-nucleotidase contribute equally to increased interstitial adenosine concentration during porcine myocaridla ischemia.* Baseic Res Cardiol, 1999. **94**: p199-207.
3. Colgan, S.P., et al., *Physiological roles for ecto-5□-nucleotidase (CD73).* Purinergic Signalling, 2006. **2**: p.351-60.
4. Fernandez, P., et al., *Extracellular Generation of Adenosine by the Ectonucleotidases CD39 and CD73 Promotes Dermal Fibrosis.* The American Journal of Pathology, 2013. **183**(6): p.1740-6.
5. Kaczmarek, E., et al., *Identification and Characterization of CD39/Vascular ATP Diphosphohydrolase.* The Journal of Biological Chemistry, 1996. **271**(61): p.33116-22.
6. Fredholm, B.B., S. Johnasson, and Y.Q. Wang. *Adenosine and the Regulation of Metabolism and Body.* Advances in Pharmacology, 2011. **61**: p.77-92.
7. Baldwin, S.A., P.R. Beal, and S.Y.M. Yao, *The equilibrative nucleoside transporter family, SLC29.* Eur J Physiol, 2004. **447**: p.735-43.
8. Young, J.D., et al., *Human equilibrative nucleoside transporter (ENT) family nucleoside and nucleobase transporter proteins.* Xenobiotica, 2008. **38**(7-8): p.995-1021.
9. Ralevic, V., and G., Burnstock, *Receptors for Purines and Pyrimidines.* Pharmacological Reviews, 1998. **50**(3): p.413-92.
10. Fredholm, B.B., et al., *International Union of Pharmacology. XXV. Nomenclature and Classification of Adenosine Receptors.* Pharmacological Reviews, 2001. **53**: p.527-52.
11. Shryock, J.C., and L. Belardinelli, *Adenosine and Adenosine Receptors in the Cardiovascular System: Biochemistry, Physiology, and Pharmacology.* Am J Cardiol, 1997. **79**(12A): p.2-10.
12. Fredholm, B.B., R.A. Cunha, and P. Svenningsson, *Pharmacology of Adenosine A_{2a} Receptors and Therapeutic Applications.* Current Topics in Medicinal Chemistry, 2002. **3**: p.1349-64.
13. Herlihy, J.T., et al., *Adenosine relaxation of isolated vascular smooth muscle.* American Journal of Physiology, 1976. **230**: p.1239-1243.
14. Donato, M., and R.J. Gelphi, *Adenosine and cardioprotection during reperfusion – an overview.* Molecular Cell Biochemistry, 2003. **251**: p.153-9.
15. Zhou, Q.Y., et al., *Molecular cloning and characterization of an adenosine receptor: The A3 adenosine receptor.* Proc. Natl. Acad. Sci, 1992. **89**: p.7432-6.
16. Liang, B.T., and K.A. Jacobson. *A physiological ole of the adenosine A_3 receptor: Sustained cardioprotection.* Proc. Natl. Acad. Sci, 1998. **95**: p.6995-9.
17. Zhan, E., V.J. McIntosh, and R.D. Lasley, *Adenosine A_{2A} and A_{2B} receptors are both required for adenosine A_1 receptor-mediated cardioprotection.* Am J Physiol Heart Circ Physiol, 2011. **301**: p. H1183-9.
18. Cass, C.E., J.D. Young, and S.A. Baldwin, *Recent advances in the molecular biology of nucleoside transporters of mammalian cells.* Biochem. Cell. Biol., 1998. **76**: p.761-70.
19. Barnes, K., *et al. Distribution and functional characterization of equilibrative nucleoside transporter-4, a novel cardiac adenosine transporter activated at acidic pH.* Circ. Res., 2006. **99**: p.510-9.
20. Young, J.D., et al., *The human concentrative and equilibrative nucleoside transporter families, SLC28 and SLC29.* Molecular Aspects of Medicine, 2013. **34**: p.529-47.

21. Thorn, J.A., and S.M. Jarvis, *Adenosine Transporters*. Gen. Pharmac, 1996. **27**(4): p.613-20.
22. Noji, T., A. Karasawa, and H. Kusaka. *Adenosine uptake inhibitors*. European Journal of Pharmacology, 2004. **495**: p.1-16.
23. Yao, S.Y.M. et al., *Molecular Cloning and Functional Characterization of Nitrobenzylthionosine (NBMPR)-sensitive (es) and NBMPR-insensitive (ei) Equilibrative Nucleoside Trasnporter Proteins (rENT1 and rENT2) from Rat Tissues.* The Journal of Biological Chemistry, 1997. **272**(45): p.28423-30.
24. Venkatesh, P.K., et al., *Dipyridamole enhances ischaemia-induced arteriogenesis through an endocrine nitrite/nitric oxide-dependent pathway*. Cardiovascular Research, 2010. **85**: p.661-70.
25. Hammond, J.R. *Comparative pharmacology of the nitrobenzylthioguanosine-sensitive and -resistant nucleoside transport mechanisms of Ehrlich ascites tumor cells*.J Pharmacol Exp Ther, 1991. **259**: p.799-807.
26. German, D.C., N.M. Kredich, and T.D. Bjornsson, *Oral dipyridamole increases plasma adenosine levels in human beings*. Clin Pharmacol Ther, 1989. **45**: p.80-4.
27. Riksen, N.P., et al., *Oral therapy with dipyridamole limits ischemia-reperfusion injury in humans*. Clin Pharmacol Ther, 2005. **78**: p.52-9.
28. Hammond, J., *Interaction of a series of draflazine analogues with equilibrative nucleoside transporters: species differences and transporter subtype selectivity*. Naunyn-Schmiedeberg's Arch Pharmacol, 2000. **361**: p.373-82.
29. Choi, D.S., et al., *The type 1 equilibrative nucleoside transporter regulates ethanol intoxication and preference*. Nature Neuroscience, 2004. **7**(8): p. 855-61.
30. Chen, J., *et al.*, *The type 1 equilibrative nucleoside transporter regulates anxiety-like behaviour in mice*. Genes, Brain and Behavior, 2007. **6**: p.776-83.
31. Bone, D.B., D.S. Choi, and J.R. Hammond. *Nucleoside/nucleobase transport and metabolism by microvascular endothelial cells isolated from ENT1-/- mice.* Am J Physiol Heart Circ Physiol, 2010. **299**: p.H847-56.
32. Warraich, S., et al., *Loss of Equilibrative Nucleoside Trasnporter 1 in Mice Leads to Progressive Ectopic Mineralization of Spinal Tissues Resembling Diffuse Idiopathic Skeletal Hyperostosi in Humans*. Journal of Bone and Mineral Research, 2013. **28**(5): p.1135-49.
33. Rose, J.B., et al., *Equilibrative nucleoside transporter 1 plays an essential role in cardioprotection*. Am J Physiol Heart Circ Physiol, 2009. **298**: p. H771- 7.
34. Aydin, S., et al., *The cardiovascular system and the biochemistry of grafts used in heart surgery*. SpringerPlus, 2013. **2**: p.612-618.
35. Safar, M.E. *Arterial Stiffness: A Simplified Overview in Vascular Medicine*. Adv Cardiol. 2007. **44**: p.1-18.
36. Bezie, Y., et al., *Connection of Smooth Muscle Cells to Elastic Lamellae in Aorta of Spontaneously Hypertensive Rats*. Hypertension, 1998. **32**: p.166-9.
37. Linden, A.V., and H.K. Eltzschig, *Role of pulmonary adenosine during hypoxia: extracellular generation, signaling and metabolism by surface adenosine deaminase/CD26*. Expert Opin. Biol. Ther., 2007. **7**(9): p.1437-47.
38. Liu, S.L., et al. *Aldosterone regulates vascular reactivity: short-term effects mediated by phosphatidylinositol 3-kinase-dependent nitric oxide synthase activation*. Circ, 2003. **108**: p.2400-6.

39. Olsson, A.K. et al. *VEGF receptor signaling- in control of vascular function.* Nat Rev Mol Cell Biol, 2006. **7**(5): p.359-71.

40. Ren, Z., *et al.*, *Hypoxic Preconditioning in Coronary Microarteries: Rold of EDHF and K^+ Channel Openers.* Ann Thorac Surg, 2002. **74**: p.143-8.

41. Furchgott, R.F., and J.V. Zawadski, *The obligatory role of endothelial cells in the relaxation of arterial smooth muscle by acetylcholine.* Nature, 1980. **288**: p.373-6.

42. Jin, R.C., and J. Loscalzo, *Vascular nitric oxide: formation and function.* Journal of Blood Medicine, 2010. **1**: p.147-62.

43. Ray, C.J. and J.M. Marshall. *The cellular mechanisms by which adenosine evokes release of nitric oxide from rat aortic endothelium.* J Physiol, 2006. **570**: p.85-96.

44. Coleman, R.A. et al. *A novel inhibitory prostanoid receptor in piglet saphenous vein.* Prostaglandins, 1994. **47**(2): p151-68.

45. Suzuki, K., et al., *Differential roles of prostaglandin E-type receptors in activation of hypoxia-inducible factor 1 by prostaglandin E_1 in vascular-derived cells under non-hypoxic conditions. PeerJ, 2013. **220.***

46. Gerczuk, P.Z., and R.A. Kloner, *An Update on Cardioprotection: A Review of the Latest Adjuctive Therapies to Limit Myocardial Infarction Size in Clinical Trials.* Journal of the American College of Cardiology, 2012. **59**: p.969-78.

47. Minamino, T., *Cardioprotection from Ischemia/Reperfusion Injury.* Journal of the Japanese Circulation Society, 2012. **76**: p.1074-82.

48. Feoktistov, I. et al., *Differential Expression of Adenosine Receptors in Human Endothelial Cells: Role of A2B Receptors in Angiogenic Factor Regulation.* Circ Res, 2002. **90**: p.531-8.

49. Dongo, E., et al., *The cardioprotective potential of hydrogen sulfide in myocardial ischemia/reperfusion injury.* Acta Physiologica Hungarica, 2011. **98**(4): p.369-81.

50. Figueredo, V.M. et al. *Chronic dipyridamole therapy produces sustained protection against cardio ischemia-reperfusion injury.* Am J Physiol, 1999. **277**: p.H209-7.

51. Abd-Elfattah, A.S.A. *et al.Role of Nucleoside Transport in Myocardial Injury and Protection: Seperation Between Ischemic and Refeusion Injury Using a Selective Nucleoside Trasnport Blocker, p-Nitrobenzylthioinosine, NBMPR.* Developments in Cardiovascular Medicine, 1996. **181**: p165-181.

52. Rose, J.B., et al., *Absence of equilibrative nucleoside trasporter 1 in ENT1 knockout mice leads to altered nucleoside levels following hypoxic challenge.* Life Sciences, 2011. **89**: p.621-30.

53. Kohler, D., et al., *CD39/Econucleoside Trisphosphate Diphosphohydrolase 1 Provides Myocardial Protection During Cardiac Ischemia/Reperfusion Injury.* Circ., 2007. **116**: p.1784-94.

54. Eckle, T., et al., *Cardioprotection by Ecto-5□-Nucleotidase (CD73) and A_{2B} Adenosine Receptors.* Circulation, 2007. **115**: p.1581-90.

55. Deussen, A. et al. *Mechanisms of metabolic coronary flow regulation.* J Mol Cell Cardiol, 2012. **54**(4): p.794-801.

56. Gros, R., K.R. Borkowski, and R.D. Feldman. *Human insulin-mediated enhancement of vascular beta-adrenergic responsiveness.* Hypertension, 1994. **23**: p.551-5.

57. Robillard, K.R., D.B.J. Bone, J.R. Hammond, *Hypoxanthine uptake and release by equilibrative nucleoside transporter 2 (ENT2) of rat microvascular endothelial cells.* Microvascular Research, 2008. **75**: p.351-7.

58. Wu, M., C. Rementer, and C.M. Giachelli. *Vascualar Calcification: An Update on Mechanisms and Challenges in Treatment.* Calcified Tissue International, 2013. **93**(4): p.365-73.

59. Clark, J.M., and S. Glagov, *Transmural organization of the arterial media. The lamellar unit revisited.* Arterioscler Thromb Vasc Biol., 1985. **5**: p.19-34.

60. Wagenseil, J.E. and R.P. Mecham, *Elastin in Large Artery Stiffness and Hypertension.* J. of Cardiovasc. Tans. Res, 2012. **5**: p.264-73.

61. McEniery, C.M., and J.R. Cockcroft, *Does Arterial Stiffness Predict Atherosclerotic Coronary Events?* Adv Cardiol. Basel, Karger, 2007. **44**: p.160-72.

62. Yan, L.L., *Psychosocial factors and risk of hypertension.* JAMA, 2003. **290**: p.2138-48.

63. Sgoifo, A., L. Carnevali, and A.J. Grippo, *The socially stressed heart. Insights from studies in rodents.* Neuroscience and Behavioural Reviews, 2014. **39**: p.51-60.

64. Thurston, R.C., M. Rewak, and L.D. Kubzansky, *An Anxious Heart: Anxiety and the Onset of Cardiovascular Diseases.* Progress in Cardiovascular Diseases, 2013. **55**: p.524-37.

65. Hildrum, B., *et al. Effect of anxiety and depression on blood pressure: 11-year longitudinal population study.* Br J Psychiatry, 2008. **193**:p.108-13.

66. Jansen, A.S.P. *et al. Central Command Neurons of the Sypathetic Nervous System: Basis of the Fight-of-Flight Response.* Science, 1995. **270**: p.644-6.

67. Triposkiadis, F., *et al. The Sympathetic Nervous System in Heart Failure.* J Am Coll Cardiol, 2009. **54** (19): p.1747-62.

68. Zurlo, F., S. Lillioja, and A. Puente, *Low ratio of fat to carbohydrate oxidation as a predictor of weight gain: study of 24-RQ,* American Journal of Physiology, 1991. **259**: p.650-7.

69. Seidell, J.A. *et al. Fasting respiratory exchange ratio and resting metabolic rates as predictors of weight gain: the Baltimore Longitudinal Study on Aging.* International Journal on Obesity, 1992. **16**: p.667-74.

70. Kouni, M.H. *et al. Metbolism and Selective Toxicity of 6-Nitrobenzylthioinosine in Toxoplasma gondii.* Antimicrobial Agents and Chemotherapy, 1999. **43**(10): p.2437-43.

71. Cohen, M.L. *Further evidence that vascular serotonin receptors are $5HT_2$ type.* Biochemical Pharmacology, 1983. **32**: p.567-70.

72. Luttrell, L.M. and R.J. Lefkowitz. *The role of β-arrestins in the termination and transduction of G-protein-coupled receptor signals.* J Cell Sci, 2002. **115**: p.455-65.

73. Hennenberg, M. *et al. Vascular dysfunction in human and rat cirrhosis: Role of receptor desensitizing and calcium-sensitizing proteins.* Hepatology, 2007. **45**: p.495-506.

74. Xu, J. *et al. Serotonin Mechanisms in Heart Valve Disease II: The 5-HT_2 Receptor and Its Signally Pathway in Aortic Valve Interstitial Cells.* American Journal of Pathology, 2002. **161**: p.2209-18.

75. Kalant, H. Grant, D., Mitchell, J.(2007). *Principles of Medical Pharmacology.* Toronto, ON: Elsevier Canada.

76. Davis, J.S. *et al. Prostaglandin F2 alpha stimulates phosphatidylinositol 4,5-bisphosphate hydrolysis and mobilizes intracellular Ca2+ in bovine luteal cells.* Proc Natl Acad Sci, 1987. **84**(11): p.3728-32.

77. Li, J. *et al. Adenosine A_{2A} Receptors Increase Arterial Endothelial Cell Nitric Oxide.* Journal of Surgical Research, 1998. **80**: p.357-64.

78. Chaudary, N., *et al.*, *Hypoxia regulates the adenosine transporter, mENT1, in the murine cardiomyocyte cell line, HL-1.* Cardiovasc Res, 2004. **61**: p.780-8.

79. Andresen, J.J., F.M. Faraci, and D.D. Heistad. *Vasomotor responses in MnSOD-deficient mice.* American Journal of Heart and Circulatory Physiology, 2004. **287**: p.1141-8.

80. Kim, N. *et al. Oxygen tension regulates the nitric oxide pathway. Physiological role in penile erection.* J. Clin. Invest., 1993. **91**(2): p.437-42.

81. Kim, N.N *et al. Altered contractility of rabbit penile corpus cavernosus smooth muscle by hypoxia.* Journal of Urology, 1996. **155**: p.772-8.

82. Marshall, J.M. *Adenosine and muscle vasodilatation in acute systemic hypoxia.* Acta Physiol Scand, 2000. **168**: p.561-73.

83. Vorbach, C., R. Harrison, and M.R. Capecchi. *Xanthine oxidoreductase is central to the evolution and function of the innate immune system.* TRENDS in Immunology, 2003. **24**(9): p.512-7.

84. Deussen, A. *Metabolic flux rates of adenosine in the heart.* Naunyn-Schmiedeberg's Arch Pharmacol, 2000. **362**: p.351-63.

85. Rath, G. *et al. Vascular Hypoxic Preconditioning Relies on TRPV4-Dependent Calcium Influx and Proper Intercellular Gap Junctions Communication.* Arteriosclerosis, Thrombosis, and Vascular Biology, 2012. **32**: p.2241-9.

APPENDIX A

Ethics Approval for Animal Use

Subject: eSirius Notification - New Animal Use Protocol is APPROVED2013-007::1

Date: Tuesday, 4 June, 2013 9:47:07 AM Eastern Daylight Time

From: eSiriusWebServer

To: Robert Gros

CC: auspc@uwo.ca, esiriusadmin@uwo.ca

Western 🛡️

AUP Number: 2013-007
PI Name: Gros, Robert
AUP Title: Elucidating Molecular Mechanisms In Vascular Signalling

Approval Date: 06/04/2013

Official Notice of Animal Use Subcommittee (AUS) Approval: Your new Animal Use Protocol (AUP) entitled "Elucidating Molecular Mechanisms In Vascular Signalling

" has been APPROVED by the Animal Use Subcommittee of the University Council on Animal Care. This approval, although valid for four years, and is subject to annual Protocol Renewal.2013-007::1

1. This AUP number must be indicated when ordering animals for this project.
2. Animals for other projects may not be ordered under this AUP number.
3. Purchases of animals other than through this system must be cleared through the ACVS office. Health certificates will be required.

The holder of this Animal Use Protocol is responsible to ensure that all associated safety components (biosafety, radiation safety, general laboratory safety) comply with institutional safety standards and have received all necessary approvals. Please consult directly with your institutional safety officers.

Submitted by: Copeman, Laura
on behalf of the Animal Use Subcommittee
University Council on Animal Care

The University *of* Western Ontario
Animal Use Subcommittee   University Council on Animal Care
Health Sciences Centre, ● London, Ontario ● CANADA – N6A 5C1
PH: 519-661-2111 ext. 86768 ● FL 519-661-2028
Email: auspc@uwo.ca ● http: www.uwo.ca animal website

Page 1 of 1

APPENDIX B

Copyright Permission for Reproduction from

Journal of Nature Neuroscience

This is a License Agreement between Keisha A Best ("You") and Nature Publishing Group ("Nature Publishing Group") provided by Copyright Clearance Center ("CCC"). The license consists of your order details, the terms and conditions provided by Nature Publishing Group, and the payment terms and conditions.

All payments must be made in full to CCC. For payment instructions, please see information listed at the bottom of this form.

License Number	3360010271422
License date	Apr 01, 2014
Licensed content publisher	Nature Publishing Group
Licensed content publication	Nature Neuroscience
Licensed content title	The type 1 equilibrative nucleoside transporter regulates ethanol intoxication and preference
Licensed content author	Doo-Sup Choi, Maria-Grazia Cascini, William Mailliard, Hannah Young, Peter Paredes, Thomas McMahon, Ivan Diamond, Antonello Bonci, Robert O Messing
Licensed content date	Jul 18, 2004
Volume number	7
Issue number	8
Type of Use	reuse in a dissertation / thesis
Requestor type	academic/educational
Format	print and electronic
Portion	figures/tables/illustrations
Number of figures/tables/illustrations	1
High-res required	n/a
Figures	The generation of ENT1-/- mouse (modified from Choi *et al.* 2004). The organization of the gene encoding mouse ENT1 as well as the targeting construct and the allele resulting from

homologous recombination are shown. Boxes represent the targeted exons (2–4). loxP sequences, the recognition sites for Cre recombination, and deleted coding exons are shown via arrowheads

Author of this NPG article   no

Your reference number   None

Title of your thesis / dissertation   Analysis of the vascular phenotype of the ENT1 knockout mouse

Expected completion date   May 2014

Estimated size (number of pages)   125

Total   0.00 USD

Terms and Conditions

K. Arielle Best

EDUCATION

Masters of Science in Pharmacology and Toxicology   **2012–2014**
University of Western Ontario

Certificate in Strategic Marketing   **2010–2014**
Ryerson University

Honors Bachelor of Science in Biology   **2005–2010**
University of Waterloo

ACADEMIC AWARDS

Western Graduate Research Scholarship
2012–2013
University of Western Ontario
(WGRS)

Canadian Society of Pharmacology and Therapeutics Travel Bursary
April 2013
Canadian Society of Pharmacology and Therapeutics
(CSPT)

RESEARCH AND PROFESSIONAL EXPERIENCE:

Research Assistant   **2012 – 2014**
Department of Physiology and Pharmacology
The University of Western Ontario
Supervisor: Dr. James Hammond, Co-supervisor: Dr. Robert Gros
Project: Analysis of the Vascular Phenotype of the ENT1-null mouse

Faculty of Biology Student Research Assistant   **2009**
The University of Waterloo
Zoology and Benthic Invertebrate
Supervisor: Dr. David Barton

Faculty of Biology Student Laboratory Assistant   **2009**
University of Waterloo
Environmental Change
Supervisor: Dr. Roland Hall

TEACHING EXPERIENCE

Teaching Assistant
2012 – 2014
Course: Pharmacology/Toxicology 3580Y laboratory course
Department of Physiology and Pharmacology
University of Western Ontario

ACADEMIC ACCOMPLISHMENTS

K. A. Best, D. Bone, R. Gros, J. R. Hammond. Characterization of the Vascular Phenotype of the Equilibrative Nucleoside Transporter 1 Knockout Mouse (2012). Experimental Biology 2013, Boston. <u>Oral Presentation and Poster Presentation</u>.International Conference.

K. A. Best, D. Bone, R. Gros, J. R. Hammond. Characterization of the Vascular Phenotype of the Equilibrative Nucleoside Transporter 1 Knockout Mouse (2013). London Health Research Day, London Convention Centre, London. <u>Poster Presentation</u>. Institutional.

K.A.Best, D. Bone, D. Quinonez, Q. Feng, R. Gros, J. R. Hammond. Characterization of the Vascular Phenotype of the Equalibrative Nucleoside Transporter 1 Knockout Mouse (2012). Department of Physiology and Pharmacology Research Day, University of Western Ontario, London. <u>Poster Presentation</u>.

PROFESSIONAL MEMBERSHIPS

Student Member (CSPT)
2012-2014
The Canadian Society of Pharmacology and Therapeutics

REFERENCES

Dr. James Hammond, Professor and Chair
University of Alberta